Georg August University, Goettingen

Washingtone Ochieng'

Immune and intrinsic correlates of protection in Rhesus macaques immunised against Simian Immunodeficiency Virus

Cuvillier Verlag Göttingen

October 2007

Immune and intrinsic correlates of protection in Rhesus macaques immunised against Simian Immunodeficiency Virus

Dissertation Submitted for the award of the
Doctoral degree of the Faculties of
Natural Sciences and Mathematics,
Georg August University, Goettingen
Germany

Submitted by

Washingtone Ochieng′

Born in Migori District of Nyanza Province of the Republic of Kenya

Goettingen 2007

Bibliografische Information Der Deutschen Bibliothek
Die Deutsche Bibliothek verzeichnet diese Publikation in der Deutschen Nationalbibliografie; detaillierte bibliografische Daten sind im Internet über http://dnb.ddb.de abrufbar.
1. Aufl. - Göttingen : Cuvillier, 2007
Zugl.: Göttingen, Univ., Diss., 2007

978-3-86727-427-2

Printed with financial support from the German Academic Exchange Services (DAAD)

D 7

Referee: Professor Hans Joachim Fritz

Co-referee: Professor Hardeland

Date of oral Examinations: 31/10/2007

Nonnenstieg 8, 37075 Göttingen
Telefon: 0551-54724-0
Telefax: 0551-54724-21
www.cuvillier.de

1. Auflage, 2007
Gedruckt auf säurefreiem Papier

978-3-86727-427-2

Dedication

To my Dad Rohi Elgibor
My wonderful parents
To my ever supportive and dearest wife
To our First-born conceived around same time as this thesis
To the Ever abundant Love

Table of Contents

Table of figures

Appendix Figures

List of tables

Appendix tables

ABBREVIATIONS

Nominal

Ad5	Adenovirus serotype 5
Ad5hr/rAd5	Human recombinant Ad5
Ad5hr-SIV	Ad5hr expressing SIV genes
Agm	African green monkeys
AIDS	Acquired Immune Deficiency Syndrome
CMV	Cytomegalovirus
HIV	Human Immunodeficiency Virus
HSV	Herpes simplex virus
Mac	Macaque(s)
Mamu	Macaca mulatta (= rhesus macaque)
MVA	Modified vaccinia Ankara
PBMC(s)	Peripheral blood mononuclear cell(s)
SIV	Simian Immunodeficiency Virus
SIVagm	SIV of agm
SIVmac	SIV of Macaque(s)

Cellular, Molecular and viral

CA	Capsid (protein of HIV/SIV)
cDNA	Complimentary DNA
Cis-acting element	a DNA region bound by other proteins to allow transcription and expression of adjacent genes without itself being transcribed.
DNA	Deoxy ribonucleic acid
dNTP	Deoxy ribonucleotide
Env	Envelope
gp	glycoprotein
LTR	Long terminal repeat
MA	Matrix (protein of HIV/SIV)
MoI	Multiplicity of infection
mRNA	Messenger RNA
Nef	'Negative factor'
PCR	Polymerase chain reaction
Pfu	Plague forming units
RNA	Ribonucleic acid

RRE	Rev responsive element
RT-PCR	Reverse transcriptase PCR
RT-RT-PCR	Real-time RT-PCR
TAR	Trans-activation response (or responsive) element
Tat	Trans activator of transcription
TATA box	a highly conserved Cis-regulatory element (DNA sequence; 5'-TATAAA-3') in the promoter of a gene, considered core promoter.
TCID50	Tissue culture infectious dose 50 %
Trans-acting element	a DNA segment coding for a particular protein needed for its own regulation/replication or those of other DNA/RNA segments'.
Vif	Virus infectivity factor

Immunology

CC	Cysteine cysteine
CCR5	CC chemokine receptor 5
CD	Cluster of Differentiation
CNAR	CD8+ T-cell noncytotoxic antiviral response
CTL	Cytotoxic T-lymphocyte
CXC	Cystein X cystein
CXCR4	CXC chemokine receptor 4
ELISPOT	Enzyme linked immunospot
FACS	Fluorescence activated cell sorter/sorting
GM-CSF	Granulocyte macrophage colony stimulating factor
HLA	Human leukocyte antigen
IFN	Interferon
IFNγ	Interferon gamma
Ig	Immunoglobulin
IgG	Immunoglobulin G
IL	Interleukin
IL-2	Interleukin 2
MCP-1	Monocyte chemotactic protein-1
MHC	Major Histocompatibility complex
MIP	Macrophage inflammatory protein
R4	Viruses tropic for CXCR4 co-receptors
R5	Viruses tropic for CCR5 co-receptors

RANTES	Regulated on Activation Normal T-cell Expressed and Secreted
V3	Variable region 3

Chemical or Biochemical

β-gal	beta galactosidase
AEC	3-amino, 9 ethyl-carbazole (AEC)
Con-A	Concanavalin A
CpG	Cytosine-phosphate-guanine
ddH_2O	Double distilled/ distilled or de-ionised water
DEAE	Di-ethyl-amino-ethyl-dextran
DMEM	Dulbelco's Modified Eagle's Medium
DMF	Dimethyl formamide
DMSO	Dimethyl sulphoxide
EDTA	Ethylene diamine tetra-acetic acid
FBS	Fetal bovine serum
H_2O	Water
H_2O_2	Hydrogen peroxide
HCl	Hydrochloric acid
HRPO	Horse radish peroxidase
Lys	Lysine
Met	Methionine
MP	Milk powder
NaCl	Sodium chloride
PBS	Phosphate buffered saline
PMA	Phorbol 12-myristate 13-acetate
RNase-A	Ribonuclease A
RNase-H	Ribonuclease H
RPMI	A cell culture medium named after the 'Roswell Park Memorial Institute'
SDS	Sodium dodecyl sulphate
STE	Sodium chloride Tris EDTA (buffer)
Taq	*Thermus acquaticus*
TE	Tris EDTA
Try	Tryptophan
Val	Valine

X-gal	5-bromo-4-chloro-3-indolyl-beta-D-galacto-pyranoside

Units of measurements and time

°C	Degree(s) centigrade (Celsius)
μL/μl	microlitre (s)
bp	base pair (s)
Hr (s)	Hour (s)
Kb	killo base
kD	Kilo Dalton
M	Molar (concentration)
Min	Minute (s)
mL/ml	Millilitre
mM	Milli molar (concentration)
nM	Nanomolar (concentration)
Sec	second (s)
U	Units

Others plus non-conventional

ΔSUP	Virus Depleted Supernatant
ABI	Applied biosystems
ca.	Circa
CFAR	Central facility for AIDS research
CFU	Spot forming unit (s)
DoC	Day of Challenge
DPZ	Deutsche Primatenzentrum (German Primate Centre)
HAART	Highly active antiretroviral therapy (treatment)
HPLC	High performance (pressure) liquid chromatography
i.m.	Intramuscular
PVDF	polyvinylidene difluoride
Rpm	revolutions per minute
SUP	Supernatant
TOPO-10	An *E. coli* cloning plasmid strain from Invitrogen
VVR	*Ex vivo* virus replication kinetics
Wdi	Weeks during immunization
Wpc	Weeks post-challenge

1.0 INTRODUCTION

1.1 The human and simian immunodeficiency viruses

1.1.1 Origin and similarities, infection and pathogenesis

Simian immunodeficiency virus (SIV) belongs to a group of lentiviruses that infect non-human primates. Though distinct, SIV is closely related to the human immunodeficiency virus type-1 (HIV-1) in its genetic structure. Figure 1.1a shows the evolutionary divergence of various lentivirus strains. The Chimpanzee species *Pan troglodytes troglodytes* is the natural and primary reservoir for HIV-1 (Gao *et al.*, 1999). Therefore, this primate species is thought to be the origin of both pandemic (group M) and non-pandemic (group N) HIV-1 (Keele *et al.*, 2006). HIV-1 group O-like viruses have also been linked to wild gorillas of West central African origin (Van Heuverswyn *et al.*, 2006), confirming that the HIV-1 pandemic may have followed the cross-species transmission route to infect their human host (Nerrienet *et al.*, 2005). SIV has also been isolated from other monkey species including Sooty mangabeys (Fultz *et al.*, 1986), African green monkeys (Fukasawa *et al.*, 1988) and Mandrills (Tsujimoto *et al.*, 1988), and shown to infect macrophages and CD4+ T-lymphocytes. The virus is associated with asymptomatic infection in its natural hosts. The SIV strains infecting these natural hosts are closely related to the HIV-2 (Anderson *et al.*, 2004), also prevalent in West Africa and from which the former is thought to have evolved. In other monkey species like the Asian macaques, infection by SIV (earlier called the Simian T-lymphotropic virus type III/STLV-III), induces acquired immune deficiency similar to human AIDS (Daniel *et al.*, 1985; Letvin *et al.*, 1985). AIDS-like symptoms can be experimentally induced in these animals, (Mann *et al.*, 1998), making them good candidates for HIV-1 infection studies.

In humans, progression of HIV-1 disease is determined by pathophysiological events occurring during infection, and also by age, immunological competence and other co-infections (Kahn & Walker, 1998; Ochieng *et al.*, 2006). While treatment leads to sustained suppression of plasma viral loads and immune recovery, (Berrey *et al.*, 2001), long-term therapy may

reverse treatment benefits (Lwembe *et al.*, 2007). Progression to simian AIDS also varies between animals (Ten Haaft *et al.*, 1998). This variation is influenced by among others, host genetic factors (Sauermann *et al.*, 1997).

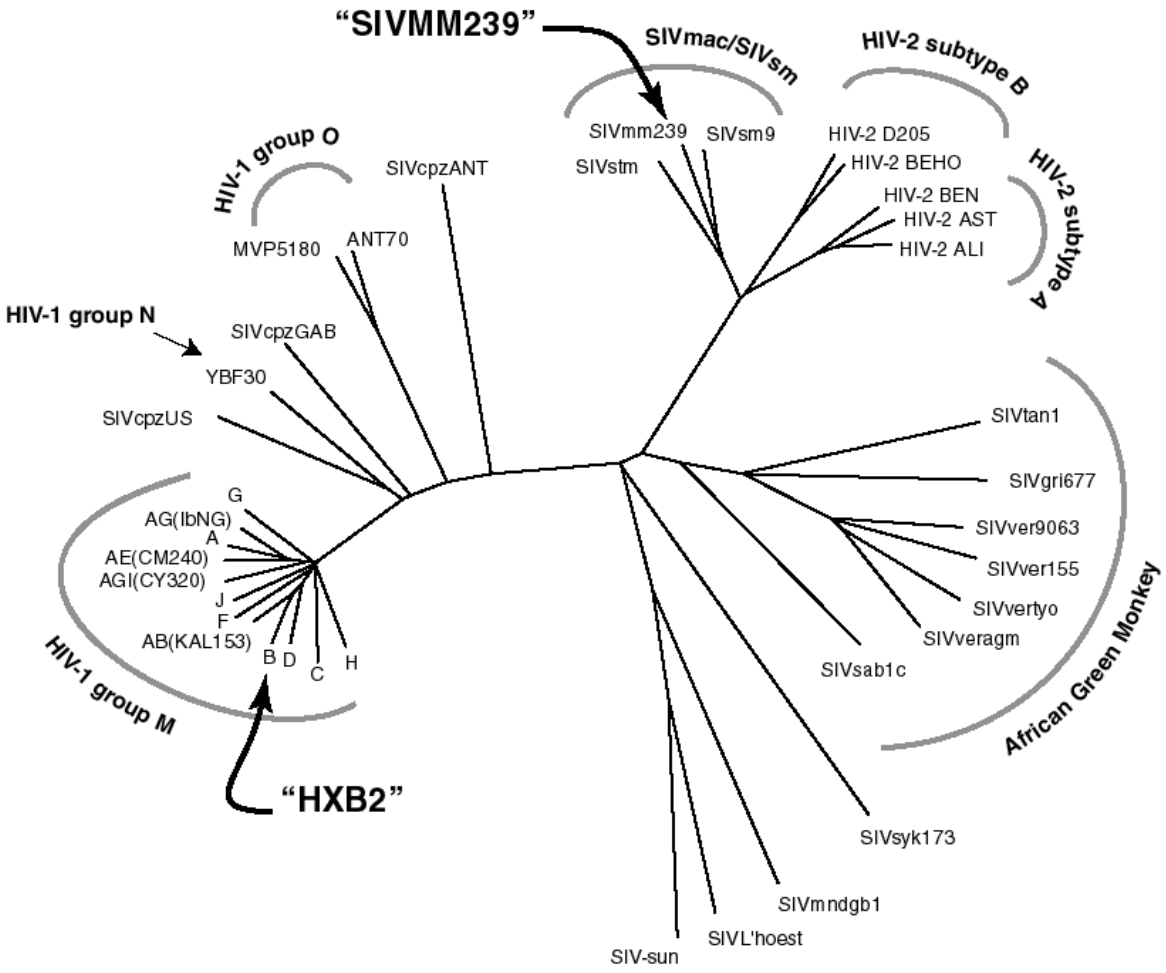

Figure 1.1a: Phylogenetic tree of the primate lentiviruses
Note the large distance between the SIVmac group and the HIV-1 M group and the wide divergence of SIVmac from other SIVs.

1.1.2 Gene structure and functions

SIV and HIV-1 are both lentiviruses that belong to the retrovirus family. The two viruses are closely related in gene structure, function and biology. They have a diploid genome that consists of two plus-stranded RNA copies, approximately 9

kilo base (kb) long. The RNA genome encodes at least 9 different proteins; Gag, Pol, Env, Tat, Rev, Nef, Vif, Vpu and Vpr.

Gag, Gag-Pol and the Protease genes

The *gag* gene product is a 55-kilodalton (kD) precursor protein known as p55. It is expressed from unspliced viral mRNA. The p55 N terminus is myristoylated during translation (Bryant & Ratner, 1990), a process that triggers its association with the cell membrane and which is essential for efficient viral assembly. The membrane-associated Gag polyprotein recruits two copies of the viral genomic RNA along with other viral and cellular proteins that trigger budding of the viral particle from the surface of an infected cell. During viral maturation and after budding, p55 is cleaved by the virally encoded protease into four smaller proteins; (i) MA or matrix (p17), CA or capsid (p24), NC or nucleocapsid (p9) and p6 (Gottlinger *et al.*, 1989). The MA polypeptide stabilizes the virion particle and also constitutes the complex required to transport proviral DNA to the nucleus to facilitate HIV infection (Gallay *et al.*, 1995; Lewis *et al.*, 1992). The CA also includes the p24 protein (p27 for SIV) which forms the viral core. The NC facilitates reverse transcription and is also required for viral packaging (Lapadat-Tapolsky *et al.*, 1993). It recognizes the packaging signal that mediates incorporation of a heterologous RNA into the virions. The p6 polypeptide mediates interactions between p55 Gag and the Vpr protein that are required for the incorporation of Vpr into the assembling virions (Paxton *et al.*, 1993). It also contains a 'late domain' needed for the release of budding virions. The viral protease (Pro), integrase (IN), RNase H, and reverse transcriptase (RT) are expressed as a Gag-Pol fusion protein (Jacks *et al.*, 1988). The Gag-Pol precursor (p160) is a product of a ribosomal frame shift triggered by a specific cis-acting RNA motif (Parkin *et al.*, 1992). Upon encounter with this motif, the ribosomes shift occasionally (5% of the times) to the *pol* reading frame. Although this shift does not interrupt translation, it leads to 20-fold more gag than Gag-Pol precursor products. The Pro is an aspartyl protease dimer that cleaves the Gag and Gag-Pol polyprotein precursors during virion maturation (Ashorn *et al.*,

1990). It accomplishes this role by cleaving the Pol polypeptide away from Gag and further digesting it to separate the protease (p10), RT (p50), RNase H (p15), and integrase (p31) activities. In the process of cleavage, about 50% of the RT protein remains linked to RNase H as a single polypeptide, the p65. Figure 1.1b shows the genome landmarks of SIVmac239 relative to HIV-1.

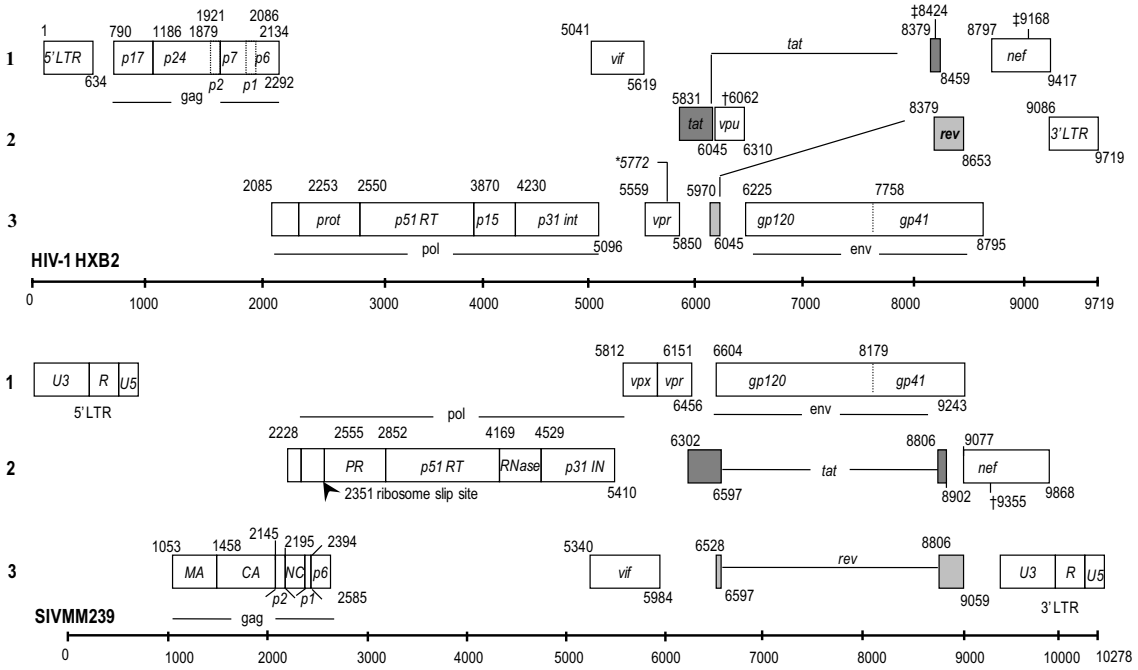

Figure 1.1b: Structural organizations of the SIVmac239 genome

Gene maps for HIV-1 (HXB2 strain, top) and SIVmac239 showing locations of the various genome landmarks. Rectangles show open reading frames (also labelled 1 to 3). The small number in the upper left corner of each rectangle records the position of the 'a' in the *ATG* start codon for the respective gene. The number in the lower right records the last position of the stop codon. For *pol*, the 5' end is the start of the open reading frame, taken to be the first 'T' in the *TTTTTTAG* sequence constituting part of the stem loop and potentiating ribosomal slippage on the RNA leading to a -1 frameshift and the translation of the gag-pol polyprotein. The *tat* and *rev* spliced exons are shown as shaded rectangles. In HXB2, *5772 marks the position of frameshift in the *vpr* gene caused by an extra "T" relative to most other subtype B viruses; †6062 indicates a defective *ACG* start codon in *vpu*; ‡8424, ‡9168 and †9355 mark premature stop codons in *tat* and *nef*. Abbreviations: MA matrix, CA capsid, NC nucleocapsid, PR protease, RT reverse transcriptase, IN integrase. Adapted from; Korber et al., Numbering Positions in HIV Relative to HXB2CG: in 'the database compendium', Human Retroviruses and AIDS, 1998. http://hiv-web.lanl.gov/HTML/reviews/HXB2.html.

Reverse Transcriptase (RT) and Integrase

The retroviral RT is encoded by the *pol* gene, which has both RNA- and DNA-dependent polymerase activities. All *pol* gene products are located within the capsid of free SIV/ HIV-1 virions. Using the dimer of single-stranded viral genomic RNA template, the polymerase synthesises a double-stranded DNA copy of the viral genome during reverse transcription. RNase H degrades the parent RNA template used to make the first DNA strand to allow synthesis of a complementary DNA. This process can be completed within 6 hours of viral entry (Zack *et al.*, 1990). Successful synthesis of proviral DNA requires several cis-acting elements found within the viral RNA. Required to initiate reverse transcription is the TAR element, a small RNA stem-loop structure located at the 5' end of viral RNAs and containing the binding site for Tat (Harrich *et al.*, 1996). The synthesised viral DNA is then integrated into the host genome or may remain in an un-integrated form for prolonged durations. The functional species of the polymerase is a heterodimer of p65 and p50. HIV-1 RT does not possess 3'- to 5'-exonuclease or proofreading activity (Laakso & Sutton, 2006). Consequently, the enzyme introduces several point mutations into each new copy of the viral genome synthesised during replication (O'Neil *et al.*, 2002).

Efficient expression of viral genes requires proviral DNA in its integrated form (Wiskerchen & Muesing, 1995). The virally encoded integrase (In) mediates the insertion of the proviral DNA into the infected host chromosome (Bushman *et al.*, 1990). This process requires three activities of this viral protein; (i) the exonuclease activity trims two nucleotides from each 3' end of the linear viral DNA duplex, (ii) the endonuclease cleaves the host DNA at the site integration and (iii) the ligase generates a single covalent linkage at each end of the proviral DNA. The site of integration is then repaired by cellular enzymes. The choice of integration sites is affected by accessibility of the chromosomal DNA within chromatin rather than by specific DNA sequences (Pryciak & Varmus, 1992).

Envelope (env) and Regulatory Proteins

The HIV envelope is a 160 kD glycoprotein (gp160) expressed from singly spliced mRNA as a precursor protein. It is synthesized in the endoplasmic

reticulum and transported to the Golgi complex where it undergoes glycosylation, a step required for virus infectivity (Capon & Ward, 1991). The gp160 is cleaved by a cellular protease into the gp41 transmembrane glycoprotein and the gp120 surface glycoprotein. The two Env proteins interact through non-covalent linkages. It is the gp120 that binds CD4 receptors on target T-cells to mediate viral internalisation and infection via gp41 (Landau *et al.*, 1988).

Tat is a 14 kD protein with three distinct functional domains that affect localisation and trans-activation of viral genes (Ruben *et al.*, 1989). It is expressed in two long forms; (i) a 72 amino acid HIV-1 Tat is expressed by early fully spliced mRNA, and (ii) the 101 amino acid form from late incompletely spliced viral mRNA. Both forms are located within the nuclei and nucleoli of infected cells and function as transcriptional activators. The trans-activation requires a cis-acting site called TAR, located on the R region of the retroviral long terminal repeat (LTR) (Feng & Holland, 1988; Roy *et al.*, 1990). The HIV-1 *tat* gene products stimulate in trans the expression of all viral genes and ensure generation of full-length transcripts during elongation phase of HIV-1. Rev is a 13-kD sequence-specific RNA binding protein with a binding site in the 'so-called' rev-responsive elements (RRE) of gag-pol and env mRNAs (Zapp & Green, 1989). It is produced from fully spliced mRNAs and acts to increase the amount of gag-pol and env messenger RNA by inducing transition from an early to a late phase of HIV gene expression (Kim *et al.*, 1989).

Accessory Proteins

HIV-1 contains four additional genes: *nef*, *vif*, *vpr* and *vpu* that code for accessory proteins. Instead of the *vpu*, SIV and HIV-2 have the *vpx*, which is a nucleocytoplasmic shuttling protein involved in nuclear import and targeting (Singhal *et al.*, 2006). These accessory proteins represent critical virulence factors (Nielsen *et al.*, 2005). Nef is a 27-kD myristoylated early gene product that is encoded by a single exon extending into the 3' LTR (Kim *et al.*, 1989). It is expressed from a multiply spliced mRNA and is therefore Rev-independent. It is required for optimal replication of both SIV and HIV during primary infection (Fackler *et al.*, 2007; Kestler *et al.*, 1991), as well as for the maintenance of

productive infection in CD4(+) T lymphocytes (Mahlknecht *et al.*, 2000). *In vitro* studies showed that exogenous Nef proteins stimulate HIV-1 LTR via *NF-kappaB* activation (Varin *et al.*, 2003), confirming that these gene products could exacerbate disease progression and increase virion infectivity (Miller *et al.*, 1994). Nef down-modulates CD4 and MHC-I and II surface expression, and polymorphisms in this gene can lead to different disease outcomes in both HIV and SIV infection (Munch *et al.*, 2005; Schindler *et al.*, 2007).

Vpr, Vpu, and Vif are products of incomplete mRNA splicing normally expressed from singly spliced mRNAs during the late Rev-dependent infection phase. The Vpr protein is incorporated into viral particles via interactions with the c-terminal of p55 Gag (Cohen *et al.*, 1990). It is needed for infection of non-dividing cells (Heinzinger *et al.*, 1994) and also acts as a nucleocytoplasmic transport factor connecting the viral genome to the nuclear pore (Vodicka *et al.*, 1998). Vpu is a 16-kD integral membrane phosphoprotein polypeptide localized in the internal cell membranes (Sato *et al.*, 1990). It functions to down-modulate CD4 and enhance virion release (Schubert *et al.*, 1996). The vpx is also incorporated into budding virions at the plasma membrane. Vif is a 23-kD polypeptide essential for the replication of HIV in peripheral blood lymphocytes, macrophages, and other target cells (Strebel *et al.*, 1987).

1.1.3 Receptor-virus interactions

Cellular tropism

HIV-1 infection is the primary cause of the acquired immunodeficiency syndrome (AIDS), a slow but progressive, degenerative and wasting disease that attacks and compromises the host immune system. Receptor and coreceptor usage by both HIV-1 and SIV plays an important role in virus tropism and pathogenesis. The primary targets for HIV-1 and SIV infections are the CD4+ T-lymphocytes and monocytes/macrophages (Dittmar *et al.*, 1997), although they can also infect astrocytes and microglial cells. Infection is initiated by binding of the virion gp120 surface glycoprotein to the CD4 receptor on T-cells (Nielsen *et al.*, 2005).

For effective binding to CD4 receptors on target cells and entry, the viral gp120 requires a coreceptor of the CC or CXC chemokine family. The two major chemokine coreceptors for HIV binding to CD4 are the CCR5 and CXCR4 (Lewis *et al.*, 1992). SIV exclusively uses CCR5, a coreceptor required by all monocytes/macrophage-tropic viruses (R5 viruses). SIV does not use CXCR4, which is used exclusively by T-cell tropic HIV-1 viruses (R4 viruses). Binding of gp120 to CD4 exposes a coreceptor binding site on gp120 which allows the formation of gp120-receptor-coreceptor complex. This interaction engages an envelope glycoprotein trimer (gp160/120/41) and initiates structural and conformational changes required for fusion of viral and host cell membranes (Chen *et al.*, 2005). The changes preceding fusion occur in the gp41 (TM), and are characterised by exposure of the N-terminal region of the TM protein (Gallay *et al.*, 1995; Gottlinger *et al.*, 1989). The gp120 subunit may also independently mediate fusion between neighbouring infected and non-infected cells via syncitium formation (Franke *et al.*, 1994). After entry, the virus integrates its genome into the host DNA and utilises the host cellular machinery to replicate. It then spreads to the lymphatic tissue and into the follicular dendritic cells where it is maintained as latent viral reservoir. This spread and subsequent reactivation of the latent virus leads to a slow and progressive destruction of the immune system.

Molecular and cellular basis of viral pathogenesis

Central to the interaction between virus envelope and cell surface chemokine receptors is the third variable region (V3) of the HIV-1 gp120. The amino acid sequence of V3 determines whether the virus binds to CCR5 (“R5 viruses”) or to CXCR4 (“X4 viruses”) in order to infect its target cells (Dittmar *et al.*, 1997). During the course of HIV-1 infection, a switch from CCR5- to CXCR4- tropic viruses occurs, which is characteristically associated with the onset of AIDS-related symptoms. This switch is associated with a single amino acid mutation at position 322 within the V3 loop, from a negatively to a positively charged residue (Fouchier *et al.*, 1992; Resch *et al.*, 2001). The presence of a basic (positively

charged) residue at position 306 or 322 is associated with X4 and the dual-tropic X4R5 viruses, whereas the presence of a negatively charged (acidic) and a neutral residue respectively at positions 322 and 306, is associated with R5 viruses. The presence of positive and negative residues at positions 304 and 322 respectively, introduces opposite electrostatic forces at the beta-hairpin structure of the V3 loop which is thought to stabilize the R5 conformation (Rosen *et al.*, 2006). It is this V3 loop that triggers membrane fusion and virus entry into human lymphocytes and macrophages (Cardozo *et al.*, 2007).

1.1.4 Replication, transcription and regulation of gene expression

After entry, the viral RNA is reverse transcribed and the proviral DNA integrated into host cell chromosome (O'Neil *et al.*, 2002). The virus may then enter into a period of latency characterised by low-level viral replication or undergo active replication and expression to produce several copies of infectious virions. Latent infection is influenced by a variety of events including virus suppression by soluble CD8+ T cell-derived factors (Chun *et al.*, 2001) or treatment (Chun *et al.*, 1997). The presence of un-integrated HIV-1 DNA in infected resting CD4+ T cells as well as replication-competent integrated proviral DNA in cells from patients receiving HAART treatment demonstrates that latent virus can undergo a normal replication cycle upon cellular activation (Chun *et al.*, 1997). Replication is initiated by binding of nuclear factor kappa-B (*NF-κB*) transcription factors to the HIV-1 LTR (Faure *et al.*, 1997). NF-kB is a family of eukaryotic transcription factors that regulate various cellular genes involved in inflammatory immune responses. The LTR has two tandem NF-κB sites and three repeated Sp1 sites upstream of the *TATA* box (Jones *et al.*, 1986; Nabel & Baltimore, 1987). The Sp1 transcription factor binds to promoter sequences within the HIV-1 LTR to activate RNA synthesis. An additional NF-κB site is located within the TAR element of the 5' untranslated region (UR) (Mallardo *et al.*, 1996), and is required for both SIV and HIV-1 replication (Palmieri *et al.*, 2004; Quinto *et al.*, 2004). When activated by specific stimuli such as the pro-inflammatory cytokines (Devadas *et al.*, 2004) or DNA alkylating agents, phorbol 12-myristate 13-

acetate, the *NF-kB*-responsive element in the *TAR* region fully induces the HIV-1 *LTR* to initiate gene expression. Cellular localization and transcriptional activity of *NF-kB* is tightly regulated by its partner *IkappaBalpha* (*IkB*) (Kiernan *et al.*, 2003). When stimulated, IκB proteins undergo phosphorylation, ubiquination and proteasomal degradation to release cytoplasmic NF-κB into the nucleus (Brown *et al.*, 1995; Chen & Greene, 2004), which activates the transcription of responsive genes. The functions of NF-κB are also regulated by reversible acetylation (Chen & Greene, 2003; Greene & Chen, 2004). In SIV infection, the p50/p65 NF-kB transcription factors enhance Tat-mediated transcriptional activation while IkB S32/36A, a proteolysis-resistant inhibitor of NF-kB, inhibits Tat-mediated transactivation of SIVmac239 (Quinto *et al.*, 2004).

1.1.5 Cytokines in immune response and regulation

Cytokines are a group of proteins and peptides that act as signalling compounds. The cytokine family consists mainly of water-soluble proteins and glycoproteins. Cytokines are particularly important in regulating both innate and adaptive immune responses. Interleukin 10 (IL-10), also known as human cytokine synthesis inhibitory factor, is an anti-inflammatory cytokine. By regulating CD4+ and CD8+ T cells, IL-10 controls lymphocyte-mediated inflammatory responses (Jinquan *et al.*, 1993). IL-10 inhibits synthesis of pro-inflammatory cytokines like IFNγ, IL-2, IL.-3, TNFα and GM-CSF and also displays potent abilities to suppress the antigen-presenting capacity of antigen presenting cells. It is mainly expressed in monocytes and Type 2 T helper cells (T_{H2}), mast cells and also in a certain subset of activated T and B cells where it may have stimulatory effect. It is released by cytotoxic T-cells to inhibit the actions of NK cells during the immune response to viral infection. HIV-1 Tat induces IL-10 expression, a mechanism that amplifies immune suppression and dysregulation (Gee *et al.*, 2007). IL-10 expression on HIV-1-specific CD8+ T-cell inhibits cytolysis of infected cell via a mechanism involving direct cell-to-cell contact (Elrefaei *et al.*, 2007). This inhibition is predominant during advanced and chronic disease (Elrefaei *et al.*, 2006). Increased IL-10 during advanced disease interferes with

the normal antiviral and memory function of immune system cells (Brooks *et al.*, 2006; Ejrnaes *et al.*, 2006). IL-10 can also block T lymphocyte chemotaxis, thereby ensuring focusing of T lymphocytes to an area of T lymphocyte activation to generate a localised immune response (Tan *et al.*, 1995). Contrastingly, IL-10 has also been shown to inhibit HIV infection of monocytes by antagonising TNFα stimulation of HIV expression as well as inhibiting expression and maturation of infected host cell mRNA (Chang *et al.*, 1996; Naif *et al.*, 1996).

IFNγ plays a key role in the early immune defence against infection (Graziosi *et al.*, 1996). IFNγ also harbours pro-inflammatory effects that facilitate lentiviral replication. Indeed, the outcome of SIV infection of immunised monkeys depends on the balance between SIV-specific IFNγ T-cell responses and nonspecific IFNγ-driven inflammation (Abel *et al.*, 2004). IL-1β belongs to the IL-1 superfamily of cytokines that includes IL-1α, IL-1 receptor and a host of other relatives. Both IL-1α and IL-1β are produced by macrophages, monocytes and dendritic cells and form an important part of the body's inflammatory response. These cytokines increase the expression of adhesion factors on endothelial cells to enable transmigration of leukocytes to sites of infection. IL-1 is also important in the regulation of haematopoiesis. Both IL-1α and IL-1β bind to the same cellular receptor that is composed of two related but non-identical intracellular signalling subunits.

1.1.6 Effects of chemokines on HIV/SIV infection

Chemokines are a family of small (approximately 8-10kD in size) chemotactic cytokines that induce directed chemotaxis in nearby responsive cells (Allen *et al.*, 2007). All chemokines function by interacting with G protein-coupled transmembrane receptors (chemokine receptors) located selectively on target cell surfaces (Maghazachi *et al.*, 1996). Binding to these receptors causes conformational changes that trigger intracellular signalling pathways involved in cell movement and activation. Regulation of chemokines is critical in many disease processes including AIDS. Pro-inflammatory chemokines are released in response to stimuli from other cytokines such as IL-1, and enhance recruitment

of immune system cells to the site of infection. Homeostatic chemokines control the migration of cells during normal processes of tissue maintenance or development and control immune system cells during immune surveillance. Chemokines are classified according to shared structural characteristics (size) and the presence of four cysteine residues in conserved locations that form their 3-dimensional shape. Four groups have been identified depending on the spacing of their first two cysteine residues.

The CC chemokines

Also known as β-chemokines, they have two adjacent cysteines near their amino terminus and include the CC chemokine ligands (CCL)-1 to CCL-28. In humans, most CC and other chemokines are located on chromosome 17 (Donlon *et al.*, 1990; Fernandez & Lolis, 2002). These chemokines interact with respective cell surface receptors, the CCRs. RANTES or CCL5, MIP (Macrophage Inflammatory Proteins) 1α (CCL3) and -1β (CCL4) are implicated in HIV-1 and SIV suppression (Cocchi *et al.*, 1995; Ondoa *et al.*, 2002; Saha *et al.*, 1998). They are also associated with an AIDS-free status in HIV-1 infected individuals (Garzino-Demo *et al.*, 1999). MIP-1α and MIP-1β activate human granulocytes (neutrophils, eosinophils and basophils) to mediate acute neutrophilic inflammation. They also induce the synthesis and release of other pro-inflammatory cytokines from fibroblasts and macrophages. RANTES is an 8 kD protein that is chemotactic for T cells, eosinophils and basophils. Monocyte chemotactic protein 1 (MCP-1) or CCL2, is approximately 13 kD and recruits monocytes, T lymphocytes, eosinophils, and basophils to sites of tissue injury and infection (Donlon *et al.*, 1990; Maghazachi *et al.*, 1996). Its role in HIV is unclear and conflicting, showing both inhibitory and enhancing activities on HIV-1 infection (Vicenzi *et al.*, 2000).

The CXC chemokines

CXC or α-chemokines have their two N-terminal cysteines separated by another ('X') amino acid. They are grouped according to the presence or absence of an

amino acid sequence (or motif) of Glutamic acid-Leucine-Arginine (ELR) immediately before the first cysteine of the CXC motif. ELR-positive CXC chemokines such as IL-8, interact with chemokine receptors CXCR1 and CXCR2 to induce the migration of neutrophils. ELR negative CXC chemokines bind to CXC chemokine receptors (CXCR1-7) and are chemo-attractant for lymphocytes. CXCR4 is a coreceptor for HIV-1 entry into T-lymphocytes, with its most studied and characterised ligands being the stromal-derived factor (SDF-1/CXCL12) (Xiang *et al.*, 2004). Another CXC chemokine, the gamma inducible protein 10 (IP-10) or CXCL10, is expressed in response to IFNγ-driven inflammatory responses. Expression of IP-10 correlates positively with SIV replication (Abel *et al.*, 2004). Like all chemokine receptors, CXCRs are G protein-coupled on their C-terminal ends to mediate intracellular signalling, while the N-terminal determines ligand binding (Fernandez & Lolis, 2002; Laing & Secombes, 2004).

1.2 Pre-clinical models of HIV-1 vaccine studies

Nonhuman primates are critical for the design of vaccines against several pathogens, with precedent vaccine testing against polio and small pox viruses (Caulfield *et al.*, 2000; Chen *et al.*, 2007). The status of research on HIV vaccines has recently been reviewed (Letvin, 2005). In both SIV and HIV-1 infections, the rhesus monkeys (*Macaca mulatta*) are the most widely used species to study protective HIV-1 vaccines (Stahl-Hennig *et al.*, 2007a), as well as chemo-prophylactic regimens for infant HIV exposure (Van Rompay *et al.*, 2006). The rhesus monkeys were used in pioneer split AIDS-vaccine experiments in which immunization with Tween-ether-disrupted SIVmac showed potential for protection against the challenge virus (Stahl-Hennig *et al.*, 1992; Stahl-Hennig *et al.*, 1993). These monkeys also offer an opportunity to understand the intra-species differences in immune responses towards several vaccine strategies (Stahl-Hennig *et al.*, 2007b). The cynomolgus monkeys (*Macaca fascicularis*) have been used to study HIV-2-based subunit AIDS vaccines (Luke *et al.*, 1993; Stahl-Hennig *et al.*, 1994). Baboons and several other monkey species are useful models for studying retroviral transmission, pathogenesis and to a lesser extent,

vaccine efficacy (Casimiro *et al.*, 2003b; Pandrea *et al.*, 2006; Ploquin *et al.*, 2004). The African green monkey which is naturally infected with SIV but does not develop disease, is used to understand the natural basis for disease resistance and virus-host cell interactions (Muller & Barre-Sinoussi, 2003). All these animals form the basic reference for advancing the development and testing of human AIDS/HIV vaccines and strategies (Letvin, 2005).

1.2.1 DNA Vaccines

Cell mediated immune (CMI) response is central to the control and resolution of both HIV-1 and SIV infections. Due to their potential for inducing CMI responses, DNA plasmids are used in a wide range of vaccine candidates (Egan *et al.*, 2006; Zhang *et al.*, 2007a). These vaccines are designed to carry multiple gene segments or regions of the retroviral genome (multigenic DNA immunogens) that are capable of expressing viral proteins (Malm *et al.*, 2005). The DNA vaccines can be delivered either systemically via the intramuscular route (Luckay *et al.*, 2007), or topically to the skin (Liu *et al.*, 2001). While systemically administered plasmid DNA is taken up by the myocytes, topical application leads to uptake by the dendritic cells, Langerhans cells and/or other antigen-presenting cells which can directly mediate antigen-specific immune responses. Some limitations of DNA vaccines include failure to produce sufficient antibody responses because of limited expression of viral proteins in the host. To circumvent these drawbacks, DNA vaccines are co-administered with immunostimulatory agents like cytokines. Besides, using synthetic codon-optimised genes to mediate high levels of transgene expression also helps improve immunogenicity of DNA vaccines (Vinner *et al.*, 1999). Furthermore, immunization with a bicistronic plasmid co-expressing viral gene (gp120) and adjuvants (GM-CSF) under the control of a single promoter can effectively augment DNA vaccine-elicited cellular immunity (Barouch *et al.*, 2002b). The host's immune system can also down-regulate vaccine-elicited antigen *in vivo*, thereby attenuating virus-specific antigen expression required to sustain an immune response (Greenland *et al.*, 2007).

Because of these limitations, plasmid DNA vaccines need to be accompanied by alternative vector-based boosting regimens.

1.2.2 Viral vector vaccines

Pre-clinical vaccine testing often embrace a combination of DNA-priming and viral or bacterial vector boosting (Castaldello *et al.*, 2006; McGettigan *et al.*, 2006; Uberla *et al.*, 2007). One vector in use for HIV-1 vaccine testing is the replication-competent human adenovirus serotype-5 (hAd5) expressing HIV or SIV proteins (Ad5hr-SIV) (Casimiro *et al.*, 2003b; Patterson *et al.*, 2004). The apparent limitation with this vector is that a majority of people have been previously exposed to one or more of the human adenovirus serotypes. Pre-existing immunity to Ad5 may lower the immunogenicity of these vaccine vectors (Casimiro *et al.*, 2003a). A second limitation is common to most multigene vaccines. Expression frequencies of viral antigens from these multigene vectors is low, leading to reduced vector immunogenicity (Brave *et al.*, 2006). These two limitations have been partially overcome by sequential vector administration with or without DNA priming (Malkevitch *et al.*, 2004; Malkevitch *et al.*, 2006), and by the use of codon optimised genes to reflect codon-usage of the eukaryotic cellular machinery (Ramakrishna *et al.*, 2004). The use of replication-competent adenovirus is considered less safe, prompting the development of vectors based on replication-defective Ad5 (Shiver *et al.*, 2002). These nonreplicating vectors are now frequently used in vaccine efficacy testing, with promising results reported in mice (Fitzgerald *et al.*, 2003) as well as rhesus monkeys (Pal *et al.*, 2006). The present study focuses on DNA priming followed by replication incompetent rAd5-SIV boosting as a strategy to generate SIV specific immune responses. The study concentrates on how these vaccine-induced immune responses can be quantified prior to challenge and then used to predict protective efficacy. Overall, an intermediate surrogate for vaccine-testing and monitoring has been developed and will be described in subsequent chapters.

1.3 Rationale for the study

SIV causes a fatal AIDS-like disease in rhesus macaques (Murphey-Corb *et al.*, 1986). For this reason, infection of rhesus monkeys and other nonhuman primate species with SIV provides a strategic model for HIV-1 studies. However, HIV-1 vaccine efficacy trials in human require large numbers of subjects drawn mainly from high risk groups. These studies also rely on accidental exposure to allow evaluation of outcome (Flynn *et al.*, 2005). Moreover, there is currently no vaccine that can completely protect against HIV-1 infection (Graham & Mascola, 2005; Stahl-Hennig *et al.*, 2007a). There is need for more studies to evaluate other potential candidate vaccines using alternative study designs. The frequently measured outcome variable of pre-challenge vaccine efficacy testing is the elicitation of antigen-specific immune responses (Casimiro *et al.*, 2003b). However, viral load is the main read-out for vaccine efficacy after challenge. Hence, the specificity of the vaccine-elicited immune responses is usually assessed *ex vivo* using viral peptides. This approach does not however, allow determination of how these vaccines can affect a replicating virus after infection exposure. An *ex vivo* model that mirrors the virus-host cell interaction prior to infection of the host would provide an important interface for both pre-clinical and clinical trials. This study was designed with the hypothesises that variations in susceptibility to infection by SIV is due to intrinsic host differences, and that vaccination may or may not alter the capacity of host cells to replicate SIV *ex vivo*. The hypothesis was used to develop an *ex vivo* model that can be used to determine intrinsic (host) factors associated with the variable course of disease and to assess how this model can be applied to the assessment of vaccine efficacy before challenge and prediction of *in vivo* infection outcome.

1.4 Study Objectives

Overall Objective

To develop a surrogate pre-clinical HIV-1 vaccine model that can be used for testing and quantifying vaccine efficacy *ex vivo* and which can be used to predict *in vivo* outcome following challenge with a pathogenic strain of simian immunodeficiency virus.

Intermediate Objective 1

To develop an experimental model for determination of virus replication kinetics and examining antiviral immune responses *ex vivo*

Specific Objectives

1. To determine the effect of vaccination on susceptibility to SIV and virus replication kinetics *ex vivo*.
2. To compare the levels of vaccine-mediated induction of IFNγ *ex vivo* and CNAR *in vitro* and how they affect *ex vivo* virus replication
3. To examine the influence of MHC alleles on susceptibility to infection *ex vivo*

Intermediate objective 2

To examine the protective efficacy of a DNA-prime and rAd5SIV-boost vaccine against pathogenic Simian Immunodeficiency Virus infection of rhesus macaques.

Specific objectives

4. To examine the protective efficacy of immunization against SIV-challenge
5. To examine longitudinally, the profile of vaccine-elicited effector immune responses after infection
6. To assess the effect of immunization on plasma SIV RNA load
7. To assess the influence of immunization on memory CD4+ T-cell profiles
8. To examine the influence of MHC alleles on protection from challenge virus *in vivo*

Intermediate objective 3

To investigate the profile of cytokine secretion during *ex vivo* infection with SIV

Specific objectives

9. To determine the kinetics of cytokines and chemokines secreted in *ex vivo* infected cultures
10. To determine the associations of α- and β-chemokines and cytokines with virus replication *ex vivo*

Intermediate objective 4

To demonstrate the predictive capacity of the pre-challenge *ex vivo* model for *in vivo* outcomes of infection after SIVmac239 challenge

Specific objectives

11. To investigate whether intrinsic susceptibility *ex vivo* predicts viremia after challenge
12. To investigate whether intrinsic susceptibility *ex vivo* predicts preservation or loss of memory CD4+ T-cells after challenge
13. To analyse which chemokines/cytokines are associated with susceptibility to infection and protective efficacy of immunization post-challenge

2.0 MATERIALS AND METHODS

2.1 General Methods

2.1.1 Immunogens

The vaccine vectors used in this study were constructed and prepared by the Institute for Molecular and Life Sciences, Pohang University of Science and Technology, Republic of South Korea. The protocols detailing construction of these vectors and adjuvants have been described previously (Stahl-Hennig *et al.*, 2007b; Suh *et al.*, 2006), and were not part of the present study. Respective viral genes for the DNA vaccines were carried in a pGX10 plasmid vector. In brief, a typical pGX10-SIV/Gag-Env construct was obtained by inserting the *Gag-Env* gene of pTX GE (Fig. 2.1.1) into the plasmid vector (Lee *et al.*, 1999). The construction of recombinant adenoviruses expressing SIV and adjuvant genes (SIV *Env*, *Pol*, *Vif-Nef* and *Tat-Vpx*) was earlier accomplished by cloning each gene into the pShuttle-CMV (Qbiogene) vector followed by insertion by homologous recombination into pAdEasy-1 (E1/E3-deleted human adenovirus serotype 5 viral DNA (Qbiogene). The rAd-Gag-Pol containing synthetic (codon-optimized) *gag/pol* genes were kindly provided by Prof. Dr K. Überla, Ruhr University Bochum, Germany. The immunostimulatory peptide (Try-Lys-Tyr-Met-Val-D-Met) has been described elsewhere (Lee *et al.*, 2005).

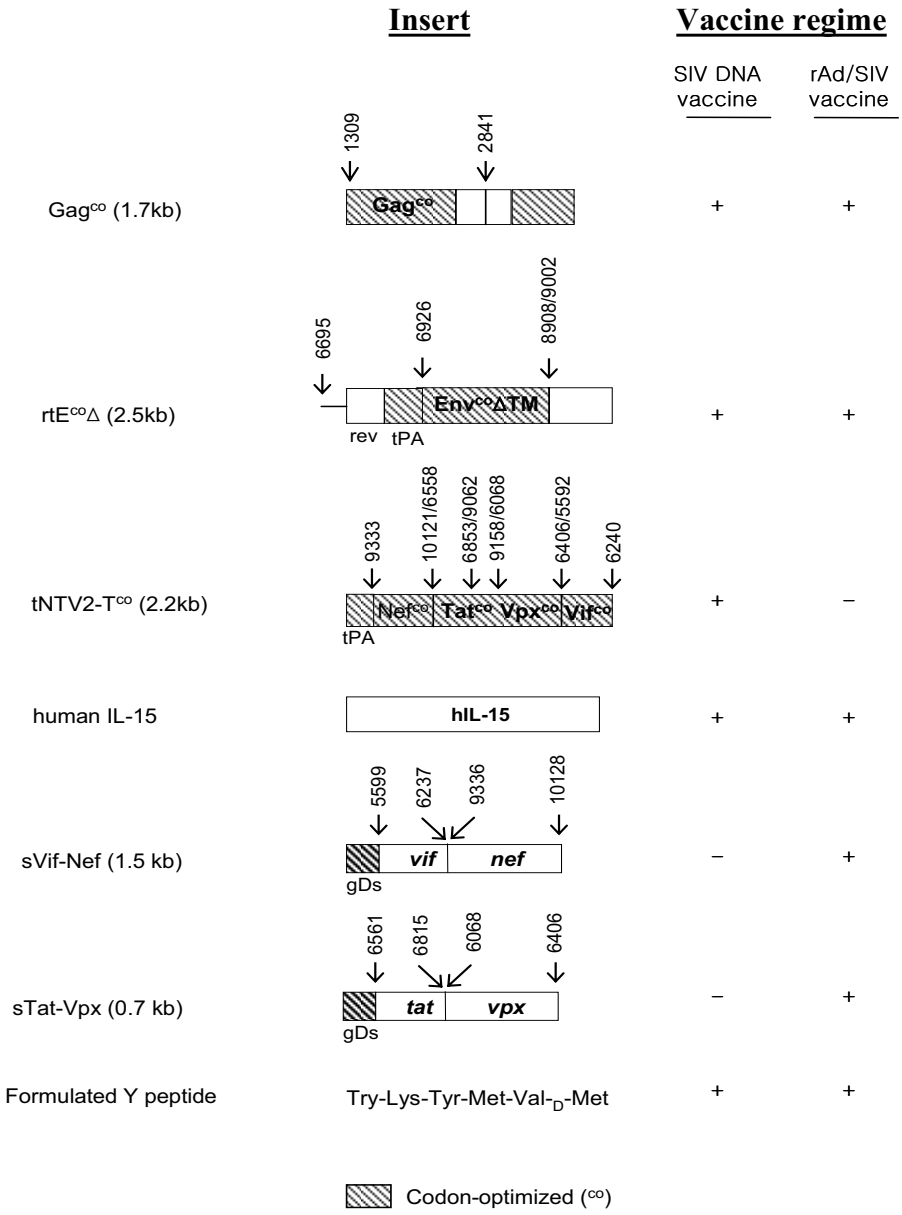

Figure 2.1.1: Vaccine inserts used in the two vaccine regimens

'co' stands for codon optimized; 'E' represents *env*; tPA, Tissue Plasminogen Activator; *E^co/Env^co* refers to codon optimized envelope; *rtE^co*Δ stands for a *rev-tPA* sequence in which the original *env* sequence was replaced by a tPA signal sequence to enhance the secretion of env. ΔTM stands for a truncated transmembrane. *Env^co*Δ*TM*; Codon optimised envelope lacking the TM protein. Deletion of TM was to enhance secretion ability env. sVif-Nef/gDs; signal sequence of herpes simplex virus (HSV) glycoprotein D (gD) (s=gDs). This modification enhances secretion and expression. + and – shows that this segment was either included in or excluded from respective vaccine regime.

2.1.2 Experimental animals and design

All SIV-infected animals were housed at the German Primate Centre (GPC) according to the German animal protection Act and in compliance with the European Union guidelines on the use of non-human primates for biomedical research. Animals were handled by the veterinarians and animal keepers of the GPC's department of virology and immunology. 18 rhesus monkeys of Indian origin were recruited into 3 experimental groups comprising 6 animals each. The groups consisted of animals that were sham-vaccinated with various vaccine buffers (control group). The other two vaccine groups received thrice DNA plasmid administered systemically weeks 0, 8 and 12 before twice boosting with rAd5-SIV at week 24 and week 32. The prime vaccine consisted of codon-optimised SIV *gag-prt*, *env*, *nef-tat-vpx-vif* DNA (1.5mg/construct) and was co-delivered with human IL-15 DNA (1.5 mg/construct) and 1 mg of the immunostimulatory peptide. The boosting consisted of a replication-incompetent recombinant adenovirus type-5 (rAd5) vector expressing various SIV proteins (rAd5-SIV) co-delivered with Ad5IL-15. One of these two groups received the boost regimen first orally ($1x10^9$ pfu/construct) then systemically ($2x10^9$ pfu/construct) (Mucosal group) while the other received the boost twice systemically (Systemic group) respectively at week 24 ($1x10^8$ pfu/construct) and week 32($2x10^9$ pfu/construct). After 44 weeks of immunization, all 18 animals received an oral challenge virus exposure at $1x10^5$ $TCID_{50}$ of the SIVmac239 strain. Fig.2.1.2 summarises these immunization schemes.

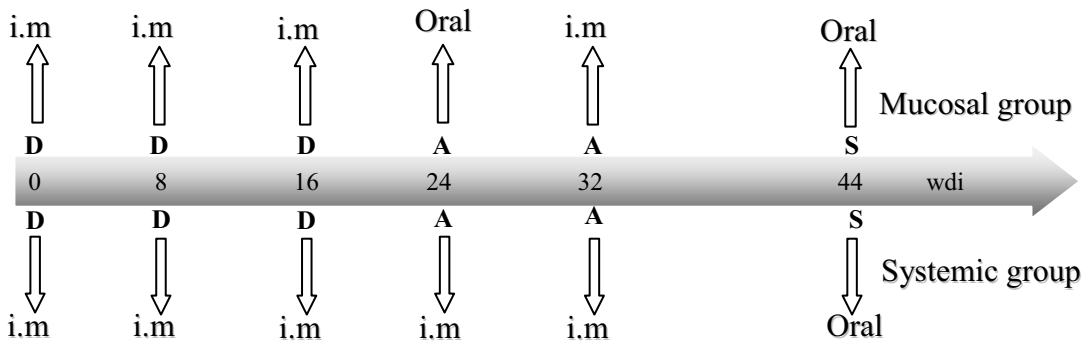

Figure 2.1.2: Flow-chart of immunization scheme showing the time-points of respective vaccine administration and challenge

Key: i.m, intramuscular; A, rAd5-SIV boost; D, DNA priming; S, SIVmac239 challenge. Arrows indicate the corresponding time-point (also indicated by numerical units in the blue bar); wdi, weeks during immunization.

2.1.3 Follow-up before and after challenge

Two exceptions applied during the follow-up. First, one animal from the control group was lost to immunization follow-up had to be replaced at week 42. Data from the replacement animal was only available after challenge and not for *ex vivo* experiments. Consequently, a description will be made for only 17 animals when describing the *ex vivo* model experiments or when comparing across the two (*ex vivo* and *in vivo*) models, whereas all the 18 animals will be included in the *in vivo* experiments. During the 44 weeks of immunisation, blood samples were obtained every 2-4 weeks and used for peripheral blood mononuclear cell (PBMC) preparation. The PBMCs were used for *ex vivo* quantitation of INFγ producing cells by enzyme-linked immunospot (ELISPOT) and to determine the *ex vivo* virus replication kinetics (VVR). In addition, culture supernatants obtained from the VVR assay were used for virus suppression and cytokine assays as described under the respective sections of the methods chapter. After challenge, EDTA blood was collected every 2-4 weeks and used for PBMC and plasma preparations. These PBMCs were used for INFγ ELISPOT and flow cytometry assays while the plasma was used for SIV RNA load analyses.

2.1.4 Preparation of Peripheral Blood Mononuclear Cells

PBMCs were isolated from 6-12 ml venous blood using Ficoll-Hypaque density gradient centrifugation. Ficoll-laid blood was centrifuged at 2200 rpm for 25 minutes at 10°C. The buffy layers containing cells were carefully transferred into new 15 ml centrifuge containing 10 ml PBS (pH 7.2) and washed twice at 1200 rpm 20°C and 10 minutes. Cell counts were determined during the second wash step using a 1:10 (in PBS) diluted aliquot laid on a haemocytometer (Neubar, Germany). The cells were used immediately for *ex vivo* infections and excess transferred to medium containing 10% dimethylsulphoxide (DMSO), 70% FS and 20% RPMI and frozen in liquid nitrogen.

2.1.5 Preparation of virus stock for *in vitro* infections

CEMx174 cell-lines were infected with 1:10 dilution of a SIVmac239-nef-open stock. The final amount of cells used per infection was 15 million. The cells were incubated with the virus at 37°C for 1.5 hours (hrs) then re-suspended at a density of $5x10^5$ cells/ml in RPMI-1640 medium containing 10% FBS and 1% penicillin/streptomycin (R-10 medium). The cells were allowed to grow for 24 hrs at 37°C in a 5% CO_2 humidified chamber before replacing the entire medium with fresh R-10 medium in order to wash out residual virus. Cell-culture supernatant at day 6 (medium syncitia) and day 7 (peak syncitia) were pooled, 0.45μm filter sterilised and frozen at -80°C in 1 ml portions in 2ml cryo-tubes. Portions of this stock were used for virus titration to determine the 50% tissue culture infectious dose ($TCID_{50}$).

2.1.6 Virus titration

For the determination $TCID_{50}$, virus titration was performed on highly susceptible freshly growing C81.66 cells. 30,000 cells were seeded to each well of a 96-well plate in 50μl R-10 medium. To each well was added in 8 replicates, 100μl of 10-fold serially diluted virus stock. Medium-only wells were included as negative controls. These were maintained in culture for 4 days after which 50μl of fresh R-10 medium was added and incubated till day 7. After 7 days, the virus titre was

determined using an indirect immunoperoxidase assay (IPA) protocol for intracellular antigen staining.

2.1.7 Indirect Immunoperoxidase Assay.

96-well plates were equilibrated with 200 µl R-10 medium at 4°C overnight or for 1hr at room temperature (RT). The plates were coated thereafter with 50µl/well of Concanavalin-A (Con-A) at a concentration of 0.5mg/ml in PBS and incubated for 1hr at RT and either used immediately or frozen at -20°C till needed. Using a multi-channel micropipette, cells from the 'virus titration' assay were re-suspended and 200µl transferred to the respective Con-A-coated plates and incubated at 37°C in a thermostated room. Plates were then decanted and cells permeabilised by immersion in methanol that was pre-equilibrated at -20°C, then incubated for 15 minutes or overnight at -20°C. Methanol was removed, plates carefully washed (x3) in cold PBS and blocked with 100µl/well of 2% milk powder (MP) (prepared in PBS) at RT for 30-60 minutes. MP was discarded and plates incubated at 37°C for another 30-60 minutes with 50µl/well of a 1:3000 diluted (in MP) polyclonal SIV anti-serum from a chronically infected macaque (SIV.S 1604, DPZ). Another washing was followed by similar incubation with 50µl/well of 1:1000 diluted anti-human IgG-HRPO conjugate, washing and a 4-10 minutes substrate reaction in 50µl substrate solution (2mg AEC, 300µl DMF, 25µl of 3% H_2O_2 and 5ml sodium acetate). The reaction was stopped by twice washing in PBS before adding 50µl/well of PBS. Plates were examined immediately for stained cells under an inverted light microscope. The $TCID_{50}$ was scored using the Reed and Muench method as described elsewhere (Fridholm & Everitt, 2005; LaBarre & Lowy, 2001).

2.2 *Ex vivo* susceptibility assays

2.2.1 Infection of peripheral blood mononuclear cells

During prospective weeks of immunisation starting from week zero before immunization through 44 weeks, PBMCs were obtained from citrated blood as described under the general methods section. To determine the differential

susceptibilities of these PBMCs to infection by SIV, the cells were incubated with SIVmac239 stock at a multiplicity of infection (MoI) of 0.0032 TCID50. To achieve this MoI, the original virus stock of $10^{5.5}$ TCID50 was diluted 1:10 in RPMI containing 10% foetal bovine serum (FBS) and 1% penicillin/streptomycin (R-10 medium). 1 ml of diluted virus was used to infect 10 million cells at room temperature for 1.5 hrs with gentle swirling every 15 minutes. After incubation, cells were washed 3-times with 10 ml PBS, (pH 7.2) by centrifugation at 1200 rpm for 10 minutes. After removing the wash-outs, cells were re-suspended at a density of 2 million/ml in RPMI containing 20% foetal bovine serum (FBS), 1% penicillin/streptomycin and 100 units/ ml IL-2 (R-20+ medium). These were transferred into tissue culture flasks and incubated at 37ºC in a 5% CO_2 humidified chamber. Every 2 to 3 days, the cells were replenished with fresh R-20+ medium by replacing half of the old medium with fresh one to maintain the same cell density. On day 5, 7 and 10, culture supernatants were aliquoted and frozen at -80 ºC for subsequent analyses. The capacity of these cells to replicate the virus was monitored by real-time reverse transcriptase PCR (RT-RT-PCR) amplification of cell-free viral RNA in culture supernatant.

2.2.2 Preparation of DNA Plasmids for PCR standards

pSTBlue plasmids containing a 349 bp SIV*gag* insert (Novagen, Madison, WI) were used to transform TOPO-10 *E. coli* cells which were then plated onto Kanamycin selective plates. The SIV insert had previously been ligated into the vector using a perfect Blunt cloning kit. Except for a slight modification (omission of a starter culture step), the plasmids were amplified and purified using QIAfilter Plasmid Midi Kits following the manufacturer's protocol (Qiagen, Germany). A single colony from freshly streaked plates was picked and inoculated into 200 ml LB medium containing the same selective antibiotic and grown for 12-16 hrs at 37ºC with vigorous shaking (ca. 300 rpm). The bacterial cells were subsequently harvested by centrifugation at 6000g for 15 minutes and re-suspended in 10 ml buffer P1 containing RNase A. Complete lysis was achieved by adding another 10 ml buffer P2 and incubating at room temperature (RT) for a maximum of 5

minutes. After incubation, 10 ml of pre-chilled buffer P3 was added to the lysate, mixed by inversion and poured into a barrel of the QIAfilter Cartridge before leaving to stand at RT for 10 minutes. The cell lysates were then filtered into a QIAtip pre-equilibrated with buffer QBT. After 2 x 30 ml buffer QC wash-steps, DNA was eluted with 15 ml buffer QF. A sample from each of the wash and elution steps was analysed on an agarose gel to confirm recovery. DNA eluate was precipitated in 10.5 ml (0.7 volumes) of RT isopropanol and centrifuged immediately at 15,000g (9000 rpm, Beckman JS-13 rotor) for 30 minutes at 4ºC. After decanting the supernatant, the DNA pellet was washed in 5 ml of RT 70% ethanol at 15,000g for 10 min and supernatant discarded. The pellet was air-dried and re-dissolved in 500 μl TE buffer, pH 8.0. Plasmid DNA was quantified and purity determined spectrophotometrically at 260nm.

2.2.3 *In vitro* transcription and preparation of RNA standards for PCR

Before *in vitro* transcription, presence of the SIVgag insert in the DNA plasmid was confirmed by double digestion with Bam H1 and EcoR1 restriction enzymes. Otherwise, only Bam H1 was used to linearise the plasmid ahead of *in vitro* transcription. A typical Bam H1 restriction digest was set up in a 20 μl reaction as follows;

- ✓ 3 μg plasmid
- ✓ 4 μl of 10X Y^+/Tango buffer (contains BSA) (MBI Fermentas)
- ✓ 14 μl RNAse-free water
- ✓ 0.5 μl (5 units) Bam H1 (MBI Fermentas)
- ✓ Made up with H_2O to 20 μl

These were quick-touch spun (2-5 sec) and incubated at 37ºC on a stationary dry heat block for 1 hr. The reaction was stopped by adding a fifth volume of DNA loading dye (50% glycerol + 50mM EDTA pH 8.8, 0.05% bromophenol blue). To confirm linearity, these were loaded onto a 1% Seakem LE agarose gel (CAMBREX Bio Science Rocklands, ME, U.S.A) containing 5-6% ethidium bromide, electrophoresed at 150-170V for 30 min, visualised under UV and photographed. For the *in vitro* transcription, the linearised DNA plasmid was used

to generate single stranded RNA using the SP6 RiboMax™ large-scale RNA production System (Promega). The assay was conducted as described in the by the manufacturer. A typical reaction set-up is indicated in table 2.2.1.

Table 2.2.1: Components of the SP6 *in vitro* transcription reaction

SP6 Reaction Component	*Sample Reaction*	*Control Reaction*
SP6 transcription buffer (5X)	20 µl	4 µl
25mM rNTPs (ATP, CTP, GTP, UTP)	20 µl	4 µl
5 µg linear DNA template plus	50 µl*	1 µl (control DNA)
Nuclease-free water		1 µl (water)
SP6 enzyme mix	10 µl	2 µl
Final volume	100 µl	20 µl

*This volume includes in-put DNA template. 25mM rNTP mix was generated by mixing equal volumes of 100mM of the individual rNTP.

After mixing, the reactions were incubated for 3 hrs at 37ºC. At the end of transcription reaction, residual DNA template was removed by DNase digestion. To do this, RQ1 RNase-free DNase was added to the reaction tubes at a final concentration of 1u/µg of template DNA and incubated for 15 minutes at 37ºC. This was followed by extraction with citrate-saturated phenol:isoamyl alcohol (25:1, Sigma). The mixture was vortexed and spun at top-speed (14,000 rpm) for 2 minutes. The upper aqueous phase was transferred to a fresh tube and mixed with 1 volume of chloroform:isoamyl alcohol (24:1) and centrifuged as before. After transferring the upper aqueous phase to a new tube, the tubes were quick-spun for 10 minutes in a microcentrifuge to remove carry-over chloroform. The bottom phase containing RNA was removed with a micro-pipette and precipitated with 0.1 volume of 3M sodium acetate (pH 5.2) plus 1 volume of isopropanol for 1 hour at 20 ºC. These were centrifuged for 10 minutes at top-speed and the supernatant carefully decanted or aspirated. The pellets were washed once with 1 ml of 70% ethanol and left to dry at room temperature. Dried pellets were re-suspended in nuclease-free water to a volume equivalent to that of the transcription reaction and stored at -70ºC till needed. To generate RNA standard for quantitative RT-PCR, RNA products of *in vitro* transcription were serially

diluted to produce 50, 10^2, 10^3……10^8 SIV RNA copy equivalents per titration. To arrive at the respective RNA copy equivalents, the following conversions were used:

X= N/ (MWtI+5 x 10E+6) = molecules/μg

X= SIV RNA molecules/microgram transcribed RNA (=RNA copies/μg)
N=Avogadro's number
MWtI= Molecular weight (g/mole) of the transcript containing SIVgag insert plus the region upstream of SP6 transcription start site

- ✓ pSTBlue vector size = 3851 base pairs (bp) (see appendix)
- ✓ SIVgag insert = 349 bp
- ✓ SP6 polymerase transcription start site = 90 bp upstream of gag
- ✓ Final length of transcript = 349+90 = 439
- ✓ Avogadro's number = 6.022E+23
- ✓ Molecular weight of RNA = 340 Daltons/base
- ✓ 1 Dalton = 1 gram/mol

MWtI = 340 x 439 bp = 1.493E+5 grams/mol = 6.022E+23 molecules/g transcript. Hence, 1.493E+5 grams of transcript contain 6.022E+23 SIV RNA molecules. These were converted into molecules/microgram RNA as

X= (6.022 x 10^{23})/ (1.493E+5 x 10E+6) = molecules/μg

For this assay, a total of 1.732 μg/μl RNA was purified after *in vitro* transcription. This was diluted to an 'X'-equivalent of 10x10^{10} RNA molecules in RNase-free water containing 30 ng/μl t-RNA (for stabilization) and was used as the starting point in the dilution series to generate required RNA standards. The standards were frozen at -80ºC into single freeze-thaw aliquots of 15 μl. This protocol has also been described elsewhere (Hofmann-Lehmann *et al.*, 2000).

2.2.4 Isolation of viral RNA for quantitative PCR

Viral RNA was isolated from frozen PBMC culture supernatants using QiaAmp RNA mini Columns (Qiagen, Germany) following manufacturer's protocol. Briefly, samples were thawed and clarified of cryoprecipitate by centrifugation at 8000 rpm for 3 minutes. 140μl of clarified supernatant or plasma was lysed for 10

minutes in 560 μl buffer AL and precipitated in an equal volume of absolute ethanol before loading onto Qia-spin columns. Viral RNA was successively washed on-column with respective buffers and eluted in 60 μl buffer AVE. Post-challenge plasma viral RNA was extracted and quantified centrally as part of the core vaccine trial by colleagues. This was done from frozen plasma using the MagAttract Virus Mini M48 kit (Qiagen GmbH). Briefly, plasma samples were thawed and clarified of cryoprecipitate as before. 200 μl of this sample was pipetted into a 2 ml tube and placed onto the M48 BioRobot work-station for automated RNA isolation following pre-defined instrument protocol. A typical RNA extraction procedure involved initial lysis of the samples in the presence of protease and buffer AL. Lysed samples are suspended in MagAttract suspension B (contains magnetic particles) and isopropanol, upon which viral RNA binds to the particles. This is followed by magnetic separation on the BioRobot workstation, successive washing in buffer AW1, AW2 and ethanol. The final stage includes a magnetic separation and elution in buffer AVE. for this protocol, RNA was eluted in 75 μl buffer. Purified SIV RNA was quantified using TaqMan-based real-time PCR on an ABI-Prism 7500 sequence detection system (ABI) and in the presence RNA standards prepared as previously described.

2.2.5 Quantitative Real-time Reverse Transcriptase PCR

Purified SIV RNA was quantified using TaqMan-based RT- PCR on an ABI-Prism 7500 sequence detection system (ABI) and in the presence of RNA standards prepared as described above. The reaction mixes (table 2.2.2) were subjected to PCR cycles as follows: reverse transcription, 50 ^{o}C, 30 min.; activation, 95 ^{o}C, 15 sec.; 45 cycles of denaturation (94 ^{o}C, 15 sec.) and annealing/extension (60 ^{o}C, 60 sec). Data acquisition was conducted during annealing/extension steps. Amplified RNA was expressed as SIV-RNA copies/ml culture supernatant or plasma. Each PCR included a non-template control. The primers used for this assay have been described elsewhere (Hofmann-Lehmann *et al.*, 2000), and are as listed under the appendix section.

Table 2.2.2: Typical RT-PCR reaction master mix showing various components, volumes and concentrations.

Component	*Volume (μL)*	*Final concentration*	**Source**
2X master mix, no AmpErase UNG	12.5	1X	Applied Biosystems
10 μM SIVgag forward primer	0.75	300 nM	Biomers GmbH
10 μM SIVgag reverse primer	0.75	300 nM	Biomers GmbH
10 μM TaqMan Probe	0.5	200 nM	Biomers GmbH
40X Multiscribe (10 U/μl) with		0.25 U/μl	
RNase inhibitor mix (16 U/μl)	0.625	0.4 U/μl	Applied Biosystems
RNAse free water	1.375		Applied Biosystems
RNA	8.5	…….	
Final volume per reaction	25		

2.3 SIVgag-specific IFNγ ELISPOT assays

IFNγ ELISPOT response assays were conducted by the animal models group of the DPZ as part of the overall vaccine trial. These data were provided by Dr. Stahl-Hennig and Dr. Suh You-Suk for purposes of comparison with *ex vivo* experiments described in this study. Briefly, PBMCs obtained from weeks 0, 12, 26 and 44 during immunization were isolated as described in the previous sections and used for the ex-vivo determination of IFNγ responses by ELISPOT. A monoclonal anti-IFNγ antibody diluted to 10 μg/ml in sterile 0.2 μM-filtered 0.1M carbonate-bicarbonate buffer was coated onto 96-well polyvinylidene difluoride (PVDF) plates (MAIPS4510, Millipore) at a volume of 100 μl/well and kept overnight at 4°C. After removal of coating antibody, plates were washed with PBS, blocked with 0.2 μm-filtered R10 medium containing 2 mM L-Glutamine+antibiotics (Gibco) and incubated at 37°C, 5% CO_2 for 2 hrs. Upon removal of blocking solution, 50 μl of fresh PBMC suspensions were seeded in triplicate wells at a final density of 200,000 cells/well and stimulated with 50 μl of the following antigens; (i) PMA+ionomycin (50 ng/ml + 1 μg/ml), (ii) SIV gag (gag p11C, C-M) or a pool of 15-mer SIV gag peptides (EVA7066.1-3, CFAR, UK) at a final concentration of 5 μg/ml for each peptide, (iii) an irrelevant peptide pool (5 μg/ml each) and (iv) medium alone as control. After a 16-hour incubation in a

low-evaporation lid in a CO_2 chamber, the plates were washed with PBS/0.05% Tween-20 and incubated as before for two hrs with 100 μl/well biotinylated detector antibody (MABTECH) diluted 1:1000 in PBS/0.5% filtered FCS. Following streptavidin-alkaline phosphatase and BCIP/NBT substrate reaction, the plates were washed and air-dried. IFNγ-producing cells were counted using a Bioreader®-3000 (Bio-Sys GmbH, Karben, Germany). Counts were normalised to background signal of medium alone plus in-put cells and reported as the number of spot-forming units (SFU)/10^6 PBMCs. Positive samples had to yield greater than 100 SFU above background and twice the signal of the medium control.

2.4 CD-8+ T-cell non-cytotoxic antiviral response (CNAR) assay

Cell culture supernatants from 7 and 10 days post *in vitro* infection (dpi) of immunization week 26 and 44 were depleted of the virus by centrifugation at 14,000 rpm for 1 hour at 4°C. Thus treated supernatant (ΔSUP) were aliquoted and frozen at -20°C until needed. For the assay, TZM-bl cell lines expressing β-galactosidase (kind gift from Prof. Kirchhoff, University of Ulm; originally from NIH) were plated onto 96-well flat-bottomed culture plates (Sarstedt, Newton NC) for 24 hrs at a density of 9,000 cells/well in Dulbecco's Modified Eagle's Medium (DMEM) containing 10% FBS + 1% penicillin/streptomycin (DMEM+). Before infection, a pre-infection stock was prepared to obtain a $2x10^4$ $TCID_{50}$ by diluting the original SIVmac239 stock in DMEM+. An infection cocktail was made by pre-incubating 48μl of the pre-infection stock with 60μL ΔSUP for 60-90 minutes at 37°C in a CO_2 chamber. This pre-incubation cocktail comprising the virus and cell culture supernatant contained an equivalence of 960 $TCID_{50}$ of SIVmac239. To this was added 20 μg (in 12 μl volume) of di-ethyl-amino-ethyl-dextran (DEAE) just before infection. Positive controls were similarly prepared but with DMEM+ instead of ΔSUP and cells plus medium as negative control. ΔSUP pus cells acted as background. Upon discarding the medium, 50 μl of the final infection cocktail was added to respective wells in duplicate or multiples of eight

for control wells. These were allowed to adsorb for 2 hrs at 37°C before adding 150 μl of DMEM+. The plates were incubated for another 42 hrs and stained in X-gal solution (Appendix table 1.1b) as described elsewhere (CAT# 3522; https://www.aidsreagent.org/reagentdetail.cfm?t=cell_lines&id=34). Dark blue stained syncitia-positive cells were counted using a Bioreader®-3000, normalised to medium control and background signal plus the input sample and expressed as infectious SIV titre/ml. The titre was converted to percentage inhibition as described elsewhere (Killian *et al.*, 2005).

2.5 Flow cytometry analyses

To demonstrate if pre-challenge *ex vivo* susceptibility was associated with memory CD4+ T-cells after challenge, data generated in parallel by colleagues in the animal models working group was retrieved and compared with VVR. Specifically, this analysis was done by Reiner Schulte as part of the main vaccine experiment. In brief, whole EDTA blood samples were stained with pre-titrated antibody mix comprising anti-CD3-Alexa700 (clone SP34-2), CD4-Alexa405 (SK3), CD8-AmCyan (SK1), CD95-APC (DX2) CD28 PerCP-Cy5.5 (L293), CD25 PE-Cy7 (M-A251), HLA-DR (L243) (Beckton Dickinson, BD), CD29-FITC (4B4) and CD45RA-ECD (2H4) (Beckmann-Coulter) antibodies. After 20-minute incubation at room temperature, lysis solution (BD) was added for 10 min and tubes centrifuged and washed with PBS/0.5% BSA. Following 10 minutes fixation in 3.5% formaldehyde, samples were pelleted, re-suspended in FACS buffer and measured on a BD LSRII flow cytometer.

2.6 Macaque MHC-class 1 typing techniques

2.6.1 DNA preparation for MHC typing

DNA was extracted from frozen whole blood as follows. 3-5 ml blood samples were left to thaw for about 30 minutes under gentle bench-top shaking. One part of the blood was transferred to 50 ml falcon tubes and mixed with 9 parts of 1X lysis buffer. While on ice, the blood-lysis buffer mixture was transferred to 4°C

and left to stand for 15 minutes with gentle periodic swirling. These mixtures were centrifuged for 15 minutes at 4000 rpm and 4°C, the supernatant removed and cell pellets left for 15 minutes on ice. Depending on size, the pellets were re-suspended in 3, 5 or 10 millilitre final volume of digestion buffer. The pellets were first loosened by vortexing in small amount of ddH_2O and STE before adding SDS and proteinase K solutions (added while gently swirling). These were incubated overnight at 55°C under gentle platform shaking. After incubation, the digest was ice-cooled in a cold room for another 15min before adding 6M NaCl to 1/3 of the digest volume. After thorough mixing and 15-minute incubation on ice, the tubes were centrifuged for 15 minutes, 4000 rpm and 4°C (with level 7 braking). The resulting DNA-containing supernatant (6.5 ml) was carefully transferred into fresh sterile 50 ml falcon tubes containing equal volume of isopropanol. Precipitated DNA was transferred using sterile loops into Eppendorf tubes containing 1 ml 80% ethanol and washed 3 times by centrifuging at 6000 rpm for a maximum of 5 minutes each. A final wash-step was done in 1 ml of 96% ethanol and the wash-out discarded. The DNA pellet was air-dried under a sterile hood and re-suspended in 100-800 μl (depending on size) TE buffer and left to dissolve overnight. Isolated DNA was quantified and checked for purity spectrophotometrically. An $OD_{260/280}$ ratio of 1.7-1.9 was considered sufficient for PCR.

2.6.2 MHC class I locus-specific PCR typing

A PCR master mix was prepared in a final volume of 25 μl to comprise 20 picomole (pmol) each of *Mamu-A*01* forward and reverse primers (VBC-Biotech, Vienna), 4 pmol each of MDRB5′ and 3′MDR (internal controls), 10 mM dNTP, 1x PCR buffer, 5μl Q-solution, 0.25μl Taq polymerase, 150 nM of DNA template and water. The individual reactions mixes were heated to 95°C for 3 min followed by 37 PCR cycles of 95°C 30 sec, 64°C 40sec and 72°C 60sec. A final extension was done at 72°C for 2 minutes. For detection, 20μl of the PCR products were mixed with 5 μl sample loading dye, loaded immediately onto a 1.5% agarose gel containing 6% ethidium bromide and electrophoresed at 180V for 50 minutes. A

10 kb DNA marker (5 μl) was included in the gel. The primers used were as described elsewhere (Muhl *et al.*, 2002), and are also listed in the appendix.

2.7 Cytokine assays

Reagents and analytes

Wash buffer (25X)	diluted with distilled water to 1X working concentration
Calibrator Diluent RD5K (2X)	diluted with distilled water to 1X working concentration
Standard Cocktails 1 & 2 (Kit A)	reconstituted each in 1 ml of 1X RD5K (for cell culture supernatants) or in Calibrator Diluent RD6-40 (for plasma/serum).
Standard (Base Kit B)	reconstituted in 1 ml Calibrator Diluent RD5-3 (for cell culture supernatants) or in Calibrator Diluent RD6-43 (for plasma/serum).

Table 2.7.1: Analytes included in the multiplex cytokine bead array test

Analytes	*Bead region*	*Concentration of 1st standard*	*Source*
Base Kit-A analytes			
IFNγ	75	1,900 pg/ml	R & D systems
IL-1β	06	1,600 pg/ml	R & D systems
IL-10	50	2,600 pg/ml	R & D systems
MCP-1/CCL2	78	2,000 pg/ml	R & D systems
MIP-1α/CCL3	59	9,000 pg/ml	R & D systems
MIP-1β/CCL4	74	4,200 pg/ml	R & D systems
RANTES/CCL5	80	2,100 pg/ml	R & D systems
TNFα	77	2,800 pg/ml	R & D systems
Base Kit-B analytes			
IP10/CXCL10	39	2,300 pg/ml	R & D systems

All the reagents for the multiplex assay were obtained from R & D Systems GmbH (Wiesbaden-Nordenstadt, Germany).

2.7.2 Preparation of Standards for the assay

Standards were prepared independently for the human base Kit A comprising 8 cytokines and base Kit B (table 2.7.1). To prepare working standards for the base Kit-A cytokines, each of the two reconstituted standard cocktails were added in

equal volumes of 100 μl to a polypropylene tube containing 300 μl respective calibrator diluents to produce the first standard concentration (table 2.7.1). After mixing, 3-fold serial dilutions were produced to achieve a total of 7 dilution series. To prepare working standard for the CXCL10/IP-10 assay, the lyophilized standard was reconstituted in 1 ml calibrator diluent and used to produce a 3-fold serial dilution of seven standards.

2.7.3 Cytokine bead array: principles of the assay

The cytokine bead array technology uses analyte-specific antibodies which are pre-coated onto color-coded microparticles. These microparticles together with standards and samples are pipetted into wells of the assay plates upon which the immobilized antibodies bind to the analytes of interest. After washing away of any unbound material, biotinylated antibodies specific for the analytes of interest are added to each well. Following a wash to remove unbound detection antibody, streptavidin-phycoerythrin conjugate (Streptavidin-PE) is added to each well to bind the biotinylated detection antibodies. A final wash removes unbound Streptavidin-PE and the microparticles are re-suspended in buffer and read using the Luminex analyzer. The analyzer has two lasers; one is specific for microparticles and determines which analyte is being detected and the other determines the magnitude of the phycoerythrin-derived signal. This signal is directly proportional to the amount of analyte bound and is used to quantify the amount of analytes.

2.7.4 Cytokine bead array: assay procedures

Except for slight modifications, the assay was conducted as described by the manufacturer in the kit protocol. The vacuum suction steps in the wash procedures were all replaced with a centrifugation step as described below. For this purpose, conical-shape plates were used instead of the flat-bottomed filter plates provided with the kits. Before the assay, reagents were brought to room temperature while protected from light. Antibodies, conjugates and microparticles were vortexed to re-suspend and spun down for 30 seconds at ca. 3000 rpm. Culture supernatants from *ex vivo* infection were thawed at room temperature,

centrifuged to remove particulate and analysed without further dilutions. Frozen plasma samples were clarified of cryoprecipitates and diluted 4-fold in buffer RD6-40 before the assay. For a complete 96-well microplate, 50 µl of each microparticle concentrate of the human Base Kit A were added to a mixing reservoir containing 5 ml microparticle diluent. For the CXCL10 assay, the human Base Kit B was used, with reagents reconstituted separately but similarly as for the Base Kit A. These preparations produced a 108-fold dilution of each microparticle of Base Kit A and a 101-fold dilution for CXCL10. Where fewer assays were conducted, all reagents were re-constituted to reflect the number of assay wells. After mixing by vortexing and inversion, 50 µl of respective microparticle master-mixes were added to each well of a microtitre plate. To this was added 50 µl of standard or 50 µl of test samples. Standards were assayed in duplicate. Securely covered with a foil plate sealer, the plates were incubated for 3 hrs at room temperature on a horizontal orbital microplate shaker set at 500 rpm. Before removing plate sealer to wash, plates were briefly centrifuged (4000 rpm, 1 minute) to settle remnant fluids from the plate sealer. Upon removal of plate sealer, 100 µl wash buffer was added per well, thoroughly mixed by pipetting, resealed and centrifuged at 4000 rpm for 5 minute to pellet the microparticles. Supernatant fluid was discarded by decantation over a paper towel, taking care to avoid loss of microparticles. Each time during washing, the microparticles were re-suspended severally (ca. 10-times) by pipetting in and out with a multichannel pipette before the next centrifugation. This wash step was repeated 3-times and is considered here as the standard modified wash procedure. After washing, 50 µl of biotin antibody dilution containing each of the diluted biotin antibody concentrates diluted 106-fold, was added per well and incubated for another 1 hour as before. After the standard wash-steps, plates were incubated for 30 minutes with 50 µl of 1x diluted streptavidin-PE conjugate at similar conditions above. After the last wash, the microparticles were thoroughly re-suspended in 100 µl wash buffer, incubated for 2 minutes in an orbital shaker and analysed within 90 minutes. Analysis was done with the Luminex Integrated System (IS-100) software for LiquiChip Workstation (Qiagen

GmbH, Hilden, Germany). The IS (Luminex Corporation) is a dual laser, flow-based sorting and detection software. Instrument settings for the analysis and data acquisition were as follows: double discriminator gates, 7500 and 15500 for Base Kit A or 6800 and 12800 for Base Kit B analytes; 100 beads (minimum 50 events/bead); sample size, 75 μl; flow-rate, fast. Standard curves were generated using the 5-PL curve fit and used to automatically calculate concentrations of each analyte. Base Kit A and B assays were run in independently using different software template and data acquisition modes.

2.8 Statistical analyses and determination of associations

The main *ex vivo* outcome variables were; SIV RNA (viral) load in culture or VVR, the number of gag-specific IFNγ-producing cells, CNAR and secreted (soluble) cytokines and chemokines. On the other hand, *in vivo* outcomes included viral load in plasma, the number of gag-specific IFNγ-producing cells, gamma inducible protein 10 (IP10/CXCL10) and CD4+ T-cells expressing the memory markers CD29 and CD95. All these variables were categorised as 'scale variables'. Because viral loads never follow a normal distribution, these were first transformed to the base 10 logarithm before computing analyses. Differences among these outcomes between the experimental groups were determined using non-parametric Mann-Whitney's U test. Effect of vaccination on the outcome variables over repeated time-points was analysed using paired sample t-Test. Pearson's correlations statistics were used to assess the associations among variables. Where regression analysis was required to determine the extent of an outcome variable's dependence on an independent variable, normal probability plot was first generated to prove non-violation of a linear association. A correlation producing a p-value of 0.05 or less was considered significant. All statistical analyses and outputs were generated using version 15.0 of the SPSS software.

3.0 RESULTS

3.1 *Ex vivo* susceptibility to SIV infection

SIV causes a fatal AIDS-like disease in rhesus macaques (Murphey-Corb *et al.*, 1986). For this reason, infection of rhesus monkeys and other nonhuman primate species with SIV provides a strategic model for HIV-1 studies. Similar to HIV-infection of humans (Munoz *et al.*, 1995), SIV-infected macaques exhibit different course of disease, and may survive for varied periods before eventual development of AIDS and death (Steger *et al.*, 1998). Macaques that progress rapidly with SIV infection demonstrate persistently high viremia accompanied by lack of virus-specific antibody responses (Dykhuizen *et al.*, 1998). These animals survive for less than 26 weeks (Sauermann *et al.*, 1997). The shared similarities between HIV-1 and SIV infections of their respective hosts have been exploited to model human AIDS vaccine and pathogenesis studies in various monkey species. Initial *in vitro* studies have been conducted to explain the variations in infection and disease profiles observed both in humans and macaques (Goldstein *et al.*, 2000; Seman *et al.*, 2000). Using these infection models, cells were shown to vary in their ability to support virus replication. Subsequent susceptibility studies demonstrated that different cell-types respond differently to HIV infection (Liu & Roederer, 2007). These and other studies support the notion that resistance to infection may be due to other intrinsic or genetic factors. This section examines the hypothesis that susceptibility to infection by SIV is an intrinsic property, and that vaccination may or may not alter the capacity of host cells to replicate SIV *ex vivo*. Because *ex vivo* viral replication kinetics (VVR) provides a way to measure the intrinsic and vaccine induced mechanisms that might limit viral replication, this study was designed to test the hypothesis that VVR correlates with vaccine induced efficacy.

3.1.1 Immunization significantly attenuates *ex vivo* susceptibility to SIV

To first determine whether VVR of individual PBMCs differed between naïve animals, cells from all 17 animals were infected before immunization (0 wdi) and

maintained in culture as described under methods. The kinetics of viral replication between lowest (LoR) and highest (HiR) replicators during *ex vivo* infection varied by >430-fold and >60-fold after 7 and 10 days of infection respectively. (Fig. 3.1.1 A-C). Animals had been assigned to three study groups before this analysis. Those with high or low VVR were evenly distributed between groups resulting in comparable mean baseline VVRs (Fig. 3.1.1 D). To determine if susceptibility changed during successive weeks of immunization, VVRs were followed until 44 weeks (total of 11 months). The individual VVRs of the sham-vaccinated control monkeys remained stable when repeatedly tested over the entire follow-up period (Fig.3.1.2A), asserting invariable intrinsic differences in susceptibility of blood cells to SIV-infection. But the analysis of VVR of all the vaccinees combined revealed striking changes, declining significantly between 0 and 12 weeks during immunization (wdi) after just two DNA immunizations ($p=0.001$) (Fig.3.1.2 B-D). At week 26, two weeks after oral rAD5/SIV boosting of the Mucosal group ($p=0.021$) (Fig.3.1.2 B) or systemic boosting ($p=0.001$) (Fig.3.1.2 C), VVR was significantly attenuated in both groups compared to baseline. This VVR attenuation was more drastic in the Systemic group. At this time, the margin between HiR (animals 2171 & 2180) and LoR (2121 & 2169) was significantly widened, with mean VVR variation of > 930-fold recorded at day 10. VVR measurements were not done two weeks after the second boost at week 36 due to insufficient material. By the day of challenge (DoC) at week 44, the Mucosal group that had now been systemically boosted, experienced further VVR attenuation compared to baseline values ($p=0.011$). Compared to the sham-vaccinated animals, these kinetics translated into significantly lower VVR for the mucosal group on DoC ($p=0.028$) and the systemic group at both week 26 ($p=0.006$) and on DoC ($p=0.045$) (Fig.3.1.2 D). Table 3.1.1 summarises VVR kinetics during the period of follow-up while inter-group differences between the control animals and the two vaccine groups are shown in table 3.1.2.

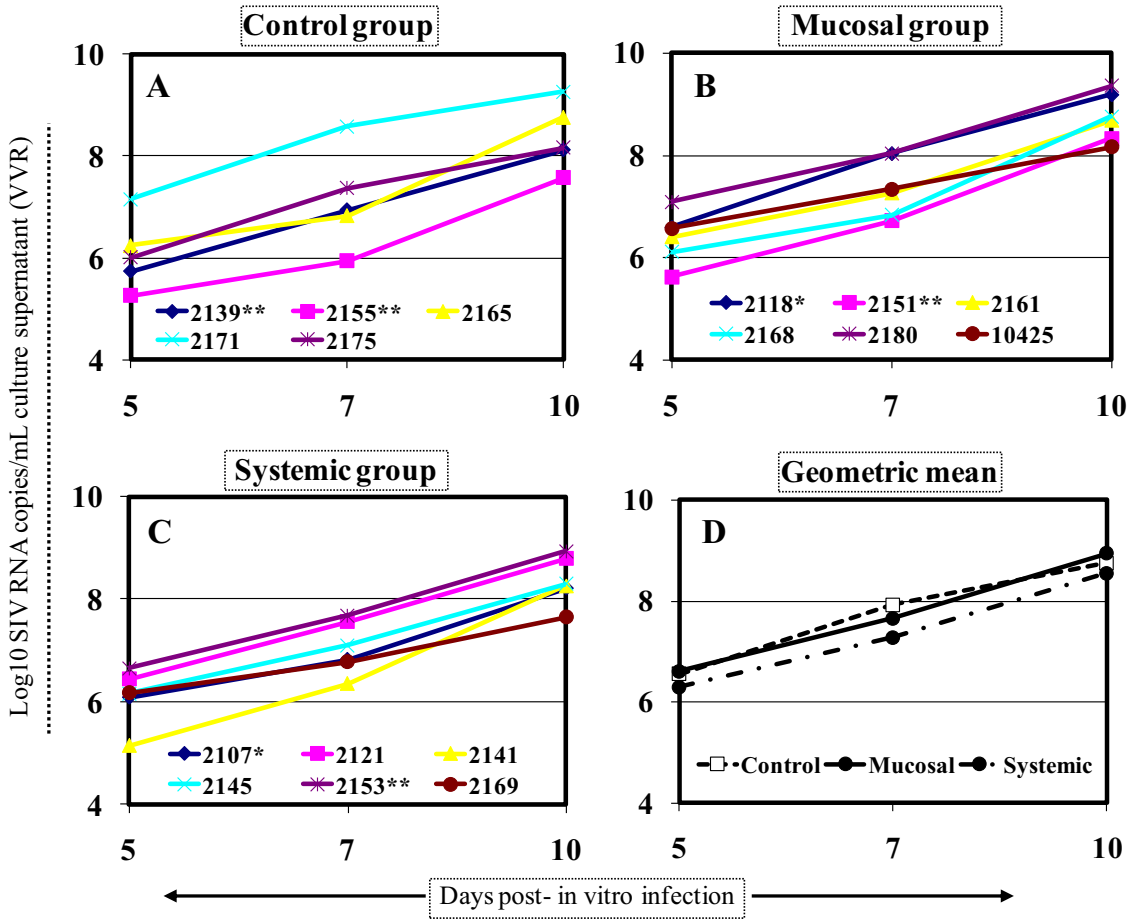

Figure 3.1.1: Susceptibility to SIV and *ex vivo* virus replication kinetics in macaque PBMCs before immunization

This figure shows the kinetics of SIV replication *ex vivo* (VVR) as measured by viral RNA load in infected peripheral blood cell cultures before any immunization was done (0 wdi). Before this analysis, animals had been grouped into respective experimental groups (controls, mucosa and systemic). The Mucosal and Systemic groups were to be immunised later. Inter-individual variations between the highest (HiR) and lowest (LoR) replicators ranged from 430-fold to 60-fold respectively on days 7 and 10 after *in vitro* infection (A-C). The HiR and LoR were evenly distributed among the groups, resulting in similar group kinetics (D). Animals expressing both *-A*01* and *-B*17* MHC-I alleles are indicated by double asterisk (**) while single asterisk (*) indicates animals positive for *-A*01* without *-B*17*.

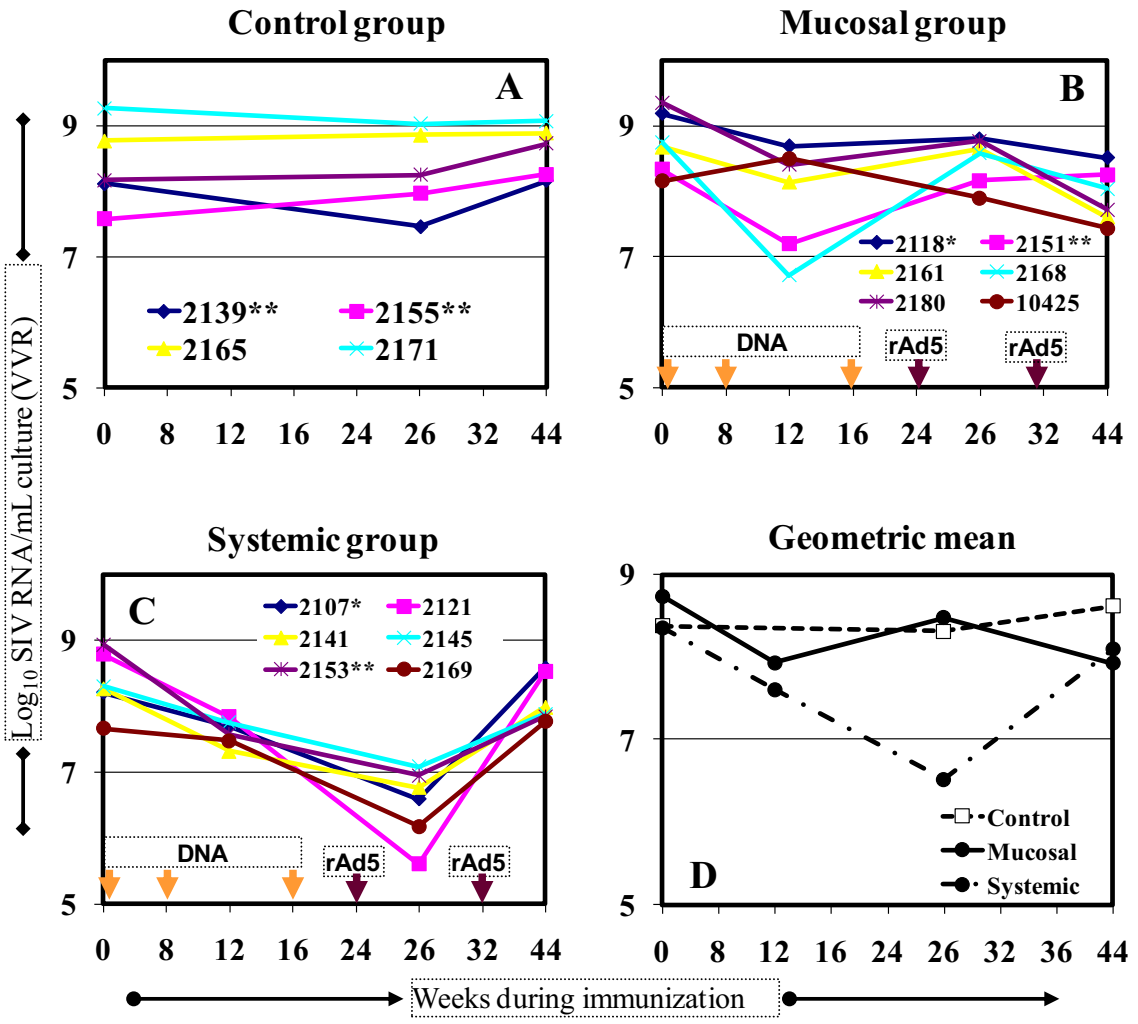

Figure 3.1.2: Longitudinal kinetics of VVR during successive weeks of immunization.
In this figure, viral RNA loads (copies/ml culture) measured 10 days after *in vitro* infection were profiled at successive weeks during immunization. VVR profiles are shown for the controls (A) and for the Mucosal (B) and Systemic (C) vaccine groups. Geometric means are shown in figure D. Compared to baseline, VVR was significantly attenuated week 26 for both the Mucosal and Systemic groups, more so for Systemic group. Only the Mucosal group VVR were still significantly attenuated from baseline on the day of challenge (DoC) at week 44. Those of control animals remained stable over the weeks. These VVRs of the Systemic group were significantly lower than those of controls at 26 wdi ($p=0.006$). VVR of both Mucosal ($p=0.028$) and Systemic ($p=0.045$) groups were lower than for controls on DoC. Immunization; DNA-prime at week 0, 8 and 16; rAd5-SIV boosting at week 24 and week 32. Animals expressing both *-A*01* and *-B*17* MHC-I alleles are indicated by double asterisk (**) while single asterisk (*) indicates animals positive for *-A*01* without *-B*17*. Arrows show points of immunization.

Table 3.1.1: Paired sample t-Test comparing the longitudinal changes in VVR between different immunization time-points

n=6,	*Paired Differences for*		*t*	*Sig. (2-tailed)*
Paired points	*SIV RNA load; Mucosal and (Systemic) groups*			
	Mean	Std. Error Mean		
0 – 26 wdi	0.26	0.08	3.32	0.021
	(1.84)	(0.29)	(6.4)	(0.001)
0 – 44 wdi	0.82	0.21	3.9	0.011
	(0.26)	(0.20)	(1.3)	(0.257)
12 – 26 wdi	-0.54	0.34	-1.58	0.176
	(1.08)	(0.26)	(4.2)	(0.009)

Viral loads in cell culture supernatants (VVR) are compared longitudinally between individual immunization weeks for the Mucosal and Systemic groups. Statistics in brackets are for the Systemic group. A positive 't' indicates a decline while a negative 't' indicates an increase from the previous point. Wdi, weeks during immunization. The column 'Sig.(2-tailed) represent p-values, which are considered significant at 0.05 and below.

Table 3.1.2: Inter-group VVR differences at various time-points of ex *vivo* infection

	VVR of Mucosal and (Systemic) groups compared to control group		
	0 wdi	**26 wdi**	**44 wdi**
Mann-Whitney U	10.0	15.0	3.0
	(12.0)	(0.00)	(4.0)
Z	-.913	0.00	-2.191
	(-0.548)	(-2.739)	(-2.008)
Asymp. Sig. (2-tailed)	0.361	0.465	0.028
	(0.584)	(0.006)	(0.045)

In this table, VVR of sham-vaccinated control animals is compared separately with VR of the Mucosal or Systemic vaccine groups. Statistics in brackets are for the Systemic group Analysis is by Mann-Whitney's U test. A p-value of 0.05 and below is considered significant. Wdi, weeks during immunization.

3.2 Immune Correlates of *ex vivo* SIV suppression

Critical to improved vaccination outcome is limiting initial viral replication and early immune damage (Zhang *et al.*, 2004), preserving CD4+ T-cell memory and deterring chronic-phase CTL dysfunction (Mattapallil *et al.*, 2006). But antiviral activity may not always be associated with cytokine production by T-cells (Chung *et al.*, 2006). Furthermore antiviral activities could still continue without evident cytotoxicity (Walker *et al.*, 1991), while T-cell suppressor activity is prominent during persistent viral infection (Kemball *et al.*, 2005). Since newly recruited T-cells help preserve antiviral CD8+ T-cell function during persistent infection (Vezys *et al.*, 2006), there is a need to explore vaccine strategies that balance between cytolytic and non-cytolytic responses (Geiben-Lynn *et al.*, 2001). Such strategies may help circumvent CTL-induced epitope selection and viral escape (Barouch *et al.*, 2002a; Friedrich *et al.*, 2004), thus widening the breadth of vaccine-elicited immune outcome measurements beyond the current T-cell response paradigms. Though mechanistically not well understood, noncytolytic pathways may involve a CD8+ T-cell antiviral factor (CAF)-mediated CD8+ cell non-cytotoxic antiviral response (CNAR) (Mackewicz *et al.*, 2003). CNAR mitigates viral burden and CD4+ T-cell loss in HIV infection (Castelli *et al.*, 2002; Stranford *et al.*, 2001; Torres *et al.*, 2006), but this has not yet been examined in the context of vaccine trials. This section assesses the vaccine-induced factors that are associated with intrinsic susceptibility to SIV *ex vivo*.

3.2.1 Suppression of SIV *ex vivo* correlates with INFγ-ELISPOT and CNAR

Because vaccination was accompanied by significant attenuation of viral replication *ex vivo*, it was important to assess how the different vaccine-elicited immune parameters were associated with this VVR suppression. This was first done by measuring the levels of INFγ-producing cells *ex vivo* and CD8+ T-cell non-cytotoxic antiviral response (CNAR) activities in culture supernatants. The changes in the profile of INFγ ELISPOT responses during the weeks of immunization are summarised in table 3.2.1.

Table 3.2.1: Paired sample t-Test comparing the longitudinal changes in IFNγ ELISPOT- producing cells between different immunization time-points

n=6	Paired Differences for		t	**Sig. (2-**
Paired points	IFNγ; *Mucosal and (Systemic) groups*			**tailed)**
	Mean	Std. Error Mean		
12 – 26 wdi	7.17	45.67	0.16	0.881
	f	(176.9)	(-3.2)	(0.025)
12 – 44 wdi	-491.5	162.55	-3.02	0.029
	(37.33)	(104.4)	(.36)	(0.735)
26 – 44 wdi	-498.67	160.18	-3.11	0.026
	(598)	(217.6)	(2.75)	(0.040)

Statistics in brackets are for the Systemic group. The two groups received DNA prime vaccine at week 0, 8 and 16. The mucosal group received rAd5-SIV boost orally at week 24 and intramuscularly at week 32. The Systemic group received the same boost intramuscularly at both time-points. A positive 't' indicates a decline while a negative 't' indicates an increase from the previous point. Wdi, weeks during immunization. The column 'Sig.(2-tailed) represent p-values, which are considered significant at 0.05 and below.

Despite vaccinees demonstrating significant reduction in their VVRs 4 weeks after the 2nd DNA immunization (seen earlier in Fig. 3.1.2D), this was not accompanied by any significant rise in INFγ ELISPOT (Fig. 3.2.1 A & B). Similarly the first Ad5-SIV boosting of the Mucosal group resulted in no demonstrable INFγ ELISPOT levels at week 26 (Fig. 3.2.1A). However, INFγ ELISPOT reached peak levels in the Systemic group at this time (Fig. 3.2.1B). These Systemic-group ELISPOT responses at week 26 were significantly above those of the Control or Mucosal groups ($p<0.006$), and appeared at a time when the Systemic group VVR was also significantly attenuated (described in Fig. 3.1.2 A-D). After the second boosting, INFγ ELISPOT peaked 4 weeks later at week 36 for the mucosal group, while those of the Systemic group were not enhanced. On the day of challenge (DoC) at week 44, INFγ of the mucosal group was significantly higher than those of either Systemic or Control animals. At this time, susceptibility to SIV as measured by VVR was correspondingly lowest for the mucosal group compared to either Control or Systemic groups.

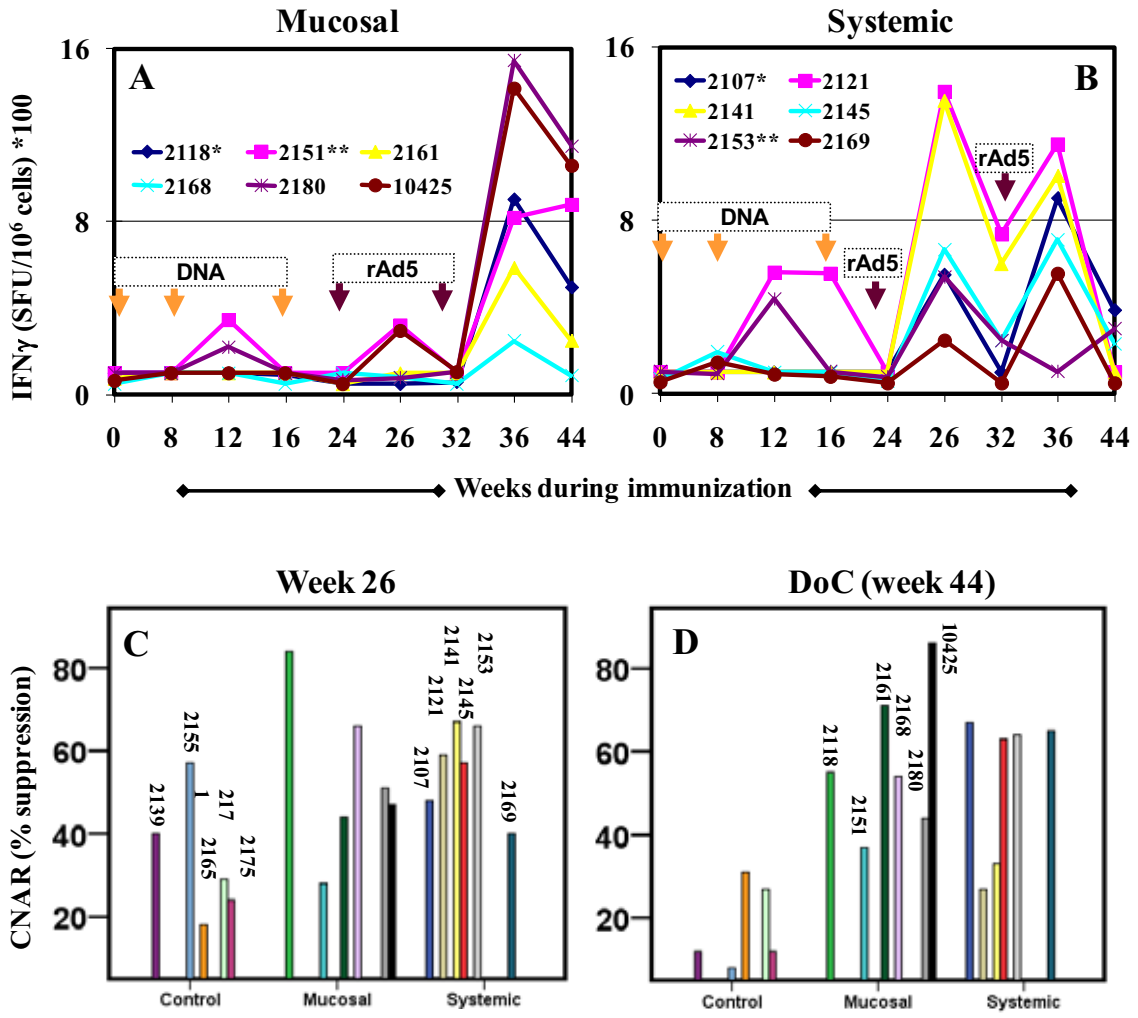

Figure 3.2.1: Profiles of gag-specific IFNγ-producing cells and CD8+ T-cell non-cytotoxic antiviral responses (CNAR) during weeks of immunization.

The number of IFNγ-producing cells was monitored *ex vivo* every 2-4 weeks using ELISPOT. Oral rAd5-SIV boosting of the Mucosal group resulted in lower IFNγ ELISPOT (A) than Systemic boosting that resulted in peak responses at week 26 (B). The second rAd5 boost given systemically for both groups resulted in significant IFNγ for both groups at week 36, peaking for the mucosal group. At week 44, IFNγ levels were still significantly higher for the mucosal group than control animals but diminished for the Systemic group. Similarly, the Mucosal and Systemic vaccine groups experienced significant elevation of their CNAR activities at both week 26 (C) and week 44 (D) compared to controls. These CNAR and IFNγ responses appeared at points where viral replication *in vitro* was significantly compromised (see fig. 3.1.2). Animal identities are comparable in both fig. C and D. Arrows indicate immunization points; rAd5, recombinant adenovirus type-5; DoC, day of challenge. Animals expressing both *-A*01* and *-B*17* MHC-I alleles are indicated by double asterisk (**) while single asterisk (*) indicates animals positive for *-A*01* without *-B*17*.

Next was to investigate whether vaccination mediated VVR suppression through soluble factors. This analysis was conducted selectively for week 26 and week 44 where significant attenuation of VVR was observed. Using a β-galactosidase indicator assay platform, the ability of these cell culture supernatants to inhibit SIV replication via a non-cytotoxic mechanism was examined. Compared to naïve controls, pre-incubation of infecting virus stock with day 7 and day 10 culture supernatants from the VVR assays of week 26 (Fig. 3.2.1C) and week 44 (Fig. 3.2.1D) resulted in increased suppression of SIV replication by supernatants of vaccinees in the TZM-bl/CCR5/β-gal cell-lines. By comparison, the suppression was significantly higher in the Systemic group at 26 wdi ($p=0.028$) and for both Mucosal ($p=0.006$) and Systemic ($p=0.013$) groups on DoC than in the controls (Fig. 3.2.2A). Pearson's correlations were computed to examine whether the VVR attenuation (see Fig. 3.2.2B) was associated with the correspondingly increased INFγ (Fig. 3.2.2C) or CNAR. The number of INFγ-producing cells was significantly and inversely associated with VVR in the individual *ex vivo* infection cultures at week 26 (Fig. 3.2.2D) but not with VVR on DoC (data not shown). On the other hand, CNAR was significantly and inversely associated with VVR both at week 26 (Fig. 3.2.2E) and on DoC (Fig. 3.2.2F). But INFγ was not associated with CNAR (data not shown), suggesting two independent activities. Assuming a linear dose response, regression analyses were computed to determine the extent of VVR dependence on either IFNγ or CNAR (Table 3.2.2). A preliminary normal probability plot confirmed non-violation of the linear model. The resulting ANOVA showed that combined, week 26 IFNγ ELISPOT and CNAR contributed up to 67% ($R^2=0.674$, $p=0.001$) of antiviral activity *in vitro* while independently, IFNγ-producing cells contributed 58% ($R^2=0.579$, $p=0.001$) and CNAR 41% ($R^2=0.405$, $p=0.011$) of this activity. On DoC, VVR was significantly influenced by CNAR and not IFNγ-producing cells.

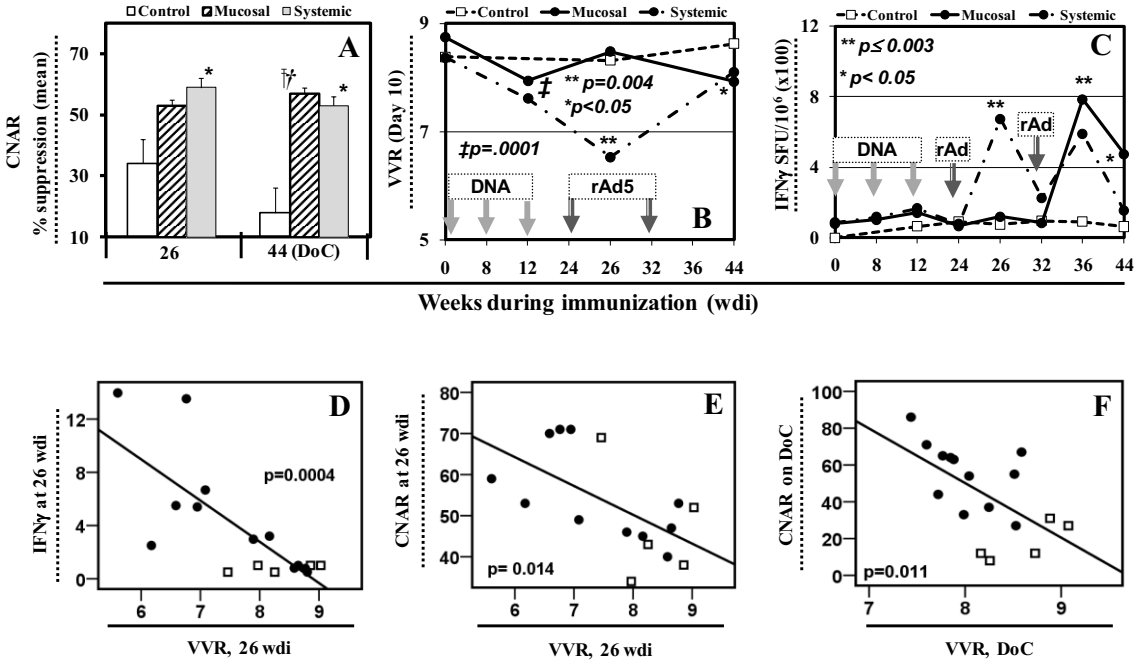

Figure 3.2.2: Associations of IFNγ-producing cells and CD8+ T-cell non-cytotoxic response (CNAR) with VVR.

Open squares, sham-vaccinated controls; closed circles, vaccinees. Compared to controls, CNAR was significantly higher in the Systemic group at week 26 (*p=0.028) and in both the Mucosal (†p=0.006) and Systemic (*p=0.013) groups on DoC (A). Group mean VVR (B) and IFNγ ELISPOT levels (C) are revisited to show points of convergence for VVR suppression and vaccine-induced boosting effects. DNA immunization resulted in significant VVR attenuation at week 12 (B) but not IFNγ responses (C). rAd5 resulted in significant VVR attenuation and IFNγ responses for the Systemic group at week 26 but not for the Mucosal group which however, were significantly boosted on DoC. These IFNγ ELISPOT levels were significantly associated with VVR at weeks 26 (D) but not other points. CNAR at both week 26 (E) and on DoC (F) were significantly associated with VVRs at similar time-points. DoC, day of challenge. ‡Paired comparison between baseline and week 12; DoC, day of challenge.

Table 3.2.2: Analysis of variance showing the dependence of VVR on CNAR and IFNγ

A

ANOVA[b]

Model		Sum of Squares	df	Mean Square	F	Sig.
1	Regression	10.987	2	5.493	12.393	.001[a]
	Residual	5.319	12	.443		
	Total	16.306	14			

a. Predictors: (Constant), % suppression in vitro (CNAR) and IFN gamma ELISPOT

B

ANOVA

Model		Sum of Squares	df	Mean Square	F	Sig.
1	Regression	9.438	1	9.438	17.864	.001[a]
	Residual	6.868	13	.528		
	Total	16.306	14			

a. Predictors: (Constant), IFN gamma ELISPOT

C

ANOVA[b]

Model		Sum of Squares	df	Mean Square	F	Sig.
1	Regression	6.606	1	6.606	8.854	.011[a]
	Residual	9.700	13	.746		
	Total	16.306	14			

a. Predictors: (Constant), % suppression in vitro (CNAR)

b. Dependent Variable: Log SIV RNA load in day 10 cultures

This table shows the results of regression analysis computed with VVR as the dependent variable and CNAR and IFNγ-producing cells as controlling variables either separately or combined. The analysis was conducted for week 26 variables when vaccination significantly lowered VVR for the systemic group. The regression sum of squares shows that the combined effect of both CNAR and IFNγ ELISPOT contributed up to 67% antiviral effect (panel A), while individually, IFNγ ELISPOT (B) and CNAR (D) respectively contributed 58% and 41% antiviral activities at week 26. At week 44, similar analysis showed that only CNAR contributed to the observed antiviral activity (analysis not shown).

3.3 Progression to SIV infection after challenge

Efficacy studies of HIV-1 vaccines support the idea that an effective AIDS vaccine should induce strong, lasting and protective immunity (Malkevitch *et al.*, 2006). Because human efficacy trials require large numbers of subjects and rely on accidental exposure to allow stringent evaluation of outcome (Flynn *et al.*, 2005), pre-clinical studies using SIV are critical requisites for candidate vaccine efficacy testing (Patterson *et al.*, 2004). Existing strategies under evaluation in rhesus monkeys include both the replication-competent adenovirus type-5 (rAd5)

and a replication-defective Ad5 vector expressing SIV proteins (Malkevitch *et al.*, 2006; Shiver *et al.*, 2002). The replication-defective Ad5 vectors have been shown to induce consistently strong and durable immunological responses (Casimiro *et al.*, 2005). A study conducted by the group at the German Primate Centre using this vector showed strong vaccine-elicited SIV-specific IFNγ responses that were associated with significant reduction in post-challenge viremia in macaques (Suh *et al.*, 2006). Since complete protection is still elusive, more studies are needed to evaluate different candidate vaccines. This section examines the capacity priming with DNA and boosting with replication-incompetent Ad5 vector expressing codon-optimised SIV genes to protect rhesus macaques from a pathogenic SIVmac239 challenge. Effects of this vaccine on acute viral load and memory CD4+ T-cells will the discussed.

3.3.1 Immunisation leads to significant control of acute viremia after challenge

Following 11 months of immunization (or sham vaccination) and until 64 weeks after challenge, SIV RNA load in plasma was quantified and compared between individual animals as well as between different vaccine groups. The same was done for IFNγ ELISPOT results. Differences in plasma viremia and IFNγ-producing cells between sham-vaccinated controls and all vaccinees combined are shown in table 3.3.1.1. Compared to controls, immunization resulted in significant reduction of acute viremia of vaccinees 2 to 4 weeks after challenge ($p=0.002$). This relative control of viremia by vaccinees lasted until 12 weeks after challenge. At this time, one rapid progressor in the control group was sacrificed due to AIDS-related symptoms. This loss narrowed the difference in viremia between control and vaccinated animals during the chronic phase.

Table 3.3.1.1: Effect of immunization on viral load and IFNγ-producing cells as determined by comparative analysis between control animals and vaccinees

	Acute-phase		Post-acute-phase			†Chronic
	2 wpc	**4 wpc**	**8 wpc**	**12 wpc**	**8-16 wpc**	***28-64 wpc***
Mann-Whitney U	3.000	2.000	16.000	29.000	26.000	19.000
	(15.0)	(8.0)	(12.0)	(10.5)	(7.0)	(15.0)
Z	-3.091	-3.184	-1.873	-.656	-.937	-.392
	(-1.97)	(-2.62)	(-2.26)	(-2.40)	(-2.72)	(-1.42)
Asymp. Sig. (2-tailed)	.002	.001	.061	.512	.349	.695
	(.049)	(.009)	(.024)	(.016)	(.006)	(.157)

This table tests the differences between control animals (n=6) and vaccinees (n=12) with respect to plasma SIV RNA load and the number of IFNγ-producing cells during weeks of infection. Statistics in brackets are for IFNγ-ELISPOT. The tests were computed using the nonparametric Mann Whitney's U statistics. †Chronic setpoint values for IFNγ are taken as average between 28- 49 wpc for, since data was not available beyond this point. Wpc, weeks post-challenge.

The profiles of plasma viral load are shown for the Control (Fig. 3.3.1.1A), Mucosal (Fig. 3.3.1.1B) and Systemic (Fig. 3.3.1.1C) groups as well as for the group mean (Fig. 3.3.1.1D). Statistical comparisons (data not shown) revealed lack of any significant difference in the control of viral load between the two vaccine groups, suggesting the route of vaccination did not affect protective efficacy of the vaccine.

IFNγ ELISPOT revealed weak responses for the control animals after challenge (Fig. 3.3.1.2A). But strong anamnestic responses were observed in most of the immunized animals of the Mucosal (Fig. 3.3.1.2B) and Systemic (Fig. 3.3.1.2C) groups, peaking 2 weeks after challenge. The differences between these groups are exemplified in Fig. 3.3.1.2D. All vaccinated animals maintained significantly higher IFNγ ELISPOT during post-acute (8-16 wpc) through chronic setpoint. Correlation analysis confirmed significant associations between plasma viral load and IFNγ-producing cells during these periods (Table 3.3.1.2). These associations were not observed during the late chronic setpoint (28-49 wpc).

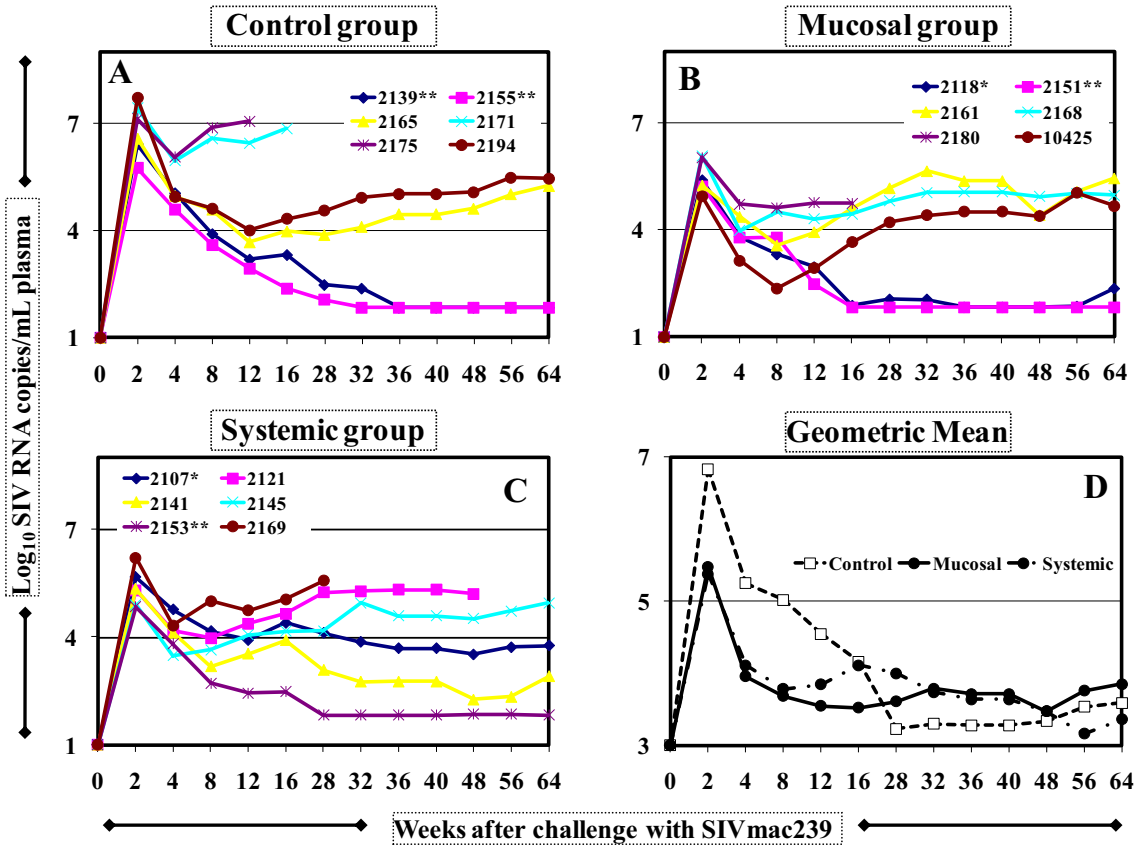

Figure 3.3.1.1: Kinetics of plasma SIV RNA load in both immunized and unimmunized macaques after SIVmac239 challenge.

SIV RNA load was measured in plasma during successive weeks of infection using real time RT-PCR. Individual viral load profiles are shown for the control (A), Mucosal (B) and Systemic (C) groups as well as geometric mean profiles for each group (D). Control of viremia following acute infection lasted until 12 weeks. Animals expressing both *-A*01* and *-B*17* MHC-I alleles are indicated by double asterisk (**) while single asterisk (*) indicates animals positive for *-A*01* without *-B*17*. These animals had the lowest viremia in respective groups. Week 'zero' (0) is taken as an arbitrary baseline.

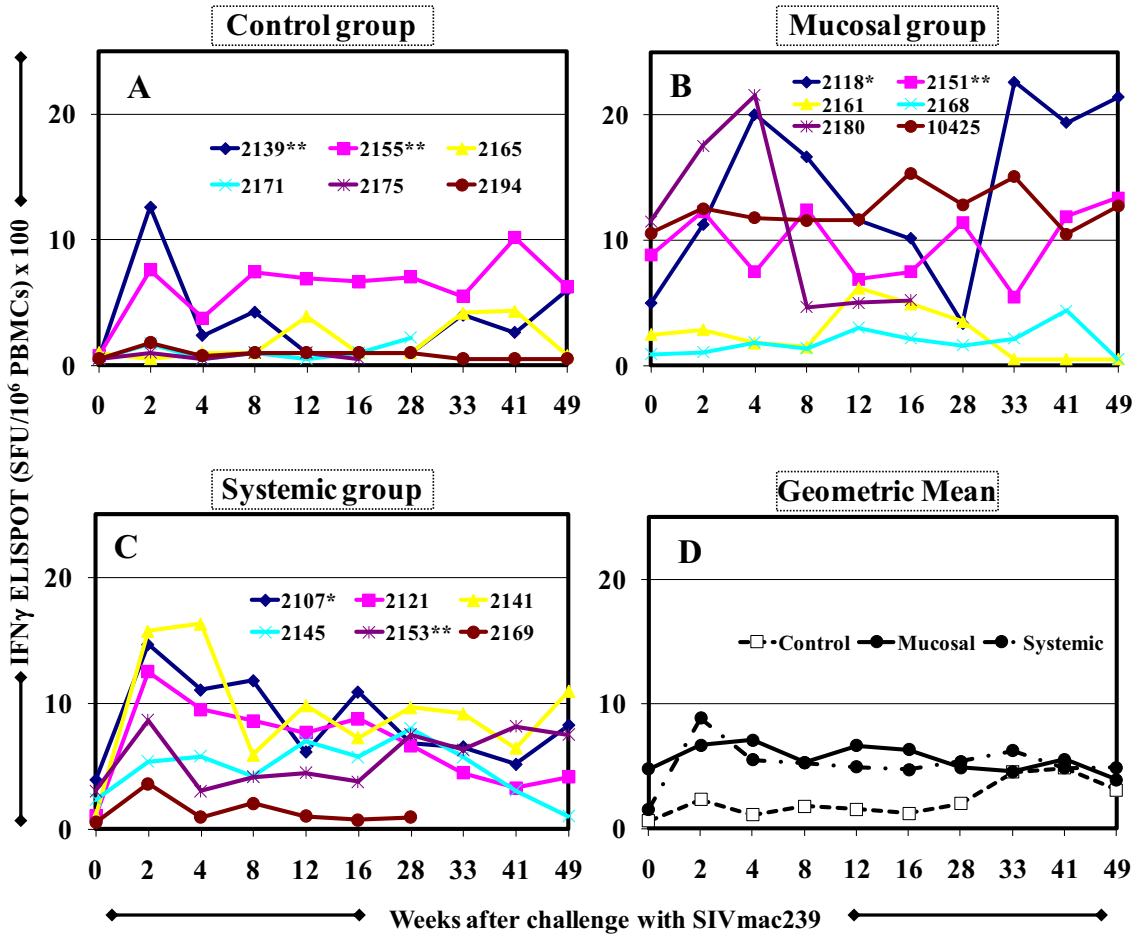

Figure 3.3.1.2: Profiles of IFNγ-producing cells during successive weeks after challenge

The number of IFNγ-producing cells was determined using ELISPOT on freshly prepared PBMC. Profiles are shown for sham vaccinated controls (A) and for the mucosally (B) and systemically (C) boosted groups. Group (D). Significant anamnestic responses occurred after challenge in 9/12 immunised but not control animals. Animals expressing both *Mamu-A*01* and B*17 MHC-I alleles are indicated by double asterisk (**) while single asterisk (*) indicates animals positive for *Mamu-A*01* without *B*17*. These alleles are usually independently associated with strong virus-specific immune responses. Week 'zero' (0) represents ELISPOT responses on the day of challenge measured before inoculation with SIV.

Table 3.3.1.2: Associations between IFNγ ELISPOT and SIV RNA load in plasma after challenge with SIVmac239

			SIV RNA copies/ml plasma at wpc			
	(wpc)		(2)	(8-16)	(28)	(32)
IFNγ-producing T- cells (SFU/10^6 PBMCs) at wpc	(2)	Pearson Correlation	-.53(*)	-.48(*)	-.44	-.48
		Sig. (2-tailed)	.024	.042	.102	.083
	(8-16)	Pearson Correlation	-.70(**)	-.61(**)	-.31	-.25
		Sig. (2-tailed)	.001	.008	.267	.38
		N	18	18	15	14
	(28)	Pearson Correlation	-.73(**)	-.53(*)	-.32	-.24
		Sig. (2-tailed)	.001	.034	.250	.418
		N	16	16	15	14
	(33)	Pearson Correlation	-.41	-.59(*)	-.40	-.41
		Sig. (2-tailed)	.144	.026	.152	.15
		N	14	14	14	14

This table examines associations between the number of IFNγ-producing cells and SIV RNA load in plasma. Wpc, weeks post-challenge; Acute-phase, 2 wpc; post-acute setpoint, 8-16 wpc. *Correlation is significant at p-level 0.05, otherwise ** at p-level 0.01 (2-tailed).

3.3.2 Immunization preserves memory CD4+ T-cells after challenge

The extent of memory T-cell preservation has been shown to predict the outcome of HIV/SIV infection (Letvin *et al.*, 2006). The group at DPZ recently showed that animals that controlled acute viremia also had a delayed loss of their CD4+ T-cells (Suh *et al.*, 2006). In order to show whether intrinsic susceptibility predicts the extent of preservation of memory CD4 T-cells, Flow-cytometry data was provided from the ongoing vaccine study of the Animal Model group of the DPZ (headed by Dr Stahl-Hennig). Compared to controls, all vaccinated animals demonstrated significant preservation of CD4+ T-cells exhibiting memory cell phenotype as evident by combined expression of high levels of CD29 and CD95 (see Fig. 3.6.2A). To examine whether preservation of these T-cell sub-sets was associated with improved viremia outcome, correlation analyses were computed between SIV RNA copies in plasma and levels of these CD4+ T-cell subsets at successive weeks after challenge (table 3.3.2). This analysis revealed significant

and inverse association between plasma viremia and memory CD4+ T-cells during acute (2-4 wpc) and post-acute (8-16 wpc) phases of infection. The observation implied that animals that maintained high viral load in plasma also significantly lost their memory CD4+ T-cells while those with low viral loads better preserved these T-cell subsets. On the contrary, IFNγ ELISPOT responses were not associated with levels of memory CD4+ T-cells at any time during infection (data not shown).

Table 3.3.2: Associations between memory CD4+ T-cells and plasma viral load after challenge

			SIV RNA copies/ml plasma at wpc			
CD4+95+29+ T-cells (% baseline) at wpc	wpc		(2-4)	(8)	(12)	(8-16)
	(2)	Pearson Correlation	-.456	-.497(*)	-.342	-.353
		Sig. (2-tailed)	.057	.036	.165	.151
	(4)	Pearson Correlation	-.683(**)	-.645(**)	-.459	-.500(*)
		Sig. (2-tailed)	.002	.004	.055	.035
	(2-4)	Pearson Correlation	-.611(**)	-.611(**)	-.429	-.457
		Sig. (2-tailed)	.007	.007	.076	.056
	(8)	Pearson Correlation	-.565(*)	-.630(**)	-.502(*)	-.511(*)
		Sig. (2-tailed)	.015	.005	.034	.030
		N	18	18	18	18

All vaccinees had significantly higher CD4+ T-cells expressing CD29 and CD95 memory markers between 2 and 4 weeks after challenge than control animals. These memory CD4+ T-cells are expressed as percent of baseline, with baseline arbitrarily taken to be 100%. Individual levels of these memory CD4+ T-cells were inversely associated with plasma viral loads. Wpc, weeks post-challenge; ** Correlation is significant at p-level 0.01 or * p-level 0.05 level (2-tailed).

3.4 Influence of MHC class-1 allele on susceptibility to SIV

In humans, products of the classical MHC class I genes, also known as the human leukocyte antigen (HLA), are highly polymorphic and play a critical role in immune defence (Robinson *et al.*, 2003). These MHC glycoproteins are expressed on nucleated cells and present foreign peptides of intracellular origin to cytotoxic T lymphocytes (CTLs) (Parham & Ohta, 1996). By doing so, they mediate destruction of the infected cells. Different HLA alleles are associated with varied disease patterns in humans (Hendel *et al.*, 1999). HLA-B*57 for

example, is associated with slower progression to AIDS, and CD8+ T cell responses to B*57-restricted epitopes are thought to contribute to protection. Features of the B*57 that influence disease progression include the induction of CD8+ T cell epitope cross-specificities for HIV-1 escape variants (Turnbull *et al.*, 2006). Because the control of HIV-1 replication is largely dependent on CTLs specific for immunodominant viral epitopes, vaccine strategies that increase the breadth of dominant epitope-specific responses may contribute to containing the spread of HIV-1.

Similar to humans, Mhc class 1 restriction is a critical component of viral containment and disease progression in SIV infected rhesus monkeys. SIV infected macaques homozygous for the Mhc class II allele *DQ-DRB* progress rapidly disease (Sauermann *et al.*, 2000). In addition, the rhesus macaque equivalents of the human classical *HLA-A* and *HLA-B* genes have been identified and respectively designated *Mamu-A* and *Mamu-B* (Miller *et al.*, 1991; Vogel *et al.*, 1999). CTL epitopes restricted by the Mhc class 1 *Mamu-A*01* allele are associated with slow viral replication in SIV-infected macaques (Muhl *et al.*, 2002; Seth *et al.*, 2000). This *-A*01* allele is responsible at least in part, for the resolution acute infection and prolonged survival. Evidence shows that the strength of CTL responses in macaques influence viral setpoint (Kuroda *et al.*, 1999), and that depletion of $CD8^+$ T cells results in rapid rebound of viremia and progression to simian AIDS. The frequencies of different *Mhc-1* alleles also correlate with viremia and disease course in humans (Trachtenberg *et al.*, 2003). Conversely, a high frequency *Mamu-B*01* allele was found to lack the capacity to elicit SIV-specific CTL responses In monkeys (Loffredo *et al.*, 2005). Developing vaccine strategies that elicit broadly active CTL responses require an understanding of the mechanisms responsible for focusing CD8+ T lymphocyte recognition on a limited number of epitopes (Newberg *et al.*, 2006). This section examines the effects of different *Mhc* class 1 alleles and their frequencies on containing SIV replication both *ex vivo* and *in vivo*. Comparison will be made between animals expressing the highly restrictive *Mamu-A*01* allele and those

lacking this allele as well as those expressing or lacking selected high frequency *Mhc* alleles.

3.4.1 PCR typing and MHC- class 1 *Mamu* allele frequencies

Figure 3.4.1 shows the PCR amplification of the 750 base pair *Mamu-A*01* fragment for the 18 animals.

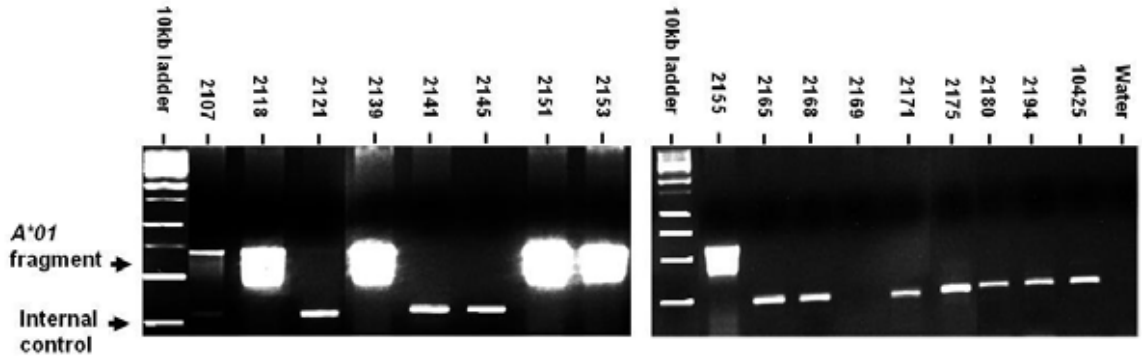

Figure 3.4.1: Amplification of a 750 bp DNA fragment of the Mhc-1 *Mamu-A01 allele.**
A typical PCR amplification of the macaque MHC *Mamu-A*01* gene is shown. Six of the 18 animals screened were positive for this allele. One animal was typed previously and its data is not part of this photograph. The rest of MHC-1 alleles detected in the study animals are summarised in table 3.4.1.

Each of the 3 experimental groups consisted of two animals positive for the low frequency *Mamu-A*01* allele. In addition, both the two sham-vaccinated control animals expressing *A*01* allele and one of the two *A*01*+ animals in each of the immunization group also expressed the low frequency *Mamu-B*17* allele. Products of these alleles are known to be associated with longer survival and a relatively controlled virus replication (Bontrop & Watkins, 2005). Alleles that were present in at least half (≥ 50%) of the animals were considered to be high frequency alleles. Consequently, *Mamu-A*04* and A*08 for MHC class 1A and *Mamu-B*22*, *B*30* and *B*57* for MHC class 1B were all high frequency alleles. Table 3.4.1 summarises the frequencies of different alleles identified in the study cohort.

Table 3.4.1: Frequency of *Macaca mulatta* (*Mamu*) MHC class A and B alleles in the studied monkey cohort

	MHC-1 *Mamu-A* positivity				MHC-1 *Mamu-B* positivity				
	A*01	A*02	A*04	A*08	B*17	B*29	B*22	B*30	B*57
2107	+		-	+	-	-	+	+	+
2118	+	+	-	-	-	-	+	+	-
2121	-	+	-	-	+	+	-	+	+
2139	+	-	-	+	+	+	-	-	-
2141	-	-	+	+	/	-	-	-	-
2145	/	-	+	+	/	-	-	-	-
2151	+	-	-	+	+	+	-	-	-
2153	+	-	-	+	+	+	-	-	-
2155	+	/	-	+	+	+	-	-	-
2161	/	-	+		/	-	+	+	+
2165	-	-	+	+	/	-	+	+	+
2168	-	+	+	+	/	-	-	+	+
2169	-	-	+	+	/	-	+	+	+
2171	-	-	+	-	-	-	+	+	+
2175	-	/	+	-	-	-	+	+	+
2180	-	/	+	-	-	-	+	+	+
§2194	-	-	-	-	-	-	+	+	+
10425	-	-	+	-	/	-	-	-	-
n+/total	6/18	3/18	10/18	9/18	5/18	5/18	9/18	11/18	10/18

+ indicates positivity for that particular allele; - indicates negativity for that particular allele; /indicates animals not tested since both parents were negative for this allele; n, number of animals

3.4.2 MHC- class 1 allele did not affect *ex vivo* susceptibility to SIV infection.

Because MHC genes have been shown to affect virus replication, differences in susceptibility to SIV was examined in *ex vivo* infected macaque PBMCs and virus replication (VVR) compared between those positive or negative for particular alleles. Viral loads in 10 day *ex vivo* infected culture supernatants were used as indices for VVR and susceptibility. Using Mann Whitney's U test, VVR differences between animals positive or negative for *Mamu-A*01* allele were examined before immunization (week 0) and thereafter at 12, 26 and 44 weeks during immunization (wdi). As expected, no significant differences were observed in

susceptibility to SIV infection between *A*01* positive and *A*01* negative sham-vaccinated animals (table 3.4.2a). Similarly, VVR of immunized animals did not differ between those expressing and those lacking the *Mamu-A*01* allele (table 3.4.2b). No difference was observed even after combining the two immunization groups, or when all animals were considered without respect for immunization (data not shown).

Changes in these VVR profiles were subsequently assessed overtime during successive weeks of immunization using the Student T-test. Since in the previous section a significant decline in VVR was demonstrated between 26 and 44 wdi, these two time-points were taken as the focus of analysis for the longitudinal variations. *Mamu-A*01* positive animals did not demonstrate any significant decline in their VVR between these two points. On the contrary, VVRs of the mucosally and systemically boosted animals that were negative for the *Mamu-A*01* allele declined significantly at week 26 (p=0.017) and week 44 (p=0.018) in comparison to baseline VVRs. These analyses precluded any influence of *Mamu-A*01* restriction from the observed VVR suppression.

Table 3.4.2a: Differences in virus replication *ex vivo* (VVR) and in plasma after challenge between *Mamu-A*01* positive and *Mamu-A*01* negative sham vaccinated control animals.

	Pre-challenge viral load (day 10, ex vivo)			*Post-challenge plasma viral load (in vivo)*		
	0 wdi	26 wdi	44 wdi	2-4 wpc (acute)	8-16 wpc	28- 64 wpc
Mann-Whitney U	,000	,000	,000	,000	,000	,000
Z	-1,732	-1,732	-1,732	-1,852	-1,852	-1,549
Asymp. Sig. (2-tailed)	,083	,083	,083	,064	,064	,121
n+/total	2/5	2/5	2/5	2/6	2/6	2/4

This table compares viral load in *ex vivo* infected cultures and in plasma after challenge. The comparison is between *Mamu-A*01* positive and *Mamu-A*01* negative control animals. Data from one animals introduced later during immunization was not available for *ex vivo* analyses but is included in the post-challenge analyses. Two *-A*01* negative animals were sacrificed with AIDS-related symptoms during the chronic phase. Wdi, weeks during immunization; wpc, weeks post-challenge; n, number of animals; 8-16 wpc, post-acute phase; 28-16 wpc, chronic phase.

Table 3.4.2b: Differences in virus replication *ex vivo* (VVR) and in plasma viral load after challenge between *Mamu-A*01* positive and *Mamu-A*01* negative immunized animals.

	Viral load ex vivo *Mucosal and (Systemic)*			*Viral load in plasma* *Mucosal and (Systemic)*		
	0 wdi	26 wdi	44 wdi	2-4 wpc (acute)	8-16 wpc	28- 64 wpc
Mann-Whitney U	4.0 (2.0)	3.0 (3.0)	.0 (2.0)	2.0 (4.0)	.0 (4.0)	.0 (3.0)
Z	.0 (-1.1)	-.46 (-.66)	-1.9 (-1.1)	-.93 (-.22)	-1.85 (-.22)	-1.73 (-.66)
Asymp. Sig. (2-tailed)	1.0 (.28)	.64 (.51)	.06 (.28)	.36 (.83)	.06 (.83)	.08 (.51)

This table compares viral load in *ex vivo* infected cultures and in plasma after challenge. The comparison is between *Mamu-A*01* positive and *Mamu-A*01* negative animals of the Mucosal and Systemic groups. Statistics in brackets are for the Systemic group. Two of the 6 animals in each group were positive for the *-A*01* allele. One *-A*01* negative animal was sacrificed with AIDS-related symptoms during the chronic phase. The row Asymp. Sig. (2-tailed) represent p-values. Wdi, weeks during immunization; wpc, weeks post-challenge; n, number of animals. , 8-16 wpc; post-acute phase; 28-16 wpc; chronic phase.

3.4.3 Influence of MHC class 1 on control of viremia after challenge

All animals positive for the *Mamu-A*01* allele replicated the virus poorly in all the experimental groups compared to those lacking this allele. Having demonstrated in the previous sections that immunized animals controlled acute viremia much better than control animals, it was investigated whether the control of viremia was dependent on or independent of *A*01* allele. All *Mamu-A*01* negative immunised animals maintained significantly lower viral load in plasma than *Mamu-A*01* negative unimmunised control animals, lasting until 12 weeks after challenge (Fig. 3.4.3A). On the other hand, there were no statistically different levels of viremia control between *Mamu-A*01* positive immunized and *Mamu-A*01* positive control animals (Fig. 3.4.3B).

Further analysis was done to examine if *Mamu-A*01* MHC-1 allele influenced viral load during late post-acute and chronic infection. During these

late phases, all immunized animals expressing the *A*01* allele had significantly lower plasma viremia than *A*01* negative immunized animals (Fig. 3.4.3C). The same pattern was observed when all animals were analysed without regard to immunization status (Fig. 3.4.3D). Overall, the observations exemplified in Fig. 3.4.3A and Fig. 3.4.3C revealed a pattern of viremia control in which vaccine-induced immunological factors influenced acute viral replication while MHC-class 1 restriction influenced viral replication during late or chronic infection after dissipation of vaccine-effect.

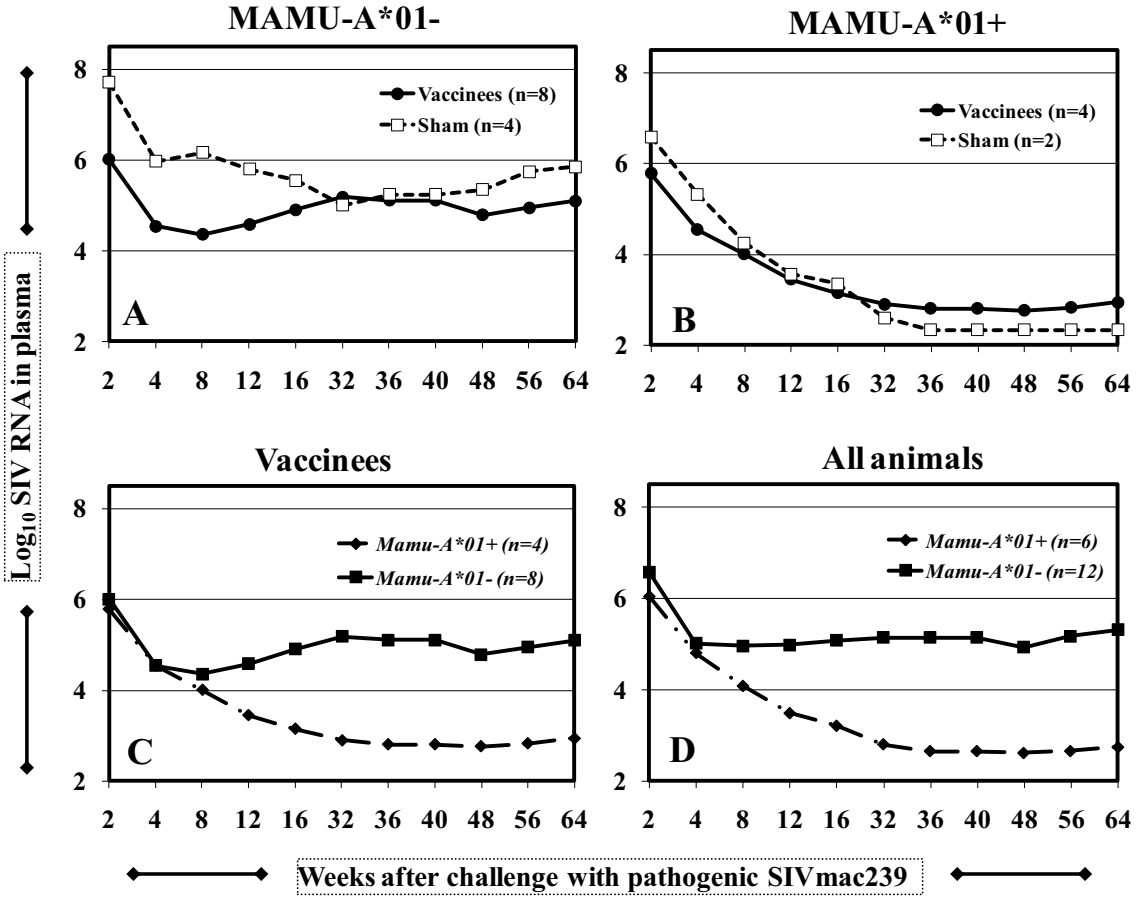

Figure 3.4.3: Influence of *Mamu-A*01* allele on plasma viral load.
Comparison between immunized and control animals lacking *Mamu-A*01* allele (A). Immunized animals showed significant reduction of their acute viremia independently of *Mamu-A*01* background. All *Mamu-A*01* positive animals are compared between those receiving the vaccine and those not receiving the vaccine (B). Vaccination did not seem to affect viremia viral load in the allele positive animals. Comparison between *Mamu-A*01* positive and *Mamu-A*01* negative immunised animals only (C) or all animals combined (D). This MHC-1 allele starts to significantly influence viral load at week 16 where the vaccine effect (in Fig A) seemed to have stopped.

3.4.4 Expression of high frequency MHC-1 alleles is linked to rapid SIV replication and viremia turnover

The role of high frequency MHC-1 alleles on the control of plasma viremia was assessed. Frequency analyses showed that *Mamu-B*22*, *B*30* and *B*57* alleles were most common in the studied macaque cohort. These alleles are presumed to be present on a single haplotype (Otting & Bontrop, 1993). Out of the 18 animals, 11 expressed all the three high frequency (HiFreq) alleles. Viral loads in *ex vivo* infected PBMC cultures and in plasma after challenge were compared between animals expressing HiFreq and those lacking the HiFreq alleles. When the two vaccine groups were considered separately, HiFreq positive animals of the Systemic group had significantly higher viral loads in cell culture than HiFreq negative animals after 26 weeks of immunization (p=0.05). Although falling short of significance, HiFreq allele positive Mucosal group animals still maintained high VVR than HiFreq negative animals in the same group (p=0.064). Plasma viral loads after challenge were significantly higher in HiFreq positive than in HiFreq negative animals. Table 3.4.4 shows these analyses separately for the immunized animals (n=12). Analyses of plasma viral loads with all the animals lumped together (n=18) still revealed comparable significance levels.

Table 3.4.4: Differences in *ex vivo* VVR and in plasma viral load after challenge between high frequency allele positive and allele negative immunised animals.

	Viral load ex vivo			*Viral load in plasma (in vivo)*		
	0 wdi	26 wdi	44 wdi	2-4 wpc (acute)	8-16 wpc	28- 64 wpc
Mann-Whitney U	12.0	15.0	13.0	1.0	3.0	5.0
Z	-.89	-.41	-.73	-2.68	-2.36	-1.83
Asymp. Sig. (2-tailed)	.37	.69	.47	.007	.019	.068
HiFreq +/total	7/12	7/12	7/12	7/12	7/12	*6/11

This table compares viral load in *ex vivo* infected cultures (VVR) and in plasma after challenge. The comparison is made between immunized animals expressing all the three frequency *Mamu-B*22*, *B*30* and *B*57* (HiFreq) alleles and immunized animals lacking this HiFreq allele combination. While no significant difference was observed in their VVRs, plasma viral loads were significantly higher for HiFreq+ than HiFreq- animals after challenge. Wdi, weeks during immunization; wpc, weeks post-challenge; n, number of animals. , 8-16 wpc; post-acute phase; 28-16 wpc; chronic phase. Asterisk (*) One animal sacrificed with AIDS-related symptoms.

3.5 Effect of chemokines and cytokines on *ex vivo* susceptibility to SIV

The ability to induce broad-range cytokine responses is increasingly becoming integral to HIV-1 vaccine efficacy assessment (Gorse *et al.*, 2001). But there are conflicting reports on how some of these soluble factors affect the outcome of HIV/SIV infections. Some chemokines inhibit HIV-1 efficiently when induced in the presence of other co-infecting pathogens (Jung *et al.*, 2005). Under such circumstances, it is not clear whether the inhibition is mediated by the chemokine, or is due to other unrelated factors. One study showed that resistance to HIV infection *in vitro* correlated with increased RANTES (Schwartz *et al.*, 1997), yet removal of RANTES did not make the cells more susceptible. Similarly, target CD4+ T-cells and PBMCs vary in their ability to respond to chemokine-mediated virus inhibition (Trkola *et al.*, 1998). Using an *in vitro* infection system, addition of MIP-1α, MIP-1β, and RANTES did not affect replication of exogenous HIV-1 in infected dendritic cells and CD4+ T-cells (Rubbert *et al.*, 1997). Beta chemokines were also not associated with replication levels of both HIV and SIV or with disease progression (Ondoa *et al.*, 2003). With these conflicting observations, it is hypothesised that other mechanisms may augment the noncytolytic-type viral suppression (Ondoa *et al.*, 2002; Rubbert *et al.*, 1997). These chemokines may regulate virus replication and expression in a mechanism tightly linked to the timing of both the infection and release of the chemokine. Indeed, there is evidence to show that chemokines may more efficiently suppress the virus during asymptomatic than late-stage infection (Garzino-Demo *et al.*, 1999; Saha *et al.*, 1998; Scarlatti *et al.*, 1997). Moreover, CD8+ T-cell supernatants can suppress HIV-1 replication independent of β-chemokine activity (Moriuchi *et al.*, 1996). These observations may imply a tilted balance between pro- and anti-inflammatory responses, which pull virus expression in different regulatory directions (Goletti *et al.*, 1996). Because CD4+ and CD8+ T-lymphocytes from HIV-1 and SIV infected cells produce high amounts of beta-chemokines (Kinter *et al.*, 1996), these soluble immune factors cannot be precluded in understanding the course of infection and disease

outcome. Using the *ex vivo* infection model, this section investigates how different cytokines and chemokines affect the outcome of SIV infection.

3.5.1 Secretion of β-chemokines and cytokines is suppressed in *ex vivo* infected cells of immunised macaques.

To determine the panel of β-chemokines and cytokines secreted during SIV infection, *ex vivo* infected cell culture supernatants and pre-challenge plasma from both immunised and sham-immunised animals were examined for production of various soluble factors. Supernatants were analysed after 24 hrs of stimulation with concanavalin-A (Con-A) and thereafter on 5 and 7 days post ex *vivo* infection (dpi). This analysis was conducted on PBMCs obtained 2 weeks after the first vaccine boosting at week 26 and at week 44 on the day of challenge (DoC). Due to the unavailability of material, this analysis could not be conducted at week 0. DoC cultures were also not examined after 24 hrs of Con-A, but after 5 and 7 days of *in vitro* infection with SIV. Except for TNF-α which was never detected, all animals demonstrated significant amounts of the other 7 cytokines 24 hrs after stimulation (Fig. 3.5.1 panel I). Soluble IFNγ in culture supernatants was highest in immunized compared to sham-vaccinated control animals, significantly more in the systemic group ($p=0.017$). Similarly, systemically boosted but not the mucosally boosted animals showed slightly elevated levels of MIP-1α and less of IL-10. At this time, the systemic group animals were also able to significantly control their viral replication in the *ex vivo* infected cultures. At week 26 when VVR was controlled, vaccinees secreted more IFNγ and less MIP-1α, MIP-1β, MCP-1, IL-1β and MIP-1β than control animals. At this time, RANTES and IL-10 were high but comparable among the groups.

These cytokine secretion kinetics nonetheless showed rapid decline after *in vitro* infection of PBMCs taken at week 26 (Fig. 3.5.1 I-III). Similar decline was observed between day 5 and 7 cultures on DoC (data not shown). This decline was more drastic for IFNγ, IL-1β and MIP-1α than the other cytokines (fig.

3.5.1A-I). Compared by cumulative production of all 7 detected cytokines/ chemokines, animals that replicated SIV rapidly (animals 2171, 2175, 2180, 2153 and 2169) also produced consistently less of all cytokines in their respective experimental vaccine groups.

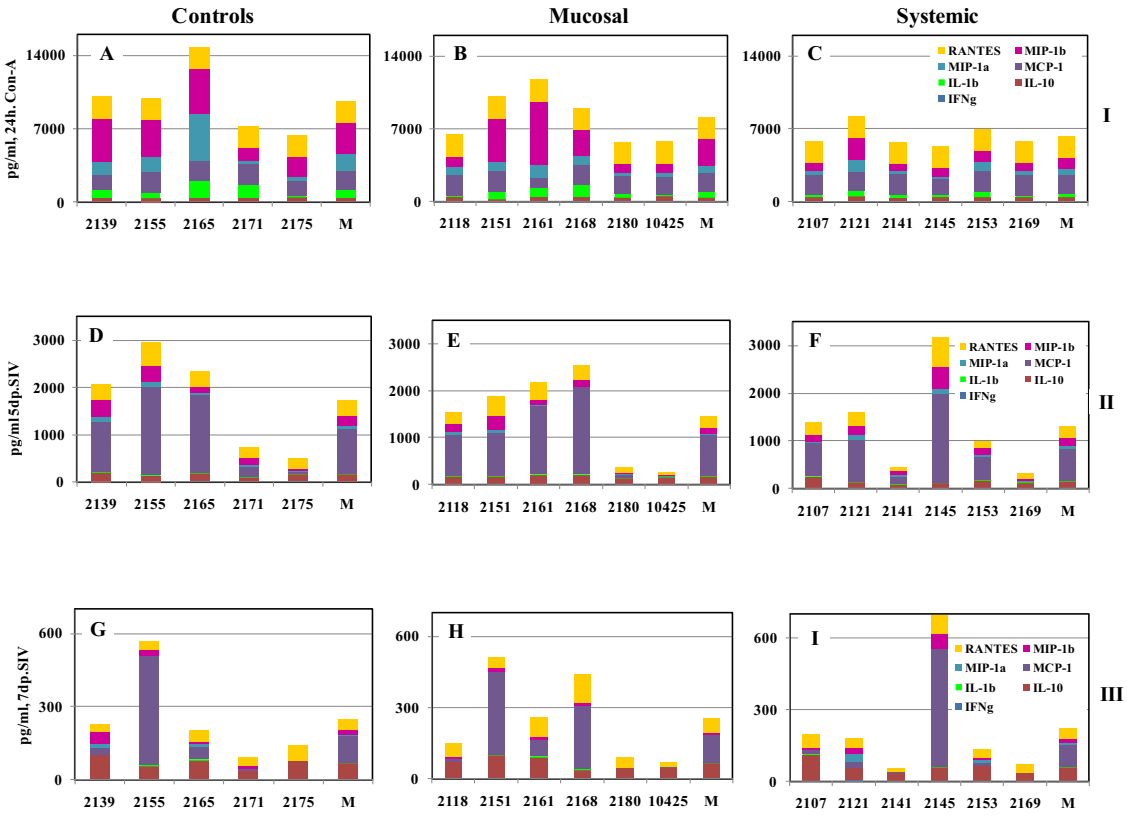

Figure 3.5.1: Cumulative profiles of β-chemokines and cytokines in immunized and control macaque PBMCs.

Cytokine levels in culture supernatants 24 hours after Con-A stimulation only (panel I) and 5 days (II) and 7 days (III) after *in vitro* infection with SIV. Measurements were done 2 weeks after the first rAd5-SIV vaccine boosting of both the mucosal and systemic groups. Except IFNγ which was higher in immunised than control animals, the control animals produced higher amounts of all the other cytokines than vaccinees before *in vitro* infection (A-C). These cytokines declined rapidly during successive days of infections (I-III), more drastically for IFNγ, IL-1β and MIP-1α (note the changing scale on the Y-axes). On average, animals (2171, 2175, 2180, 2153 and 2169) that replicated SIV rapidly *in vitro* also produced less of most cytokines except more of IFNγ in their respective experimental groups.

On DoC and similar to week 26, control animals still had significantly elevated levels of IL1β, MIP1α, MIP1β and RANTES compared to immunised animals, while MCP-1 and IL10 were comparable in both immunized and control groups (table 3.5.1). IFNγ in cultures of the Systemic group had declined to the lowest level but high in the Mucosal and highest in the Control group. These DoC cytokine levels were largely though not significantly above those occurring at week 26 after only one boost. Since (i) vaccinees had reduced cytokine secretion capacity in 24-hrour cultures compared to control animals, (ii) all cytokine/chemokine levels went down after *in vitro* infection and (iii) high *ex vivo* virus replicators secreted less amounts of cytokines/chemokines than low replicators, it was hypothesized that exposure to high amounts of viral antigens may suppress cytokine production. This exposure could be either in the form the introduced virus or the vector used for immunization.

Table 3.5.1: Differences in secreted cytokine levels between immunized and control macaque PBMCs 5 days after *ex vivo* infection of PBMCs obtained on the day of challenge.

	IFNγ	*IL10*	*IL1β*	*MCP1*	*MIP1α*	*MIP1β*	*RANTES*
Mann-Whitney U	18.0	27.0	5.0	29.0	7.0	6.0	4.0
Z	-1.27	-.32	-2.64	-.11	-2.63	-2.53	-2.74
Asymp. Sig. (2-tailed)	.204	.752	.008	.915	.009	.011	.006

Cultures were derived from Day of Challenge (DoC) PBMCs. Sham-vaccinated control animals secreted significantly elevated levels of most cytokines than immunised animals. p-values are reported in the row 'Asymp. Sig.' and are significant at level 0.05 and below.

3.5.2 Gama inducible protein 10 (IP10, or CXCL10) is lowered during effective viral control and increased during rapid virus replication

CXCL10 is an α-chemokine produced in response to IFNγ-driven inflammation and a potent suppressor of cytokine production (Abel *et al.*, 2004). Immunized macaque PBMCs secreted low amounts of CXCL10 in cultures after 26 weeks of immunization compared to sham-vaccinated macaque PBMCs (Fig. 3.5.2A). At

this time, immunized animals controlled virus replication (VVR) in these *ex vivo* infected cultures much better than control animals. On DoC, immunized animals secreted significantly higher amounts of CXCL10 in infected cultures than control animals (Fig. 3.5.2B). At this time, the immunised animals had lost much of their capacity to control VVR. All the 7 animals that replicated the virus rapidly *ex vivo* (animals 2118, 2153, 2169, 2171, 2175, 2165 and 2180) also had significant amounts of CXCL10 in infected cultures either after the first vaccine boost or on DoC (Fig. 3.5.2 A & B). Within this group of *ex vivo* high replicators, four (animals 2175, 2171, 2169, and 2180) died rapidly after infection (see Fig. 3.3.1.1A-C, section 3.3). The other three were still alive by the time of compiling this data, indicating that SIV replication cannot simply be predicted by the over-expression of only one chemokine, but by a complicated network of different regulatory factors interacting with each other.

Due to lack of material at week 44, pre-challenge plasma was analysed at week 42, 2 weeks before the actual day of challenge. For convenience of and consistency reference, this time-point is referred to simply as DoC. To corroborate the *ex vivo* infection data, CXCL10 levels were examined in both immunised and unimmunised plasma at time before inoculation with SIV (Fig. 3.5.2C) and thereafter, 2 weeks after SIVmac239 challenge (Fig. 3.5.2D). Pre-challenge uninfected plasma CXCL10 was on average higher in sham-vaccinated control compared to immunised animals. This average difference was mainly because the rapid progressor (animal 2175) had very high CXCL10 levels compared to the other control animals. Although acute-phase plasma CXCL10 was comparable between groups, these were significantly increased from pre-challenge plasma levels. In addition, plasma CXCL10 levels were highest in 3 of 4 rapid progressors (2171, 2180 and 2169) after challenge. Correlation analysis showed that high CXCL10 was associated with elevated IL-10 ($p=0.0004$).

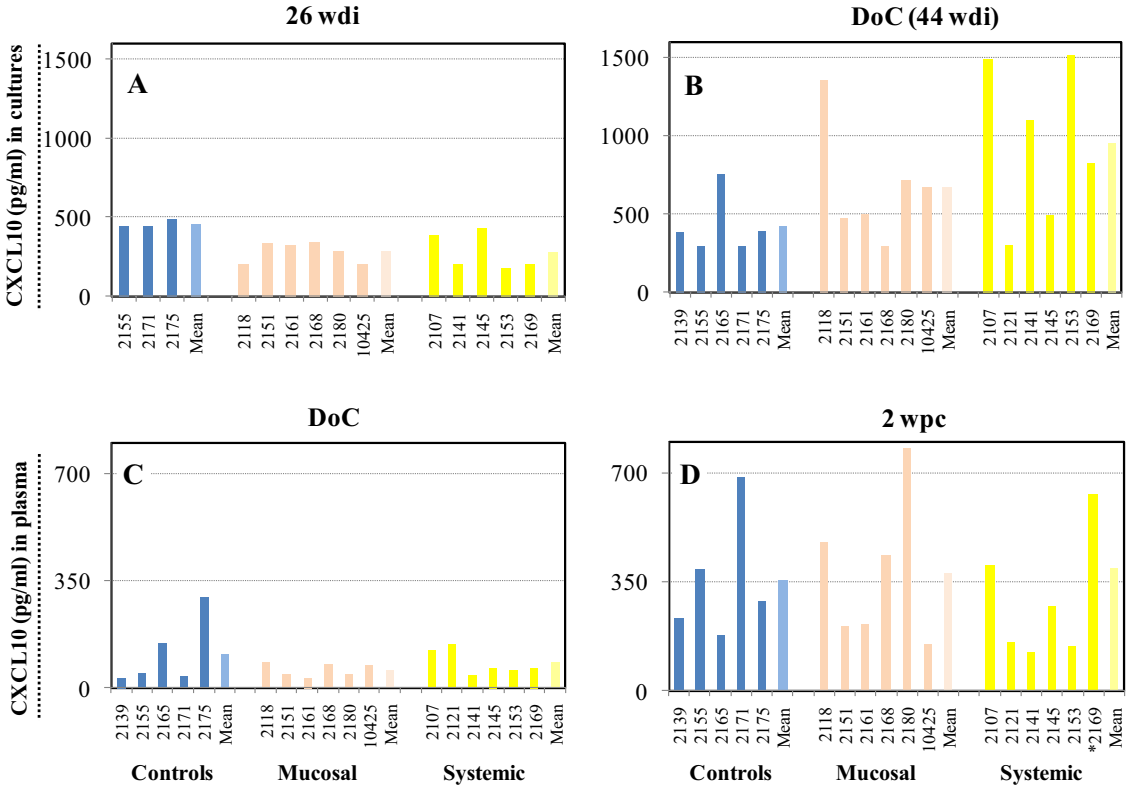

Figure 3.5.2: *Ex vivo* and *in vivo* levels of secreted gamma inducible protein 10.
CXCL10 levels are shown for the *ex vivo* infected PBMC cultures 2 weeks after first vaccine boosting (A) and on the day of challenge (DoC) (B). Only 3 of 5 control animals and 5/6 systemic group animals were tested at week 26 due to insufficient material. Y-axes are only identical in adjacent figures. CXCL10 was substantially low in immunized compared to control animals at week 26. On DoC, CXCL10 was significantly increased in immunized animals, but these were comparable to week 26 for the control animals. Pre-challenge plasma CXCL10 on DoC (C) was significantly lower than CXCL10 occurring 2 weeks after challenge (D). The animals that progressed with high plasma viremia after challenge (2175, 2171, 2180, 2169 and 2165) had elevated CXCL10 in plasma either before or after challenge. These animals also died earlier in their respective order of listing. *2169; true values for this animal is twice the presented readings.

3.5.3 Association of chemokines and cytokines with SIV replication *ex vivo*

To assess whether intrinsic susceptibility and virus replication *ex vivo* (VVR) was affected by these cytokines, correlation analyses were computed to determine associations. At week 26 when the systemic group poorly replicated the virus, viral loads in *ex vivo* infected PBMCs cultures were significantly and inversely

associated with the amount of secreted MIP-1α (Fig 3.5.3 A & B) and IFNγ (Fig 3.5.3 C & D) in respective culture supernatants. MIP-1α was still detected in day 7 cultures but at low concentrations. These cytokine levels on day 5 or day 7 still correlated significantly with day 10 VVR, suggesting a long-term effect on the virus. On the day of challenge however, high levels of IL-1β (Fig 3.5.3E), RANTES ($p=0.033$) and MIP-1β ($p=0.1$) in day 5 cultures were all associated with increased susceptibility as evident by high virus load in later cultures at day 10. These associations were not significant when correlations were computed against similar days for VVR and cytokines/chemokines (e.g. day 5VVR and day 5 IL-1β/ MIP-1β). The lack of association at similar time-points of cultures confirmed that these cytokines produce more of a long-term than short-term effect. Similarly, secretion of high levels CXCL10 in pre-challenge plasma was significantly associated with high VVR for the respective animals (Fig 3.5.3F). These observations exemplified two opposing effects of β-chemokines on virus infection and replication. At high concentrations, β-chemokines or pro-inflammatory cytokines may act in concert with the anti-inflammatory CXC-chemokines to reverse any beneficial antiviral effect of these soluble factors.

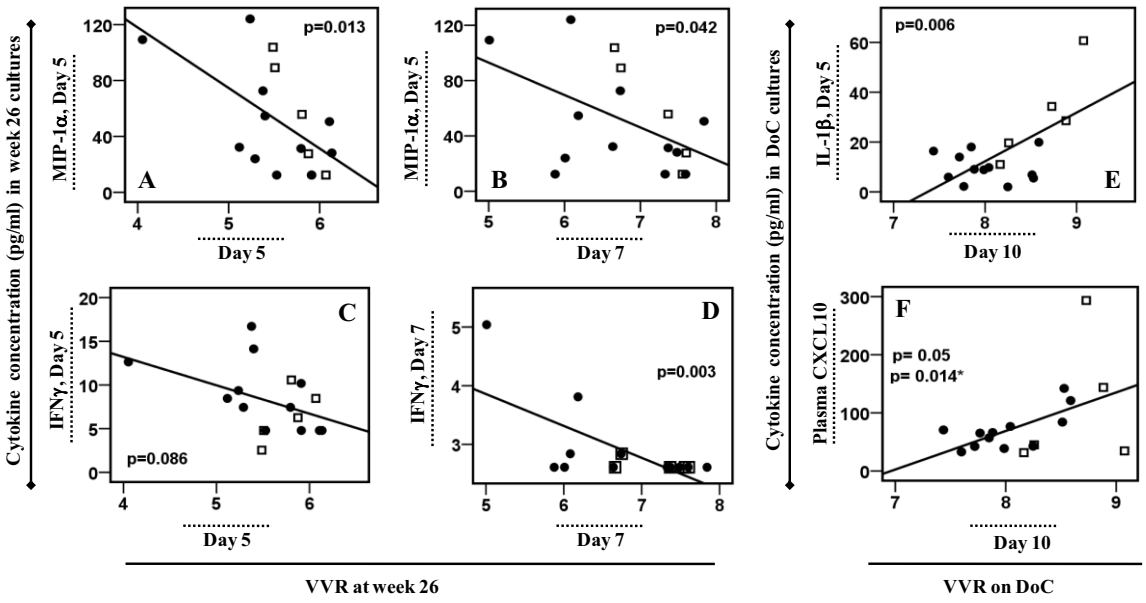

Figure 3.5.3: Associations of α- and β- chemokines/cytokines with SIV infection *ex vivo*.
Increased secretion of MIP-1α in day 5 and 7 culture supernatant of PBMCs infected after 26 immunization weeks correlated with low viral loads in the same cultures (A-D). High IFNγ secreted in these culture supernatants also correlated with reduced viral loads (C & D). On the day of challenge, high IL-1β (G) and CXCL10 (F) were all associated with increased SIV RNA load in these culture supernatants. Open squares, sham-vaccinated controls; closed circles, vaccinees. * This p-value (Fig. F) is for vaccinees only. Scaling for X-axes is not identical because VVRs varied widely at different stages of *ex vivo* infection.

3.6 Intrinsic susceptibility as an *ex vivo* surrogate for vaccine outcome.

HIV-1 infection leads to a highly variable course of disease, from rapid progression to long-term non-progression (Buchbinder *et al.*, 1994; Ochieng *et al.*, 2006). This course of disease is defined by among other factors, plasma viral RNA (Mellors *et al.*, 1996), strength the of host immune responses (MacArthur *et al.*, 2005; Zhang *et al.*, 2007b) and host genetic predisposition (Kindberg *et al.*, 2006). Strong CD8+ T-cell and innate immune responses may delay disease progression (Horton *et al.*, 2006; Milush *et al.*, 2007). Pathogenesis of SIV infection in macaques also varies between animals (Lifson *et al.*, 1997; Orandle *et al.*, 2001), and may be influenced by intrinsic host factors (Goldstein *et al.*, 2000; Hirsch *et al.*, 1996). It is possible to predict viral loads in plasma of SIV-infected monkeys using an *in vitro* SIV infection model (Goldstein *et al.*, 2000;

Seman *et al.*, 2000). But the capacity of such an infection system to predict vaccine outcome and disease course has not been examined in immunised animals. This section examines the *ex vivo* pre-challenge infection model as a surrogate for predicting outcome of a pre-clinical vaccine study following challenge with pathogenic SIV. It compares the main outcome of the *ex vivo* pre-challenge model with the outcomes of *in vivo* post-challenge model. With these comparisons, a surrogate model is described that can in several aspects, be used in macaques to predict vaccine outcomes following infection. Avenues for application of this model in human vaccine testing will be highlighted.

3.6.1 Pre-challenge VVR accurately predicts plasma viremia after challenge

Detailed description of *ex vivo* virus replication kinetics (VVR) or susceptibility to SIV infection has been captured in the previous sections. Figure 3.6.1A recapitulates the fact that immunization significantly lowered viral loads in plasma of animals receiving the vaccine regime as opposed to those receiving placebo only (sham vaccine). This was discussed in section 3.3.1. Figure 3.6.1B and C revisit the longitudinal profiles of viral replication after 7 and 10 days of *ex vivo* infection respectively, also described in section 3.1.1. This section now examines whether susceptibility to infection *ex vivo* is predictive of plasma viremia after inoculation with pathogenic SIVmac239. This assessment was achieved by correlating viral loads from days 5, 7 and 10 of infected cultures with plasma viremia after challenge. Mean day 5 VVR (Fig 3.6.1D) and day 7 VVR (Fig 3.6.1E) positively and significantly correlated with post-challenge plasma viral load during post-acute and acute infections respectively. Baseline VVR of the control animals also significantly predicted acute-phase plasma viremia 2 weeks after challenge (Fig 3.6.1F). This is in contrast to vaccinated monkeys for which no correlation existed between pre-immunization (0 wdi) VVR and acute viremia post-challenge (Fig 3.6.1F). While VVR of these immunized animals was comparable with VVR of control animals at 0 wdi before any immunization was

done, their *in vivo* acute-phase viremia was additionally influenced by 11 months of immunization. Hence significant viremia control by vaccinees at 2 wpc meant loss of correlation between intrinsic (baseline) levels of VVR and viremia *in vivo*. Further analyses showed that pre-immunization VVRs were still significantly associated with plasma viremia during chronic setpoint (Fig. 3.6.1G). Thus, the individual capacity of vaccine-naïve PBMCs to support viral replication *ex vivo* translated into a parallel susceptibility to infection *in vivo*. Moreover, VVR on DoC was significantly and positively associated with acute (Fig. 3.6.1H) and post-acute (Fig. 3.6.1I) plasma viremia. This association was still observed at 8 wpc ($p=0.01$), but was not significant at later time points ($p=0.077$). The correlations between DoC VVR and acute plasma viremia were a culmination of the influence of both genetic and vaccine induced factors.

3.6.2 Intrinsic susceptibility *ex vivo* predicts the number of memory CD4+ T-cells after challenge.

Having demonstrated that VVR was highly predictive of acute to post-acute-phase plasma viremia, it was important to assess whether VVR also predicted the number of CD4+ memory T-cells after challenge. Figure 3.6.2A demonstrates the effects of vaccination on preservation of memory CD4+ T-cells as described in section 3.3.2. This section now correlates pre-challenge susceptibility to SIV with the number of these memory T-cell subsets. Animals which were highly susceptible to infection *ex vivo* before any immunizations (Fig 3.6.2B-D) also demonstrated significant loss of acute- through chronic-phase memory CD4+ T-cells. Similarly after immunization on DoC, increased susceptibility to SIV as indicated by high VVR *ex vivo* was associated with loss of acute-phase (Fig 3.6.2E) and post-acute-phase (Fig 3.6.2F) memory CD4+ T-cells. By contrast, less susceptibility meant preservation of these T-cells after challenge.

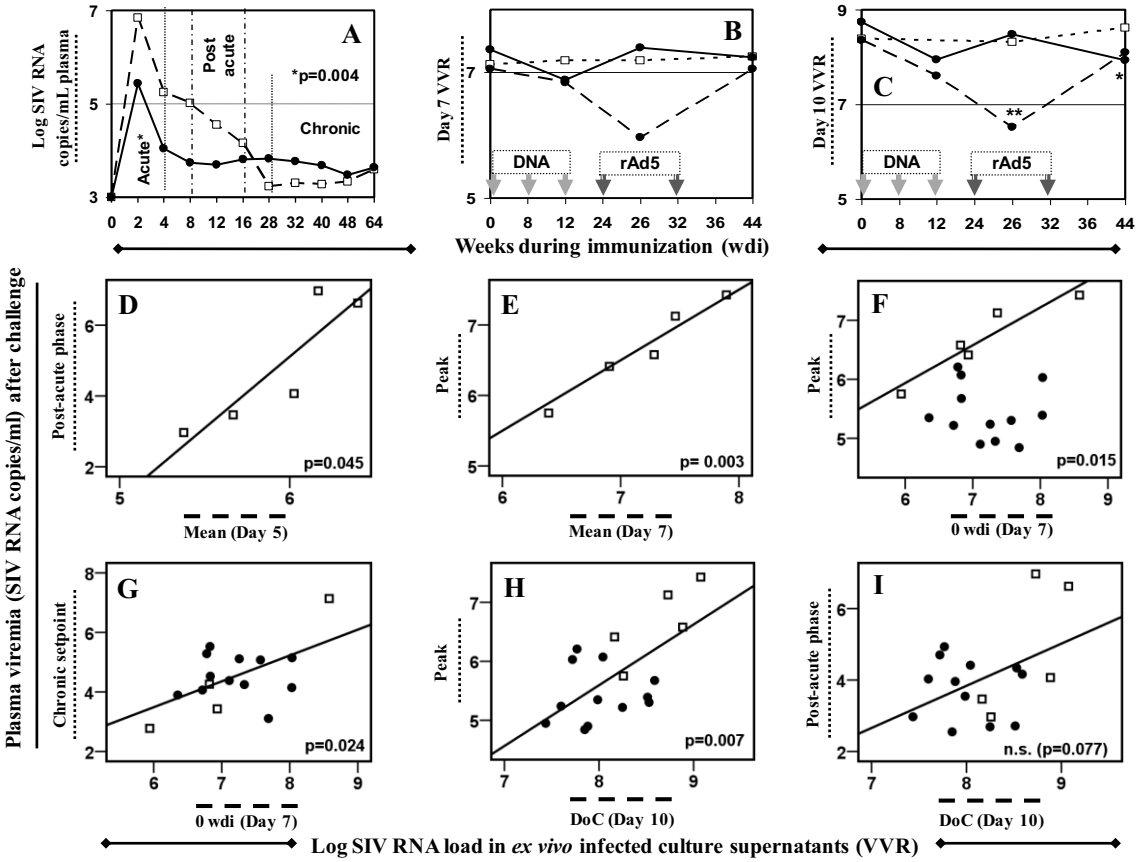

Figure 3.6.1: Associations of *ex vivo* viral load with post-challenge plasma viremia

Open squares, sham-vaccinated control animals; Filled circles, immunized animals. Vaccinees significantly controlled their acute viremia after challenge (A). The two vaccine groups are combined because of similar viremia profile and similar VVR on DoC. Viral loads in *ex vivo* infected cultures (VVR) after day 7 (B) and day 10 (C) of infection during the weeks of immunization. Individual day 5 VVR (D) and day 7 VVR (E) averaged for week 0, 26 and 44 for control animals correlated significantly with respective plasma viral loads. VVR at individual baseline (F &G) and on DoC (H & I) were significantly associated with plasma viremia at different stages after challenge Wdi, weeks during immunization; DoC, day of challenge; acute, 2 weeks post-challenge (wpc); post-acute, 8-16 wpc.

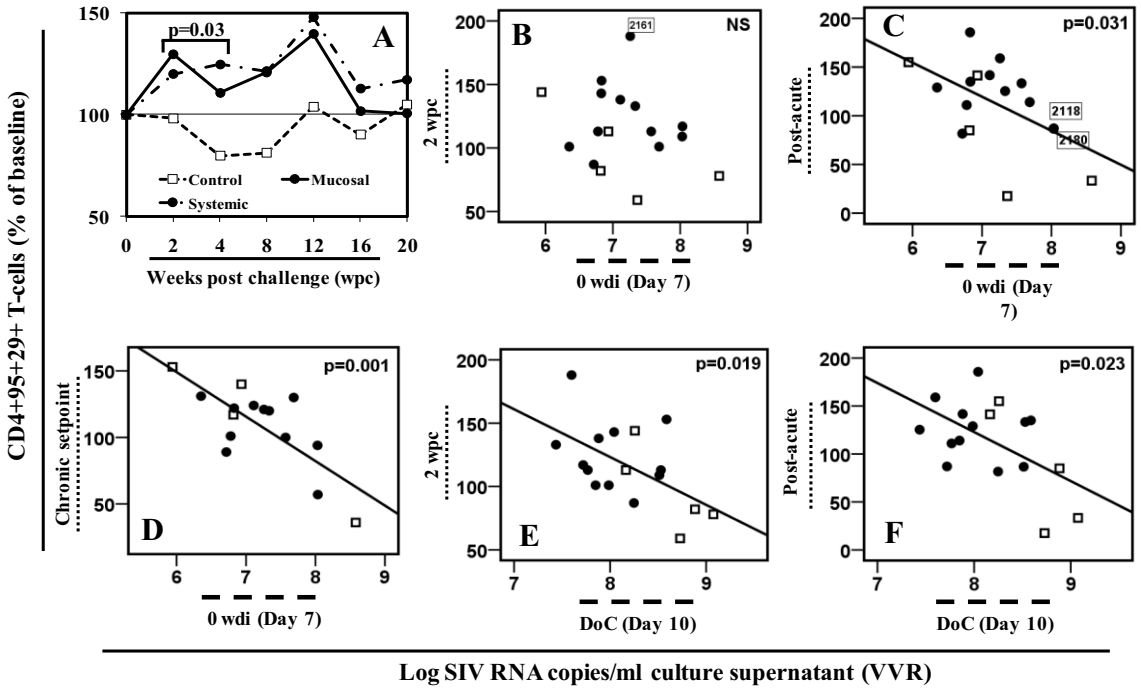

Figure 3.6.2: Association of e*x vivo* viral load with post-challenge memory CD4+ T-cells
Open squares, Sham-vaccinated control animals; Filled circles, immunized animals. Vaccinees had significantly higher acute-phase (2-4wpc) CD4+ memory T-cells than control animals (A). VVR before immunization was inversely associated with acute (B) and significantly with post-acute (C) and chronic-phase (D) memory CD4+ T-cell after challenge. In addition, VVR on DoC was inversely and significantly associated with acute (E) and post-acute (F) memory CD4+ T-cells. Wdi, weeks during immunization; DoC, day of challenge; acute-phase, 2 weeks post-challenge (wpc); post-acute, 8-16 wpc; n.s., not significant.

3.6.3 Pre-challenge CNAR but not IFNγ ELISPOT correlate with plasma viremia and memory CD4+ T-cells counts

Having shown that VVR was dependent partly on CNAR and IFNγ and that VVR predicted plasma viremia and memory CD4+ T-cell levels after challenge, the effects of pre-challenge CNAR and IFNγ on viremia control and memory CD4+ T-cell levels post-challenge were examined. Strong CNARs occurring on the day of challenge were significantly associated with control of acute plasma viremia (Fig 3.6.3A) and preservation of acute-phase memory CD4+ T-cells (Fig 3.6.3B) after challenge. Highly significant associations were still evident during post-acute and chronic phase infections as well as when these plasma viremia and CD4+

memory T-cell levels were compared with CNARs appearing 2 weeks after 1st boosting ($p<0.008$, data not shown). On the contrary, the number of IFNγ-producing cells on the day of challenge just before inoculation with SIV did not correlate with either plasma viremia (Fig 3.6.3C) or memory CD4+ T-cell levels (Fig 3.6.3D) after challenge.

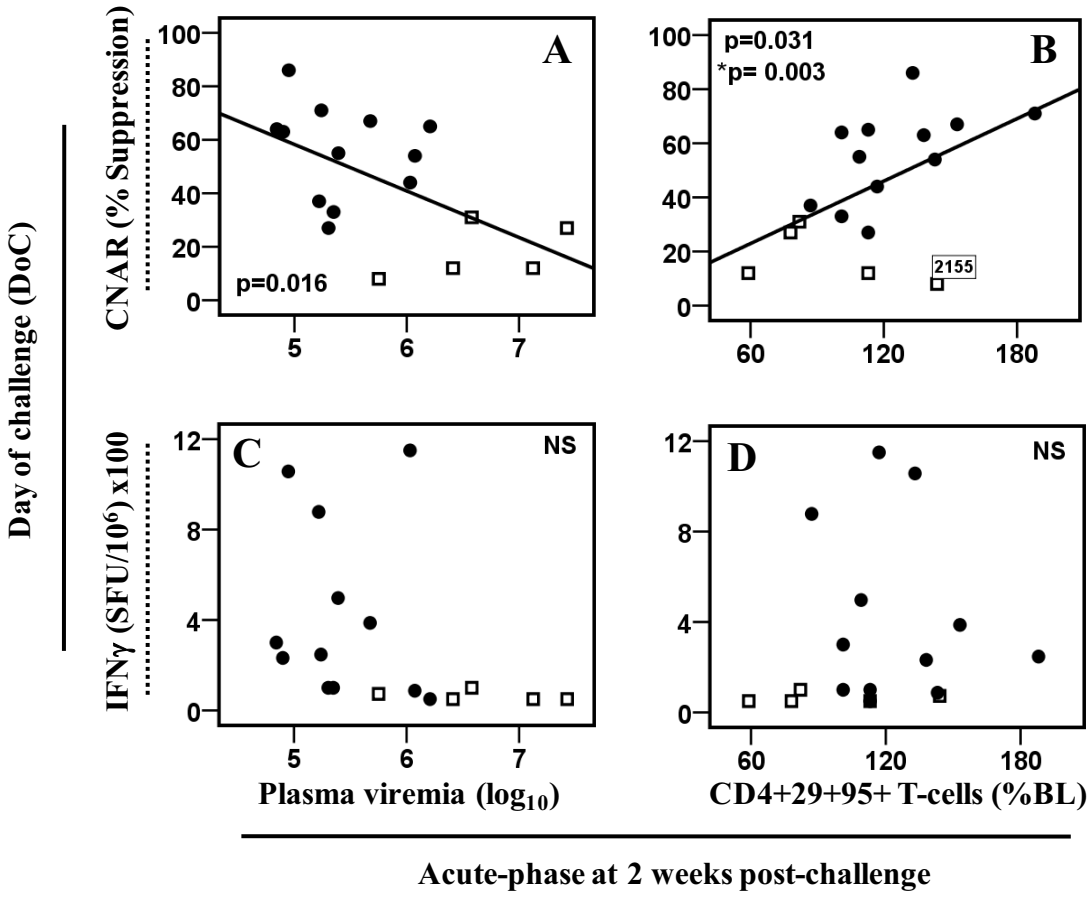

Figure 3.6.3: Associations of pre-challenge CNAR and IFNγ ELISPOT with post-challenge plasma viremia and memory CD4+ T-cells

Open squares, Control animals; Filled circles, vaccinees. Increased CNAR on DoC was significantly associated with acute plasma viremia (A) and CD4+ memory T-cells (B) after challenge. IFNγ on DoC was not associated with either plasma viremia (C) or CD4+ memory T-cells (D); N.S., not significant; %BL, percent of baseline.

3.6.4 Pre-challenge secreted cytokine levels correlate with post-challenge plasma viremia and memory CD4+ T-cell counts

Subsequent to the observations that cytokines differentially affected virus replication kinetics *ex vivo*, the capacity of these factors to predict post-challenge outcomes was assessed. Correlation statistics were computed to determine associations of the various cytokines secreted *ex vivo* on the day of challenge, with plasma viremia after challenge.

High IL-10 in infected cultures was significantly associated with reduced viral load in plasma during post-acute and chronic phases of infection (Fig. 3.6.4.1 A & B) but not with acute-phase viral load. MIP-1β was positively though not significantly associated with plasma viremia (Fig. 3.6.4.1C). MIP-1α that was significantly associated with reduced viral replication *ex vivo* did not however, correlate with plasma viremia after challenge. Further analysis showed that animals producing high amounts of IL-1β in cultures on DoC also had significantly high acute and post-acute viral load in plasma after challenge (Fig. 3.6.4.1 D & E). These animals also had high chronic phase viremia (data not shown). The same was true for animals producing large amounts of the α-chemokine CXCL10 in their DoC plasma. Increased DoC CXCL10 correlated positively with acute (data not shown) and significantly with post-acute (Fig. 3.6.4.1F) plasma viremia. Five out of 7 animals that replicated SIV rapidly *ex vivo* also produced high CXCL10 in cultures, (see fig. 3.5.2 A & B). Four of the 5 high CXCL10 producers turned out to be fast progressors with one animal (#2175) dying early at 12 weeks after challenge. Similarly, acute-phase plasma CXCL10 appearing after challenge correlated positively with acute plasma viral load ($p=0.1$). The reverse implications of these associations means that increased concentrations of MIP-1β, IL-1β and CXCL10 may be detrimental in SIV infection, and that these cytokines may either be beneficial or have non-effect at low concentrations.

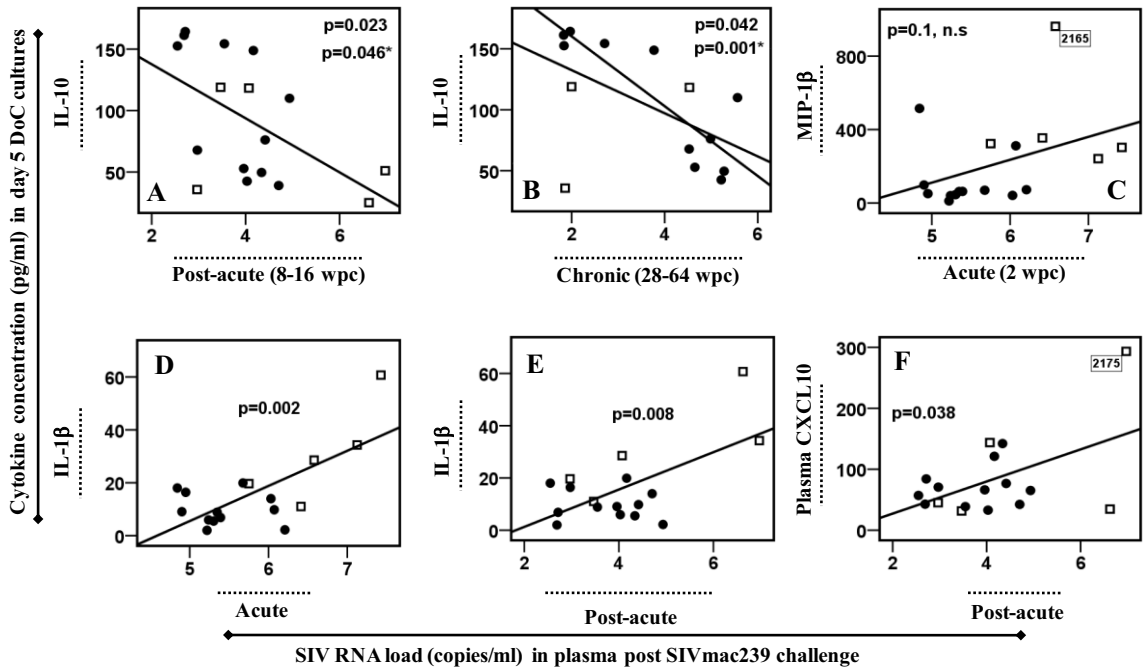

Figure 3.6.4.1: Associations of pre-challenge chemokines with plasma viral load.
Open squares, control animals; Filled circles, vaccinees. IL-10 in *ex vivo* infected DoC cell cultures correlated inversely with post-acute (A) and chronic (B) phase plasma viremia after challenge. MIP-1β correlated positively but not significantly with acute plasma viremia (C). IL-1β was associated positively with plasma viremia during the entire post-challenge phases examined. This association is shown here for acute (D) and post-acute (E) phases. Pre-challenge (DoC) plasma CXCL10 was positively and significantly associated with plasma viremia after challenge (F).

Because of the importance of memory CD4+ T-cell in progression of SIV/HIV-1 infection, the relationship between the above chemokines and CD4+ T-cells was examined. High amounts of IL-1β in infected cultures on DoC correlated significantly with loss of acute (Fig 3.6.4.2A) and post-acute (Fig 3.6.4.2B) memory CD4+ T-cells while animals producing less of this cytokine better preserved their memory T-cell pool. The same was true for MIP-1β secreted in these infected cultures (Fig 3.6.4.2C) and CXCL10 in uninfected DoC plasma (Fig 3.6.4.2D), both correlating with loss of memory CD4+ T-cells. These data complete the previous hypothesis that IL-1β, MIP-1β and CXCL10 may worsen prognosis by suppressing virus-specific immune responses.

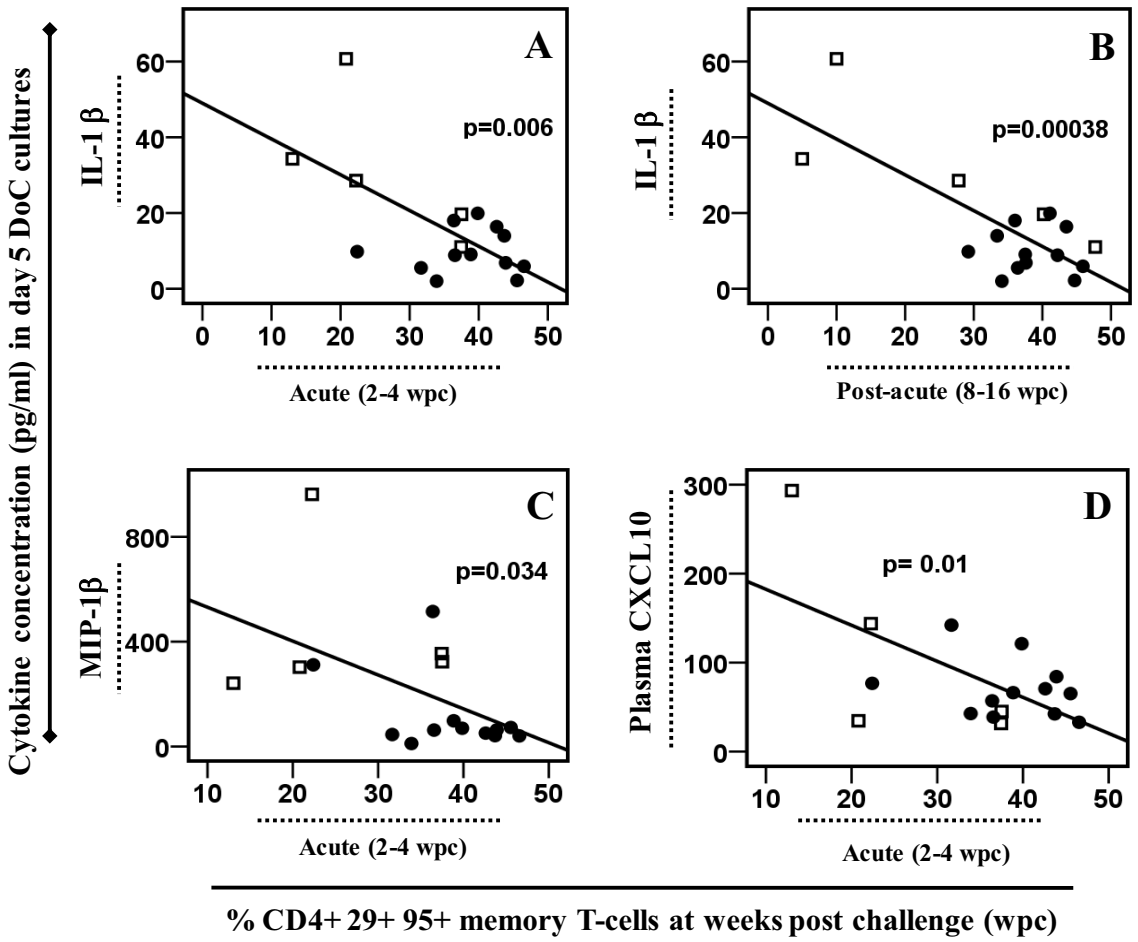

Figure 3.6.4.2: Associations of pre-challenge chemokines with memory CD4+ T- cells.

Open squares, control animals; Filled circles, vaccinees. High levels of IL-1β in pre-challenge *ex vivo* infected (DoC) cultures were associated significantly with loss of CD4+ T-cell memory during both post-challenge acute (A) and post-acute (B) infection phases. Similarly, high MIP-1β in these cultures (C) and CXCL10 in DoC plasma (D) were both associated significantly with loss of memory CD4+ T-cells after SIVmac239 challenge.

4.0 DISCUSSIONS

This chapter discusses the *ex vivo* infection model as a surrogated for measuring virus-specific vaccine-induced immune responses, and the protective efficacy of the experimental vaccine against SIV infection of macaques. Importantly, the chapter aims at interfacing the *ex vivo* infection model with the conventional pre-clinical monkey challenge model by comparing the various outcome variables across the two models.

4.1 *Ex vivo* susceptibility to SIV infection.

Using SIV RNA load in supernatants of *in vitro* infected PBMCs as an index for intrinsic susceptibility and *ex vivo* virus replication (VVR), VVR kinetics varying by more than 400-fold was observed between individual animals before immunization. When sham immunised control animals were followed over 11 months, their VVRs remained stable. These observations concur with suggestions that susceptibility to infection was an intrinsic property of the individual animal (Seman *et al.*, 2000). After immunization, the variation observed between individual high and low replicators increased to over 2000-fold, suggesting that intrinsic differences significantly pre-empted the outcome of vaccination. The number of INFγ-secreting cells is functionally linked to CTL responses (McKay *et al.*, 2002; Negri *et al.*, 2006) while noncytotoxic responses mediate viral suppression (Geiben-Lynn *et al.*, 2001; Walker *et al.*, 1991). Since both these cytolytic and noncytotoxic immunological responses constitute an integral part of cell-mediated immunity, the effects of INFγ and CNAR on susceptibility to SIV infection were assessed. Two to 4 weeks after systemic rAD5/SIV vaccine boosting, both INFγ and CNAR significantly correlated with attenuation in susceptibility to infection. This pattern was less evident after oral boosting of the mucosal group, possibly because oral rAD5/SIV administration alone did not deliver a boosting effect except when followed by a systemic rAd5-SIV application. Overall, systemic-only boosting resulted in CNAR still measurable on DoC, which also correlated inversely with DoC VVR. The number

of INFγ-producing cells was low by this time. The short stimulation time in the IFNγ ELISPOT assay allows only for measurements of effector cells which are abundant shortly after immunization but wane afterwards. On the other hand it is likely that activation of memory cells during several days of culture contributes to VVR suppression and CNAR production long after the last immunization.

Although the beneficial effect of CNAR has been reported in highly active antiretroviral treatment (HAART) of HIV-1 infected individuals (Castelli *et al.*, 2002; Torres *et al.*, 2006), this study provides the first evidence that vaccination is associated with a significantly raised non-cytotoxic antiviral response that suppresses SIV *ex vivo* independent of INFγ activity. A study in which monkeys were vaccinated with a *nef*-deleted live virus and challenged with a heterologous strain found significant correlations between soluble INFγ and CD8+ T cell-dependent antiviral activity (Goletti *et al.*, 2006). In this study, the number of INFγ ELISPOT-secreting cells did not correlate with CNAR, and statistical analyses suggested that these two influenced viral replication independently. The lack of association between these two variables may because the ELISPOT assay does not measure the amount of IFNγ available in its soluble form, while CNAR suppression is due entirely to soluble factors *In vitro* studies have shown that virus suppression does not always depend on cytokine production by T-cells (Chung *et al.*, 2006). This study provides data suggesting that virus replication is suppressed by additional hitherto unidentified factors. Put together, these data represent the first evidence that inducible innate immunity plays a significant role in the outcome of a pre-clinical vaccine trial. Whether *ex vivo* CNAR production correlates with *in vivo* parameters of protection will be discussed in the subsequent sections.

4.2 Control of viremia after challenge.

Although all animals got infected with high acute viremia 2 weeks after inoculation with SIVmac239, vaccinated animals significantly controlled acute viremia compared to non-immunized controls. However, the difference in viremia control dissipated fast as the animals transitioned into chronic phase of infection.

This was not unexpected, because acute infection is normally characterised by higher magnitudes of anti-viral cytotoxic T-lymphocyte (CTL) which offer protective advantage to immunised compared to unimmunised animals (Leslie *et al.*, 2004). But these CTL pressures eventually select for viral escape, a process that tends to reduce the protective efficacy of the vaccines that rely entirely on CTLs (Barouch *et al.*, 2002a). Moreover, control of acute infection is subject to additional individual host defence system (Blackburn & Wherry, 2007). Some viruses may however, revert to become CTL-sensitive upon transmission to an entirely different host, thus restoring the ability of these T-cells to control the infection (Friedrich *et al.*, 2004). Acute viremia control by these vaccinated animals indicates that the vaccine had induced reasonable virus-specific immunity that partially protects from SIV infection. This immune-mediated protection was associated with robust re-call responses as evident by the increased numbers of memory CD4+ T-cells. Indeed, an earlier study by the group at the German Primate Centre showed that vaccination delayed the loss of CD4+ T-cells upon infection (Suh *et al.*, 2006), while others showed that reduction in acute viremia was associated with preservation memory CD4+ T-cells (Mattapallil *et al.*, 2006) . From this and earlier data, it is possible that preservation of this T-cell lineage may occur as an early immunological event which confers progressive survival advantage during the course of infection.

To further understand the aspects of effector immune responses associated with the observed control of infection, SIV-specific IFNγ responses were investigated. The numbers of IFNγ-producing cells were significantly increased during acute infection. Correlation analysis showed that these IFNγ-producing cells were inversely and significantly associated with plasma viral loads, lasting through post-acute and early chronic setpoint. This association was instructive, because vaccinees also preserved their CD4+ memory T-cells during this phase. The vaccine-mediated preservation of these CD4+ T-cells by vaccinees supersedes their destruction (Letvin *et al.*, 2006; Sun *et al.*, 2006), thus conferring the vaccinees with functionally competent T-cells (Pal *et al.*, 2002). This preserved capacity is characterised by positive effector function,

such as strong IFNγ responses. An improved association between viral load and IFNγ-expression was found after resolution of acute infection. Post-acute phase viremia control may be associated with the levels of memory CD4+ T-cells appearing during acute infection, and/or with the short-lived expansion of MHC-class 1-restricted IFNγ-secreting virus-specific CTL epitopes (Acierno *et al.*, 2006; Cayabyab *et al.*, 2006). The peptides used for the ELISPOT assay in this study were too short to allow binding and measurement of IFNγ-producing CD4+ T cells. Hence and although viral load correlated both with IFNγ ELISPOT and CD4+ T-cells, the number of IFNγ-producing cells did not correlate with CD4+ T-cells. It is possible that this effector function was linked more to CD8+ than CD4+ T-cells (Horton *et al.*, 2006), and that a majority of CD4+ memory T-cells did not augment CD8+ T-cell responses.

Because CD8+ T-cell are less susceptible to antigen-mediated CTL killing than CD4+ T-cells (Liu & Roederer, 2007), a substantial amount of effector immune function during acute infection is expected to be linked to CD8+ T-cells. In this study, late chronic viral loads from 28 weeks post-challenge were not associated with the number of IFNγ-producing cells. This phase is established by viral mutants that escape virus-specific CTL-mediated killing during acute infection (Allen *et al.*, 2005), albeit these mutants may have reduced fitness compared to wild-type viruses (Friedrich *et al.*, 2004). Since these escape mutants continue to destroy a majority of antiviral T-cells, immune regeneration is compromised leading to progressive development of immunodeficiency. The virus may also enter latency, during which time it is inaccessible to the immune system. Controlling infection during this phase requires virus activation in order to focus the viruses to the immune defence machinery (Rabbi *et al.*, 1998). Lack of association in the late chronic phase also signified a dissipation in IFNγ-depended viremia control possibly due to the short biological half-life and an intricate pharmacokinetic or signalling pathway of this cytokine (Brysha *et al.*, 2001; Houglum, 1983; Platanias, 2005). In fact, chronic infection is intriguing because not all antigen-specific responses during this phase can control infection. One study showed that HIV-gag specific responses were associated

with control of viral replication, while responses specific for HIV envelope and accessory proteins were associated with increase viral replication (Kiepiela *et al.*, 2007). Moreover, a generalised impairment of IFN-γ-secretion during chronic viral replication may also diminish IFNγ-mediated viremia control (Sutherland *et al.*, 2006).

In conclusion, this section demonstrated that immunisation with DNA followed by recombinant adenovirus vector expressing SIV proteins partially protects from acute SIV infection. This protection is linked to preservation of CD4+ T-cell memory and other effector immune functions.

4.3 Influence of MHC-class 1 alleles on *ex vivo* and *in vivo* virus replication.

Restriction by the classical MHC class 1 regions plays a pivotal role in many disease outcomes. This section discusses the influence of MHC alleles on *ex vivo* virus replication kinetics (VVR) and on the *in vivo* outcome of infection. Infected PBMCs from all the animals before any immunization revealed no difference in their susceptibility to SIV *ex vivo*, suggesting an invariably different capacity of vaccine-naïve cells to replicate the virus. However, the susceptibility of immunized macaque PBMCs was greatly compromised. Because MHC class-1 genotype contributes to differential pattern of infection and disease, (Muhl *et al.*, 2002; O'Connor *et al.*, 2003), it was hypothesised that MHC-1 allele restrictions were key to this intrinsic property. As the first step in examining this hypothesis, differences in VVR kinetics were analysed between animals expressing the highly virus-restrictive *Mamu-A*01* allele and those lacking this allele. This analysis was done before immunization and repeated during immunization. *Mamu-A*01* positive animals maintained lower viral loads after *in vitro* infection, but these were not statistically different from VVR of *Mamu-A*01* negative animals. The small number of *Mamu-A*01* positive animals (n=6, two in each of the 3 groups) may have precluded robust statistical power to necessitate definitive conclusion. Nevertheless, it was still valid within this limited context to examine how the viral load profiles differed between *Mamu-A*01* positive and

negative animals under the influence of immunization. During the 44 weeks of follow-up, VVR was significantly attenuated after the two vaccine boosts, but these changes were not significantly influenced by the *A*01* allele. On the contrary, *A*01* negative immunized animals suppressed SIV *ex vivo* much better than their *A*01* positive immunized counterparts. This observation implied, at least in the context of this study, that MHC class 1 restriction neither influenced intrinsic susceptibility nor vaccine-mediated VVR outcome.

To further validate this observation, effect of this allele on plasma viral load was examined after challenge. Like in the *ex vivo* model, all *Mamu-A*01* positive animals poorly replicated the virus *in vivo* after challenge, although this did not differ significantly from *A*01* negative animals. Out of the 6 *A*01* positive animals, 4 also carried the *B*17* allele, both of which are associated with low viral loads (Yant *et al.*, 2006). All these 4 animals turned to be elite controllers of SIV after challenge independent of immunization status. Elite virus-control is linked to overrepresentation of some MHC alleles in the macaque population (Loffredo *et al.*, 2007). This may explain why the animals expressing both *A*01* and *B*17* alleles significantly controlled SIV after challenge. However, the presence of *Mamu-A*01* and *-B*17* alone may not be sufficient to induce elite virus control. In one study, animals that inherited the *-B*17*-containing haplotype demonstrated a widely divergent disease course (Wojcechowskyj *et al.*, 2007). Although the same limitation of sample size hampered conclusive statistical interpretations of the influence of these alleles on virus replication, the reduced viral load profiles for *-A*01+B*17+* compared to allele negative animals were a clear indication of a non-chance invariance.

Because HIV-1 or SIV infection can lead to either rapidly progressive or long-term and persistent infection, it is thought that multiple genetic factors may predispose to this different disease outcome. Expression of a rare HLA allele in human populations is associated with a slow disease progression (Trachtenberg *et al.*, 2003). By extension, the virus rapidly adapts to the most frequently expressed alleles, putting those individuals expressing these frequent alleles at a selective disadvantage. These high frequency (HiFreq) alleles may also simply

have no role in cell mediated immune response (Loffredo *et al.*, 2005). Conversely, some of these alleles have the ability to present antigen to CTL and induce virus-specific immunity (Miller *et al.*, 1991). Due to these conflicting possibilities, this section also examined the role of HiFreq *Mamu* class B alleles on viral plasma loads. This examination narrowed on the effects of a combination of multiple (*Mamu-B*22*, *B*30* and *B*57*) and not single HiFreq alleles. These alleles are thought to be present on one haplotype (Otting *et al.*, 2005). All (11/18) animals expressing all three HiFreq alleles had significantly higher viral loads in plasma than animals lacking this allele combination. This was only partly true for the *ex vivo* infected PBMC cultures. But these results did not hold true when only one of the 3 HiFreq alleles was used as the factor of analysis. These observations imply that these multiple frequently expressed MHC alleles put the host at a more disadvantaged position than singly expressed HiFreq alleles and may provide an explanation for the phenotypic differences in disease progression after challenge. Immunised monkeys seemed to respond very well during immunisation. But 12 weeks after *in vivo* infection, these responses vanished and the animals homozygous for the Mamu-B*22, B*30 and B*57 either died or started progressing to death. It is possible that CTLs restricted by Mamu-B*22, B*30 and B*57 induce very early viral escape which facilitates rapid progression.

Further analysis showed that control of acute viremia was dependent on vaccination and not on *Mamu-A*01* MHC allele (see figure 4.4.1A). It is possible that the vaccine effect that was limited to acute infection was as a result of strong acute-phase CTL responses. Immunised animals usually show strong virus-specific IFNγ ELISPOT responses (Suh *et al.*, 2006), but these diminish fast after acute infection. In the present study, the vaccine-induced viremia control disappeared after resolution of acute infection, possibly due to rapid selection of viral mutants that escape CTL (Yu *et al.*, 2007). It may be possible that the selection of these mutants is influenced by both the vaccine-induced immunological pressures and the presence of HiFreq alleles. These escape mutants evade immune surveillance to establish rapidly progressive and chronic infection independent of vaccine-mediated responses. Here, chronic viremia was

maintained at significantly low threshold for a prolonged duration in all the animals. To examine whether this chronic viral suppression was linked to particular MHC alleles, viral loads in plasma of only the immunized animals were compared between those expressing and those lacking the *Mamu-A*01* allele. This analysis revealed a significantly lower chronic setpoint viral loads in *-A*01* positive than A*01 negative animals. Put together, these observations exemplified a pattern in which acute viral infection was subject to vaccine induced viral clearance while chronic infection was under the control of MHC-driven genetic or intrinsic factors. In order to contain acute infections to their lowest thresholds, vaccine designs should focus on eliciting strong and broad CTLs that are specific for the diverse populations of escape viral variants. In addition, therapeutic vaccines should be able to activate viral replication from latent reservoirs and target them to the diverse vaccine-mediated CTLs in order to effectively control chronic infection.

4.4 Influence of cytokines and chemokines on *ex vivo* SIV infection.

Any single cytokine may possess both anti and pro-inflammatory functions that produce two opposite effects on infection outcomes (Abel *et al.*, 2004). Studies have shown that CD8+ T-cell supernatant cultures can suppress HIV-1 independently of beta chemokine activity (Moriuchi *et al.*, 1996). To assess the role of multiple cytokines and chemokine on SIV infection and susceptibility, these factors were monitored in infected cell culture supernatants and compared with viral load.

4.4.1 Kinetics of cytokines and chemokines in *ex vivo* infected PBMC cultures.

At week 26 after a single vaccine boost, PBMCs of immunised animals secreted higher amounts of IFNγ than the control group. These were also much higher for the Systemic than Mucosal vaccine groups. MIP-1α was comparable among groups though slightly elevated in the Systemic group. MCP-1, MIP-1β and IL-1β were lowest the Systemic group, low in the Mucosal group and highest in

controls animals. RANTES and IL-10 were largely comparable among groups. These profiles also coincided with better control of *ex vivo* viral replication (VVR) in the Systemic group at week 26. Surprisingly however, these cytokine kinetics reversed on the day of challenge (DoC). On DoC, PBMCs of the Systemic group animals secreted less IFNγ than either the Mucosal or control group. Control animals still secreted more IL-1β and MIP-1β and MCP-1 than vaccinees. But DoC IL10 was highest in the Systemic group followed by the mucosal group and lowest in control animals. Between the vaccinees, IL-1β and MIP-1 were high in the Systemic group and low in the mucosal group on DoC. At this time, the VVR kinetics was also reversed, with the Systemic group showing reduced ability to control VVR compared to 26 wdi. These observations suggest a concentration-dependent effect of most cytokines on virus replication. For instance, MCP-1 has been found to enhance rather than inhibit virus replication when secreted in high amounts (Vicenzi *et al.*, 2000). This is quite instructive, because elevated levels of this chemokine in the DoC cultures also coincided with increased rate of virus replication in the *ex vivo* infected cultures, confirming that MCP-1-mediated response is concentration-dependent (Loetscher *et al.*, 1994; Roth *et al.*, 1995). During the *ex vivo* infection, all cytokines declined rapidly, with IFNγ and IL-1β diminishing faster towards undetectability while TNFα was completely undetectable. It is likely that the suppressive effects of other anti-inflammatory cytokines could be attributed to this diminished cytokine secretion kinetics (Pott *et al.*, 2007). Indeed, IL10 has been has bee shown to depress TNFα secretion in HIV-1 infected adults (Andrade *et al.*, 2007), and IL-10 was highly abundant in all cultures. Finally, it is also possible that these cytokines have a shorter biological half-life that is not favoured by the longer periods of culture.

4.4.2 Association of β-chemokines and cytokines with *ex vivo* SIV replication.

Primary HIV-1 infection is accompanied by expression of high levels of both pro- and anti- inflammatory cytokines. Expansions of CD8+ T cells during primary infection influences production cytokine such as IFNγ while progression to HIV-1

disease is accompanied by increased TNFα and IL-10 (Graziosi *et al.*, 1996). In this study, IL-10 persisted during prolonged periods of *ex vivo* cultures when most pro-inflammatory cytokines had disappeared. This persistence may be attributed to the fact that IL-10 is expressed under the direct influence of the lentiviral transcriptional regulator, *tat* (Gee *et al.*, 2007). Because of this regulatory mechanism, IL-10 has been reported to be associated positively with increased rate of retroviral replication (Jinquan *et al.*, 1993). This was not the case in the present study, because most animals secreting large amounts of this cytokine in cultures also had reduced viral loads, although the associations were not statistically significant. Others have shown that IL-10 can suppress HIV infection through down-modulation of TNFα expression (Chang *et al.*, 1996; Naif *et al.*, 1996). This fits in the present framework, because TNFα was not detected even after only 24 hrs of polyclonal stimulation of these cells. It has also been demonstrated that IL-10 inhibits HIV-1 replication in primary monocytes and macrophages at various stages of maturation (Chang *et al.*, 1996). This inhibition of HIV-1 gene expression is more potent when IL-10 is present before infection than when administered after infection (Naif *et al.*, 1996). Parallel studies asserted this position, showing that IL-10 given 72 hrs before infection or within 24 hrs of infection delayed the onset of HIV-1 LTR reverse transcription and reduced the amounts of viral transcripts in tissues culture (Montaner *et al.*, 1994). The latter study also hypothesised that IL-10 induces viral latency *in vitro* without modulating cell surface CD4+ expression. Based on these studies, the lack of significant association between IL-10 and suppression of SIV *ex vivo* despite being secreted in large amounts can be inferred. In the present *ex vivo* infection model, the virus was introduced 24 hrs after stimulation and not before, thereby potentiating a reduction in the antiviral efficacy of this cytokine (Naif *et al.*, 1996).

RANTES, MIP-1α and MIP-1β are all associated with suppression of both HIV-1 and SIV (Chelucci *et al.*, 1999; Cocchi *et al.*, 1995; Ondoa *et al.*, 2002). These chemokines/cytokines correlate with immune activation and inflammatory responses in the genital mucosa of HIV-1 positive individuals (Behbahani *et al.*, 2007). Their increased secretion also correlates with lack of AIDS (Garzino-

Demo *et al.*, 1999). But these factors may also induce the synthesis and release of other pro-inflammatory cytokines associated with acute inflammation. Here, high MIP-1α was significantly associated with depressed virus replication *ex vivo*. Conversely, increased production of MIP-1β and IL-1β were both associated with increased susceptibility. In addition, these cytokines were secreted in higher amounts in cultures of unimmunised animals that did not suppress SIV than in immunised animal cultures that suppressed SIV. Expression of IL-1β is induced by the HIV-1 gp120 protein (Corasaniti *et al.*, 2001), and increased expression of this cytokine correlates with disease pathology in humans (Bagetta *et al.*, 1999; Russo *et al.*, 2007; Zhao *et al.*, 2001). In tissues and certain cell-types, IL-1β achieves a toxic potential via activation of inflammatory enzymes such as nitric oxide synthase (Boven *et al.*, 2003), further worsening AIDS pathogenesis. The data presented here suggest that immunization may selectively induce cytokine secretion which in turn, suppresses virus replication in a concentration-dependent manner.

In the presence of IL-2 and IFN-γ, RANTES induces the proliferation and activation of certain natural killer (NK) cells to become CC-Chemokine-activated killer (CHAK) cells (Maghazachi *et al.*, 1996). In addition RANTES competes with SIV with the CCR5 coreceptors. Because of this, high RANTES should correlate with reduced viral load and resistance to infection. However, RANTES was not associated with *ex vivo* resistance to SIV in this study. This observation is consistent with reports that RANTES may not after all, correlate directly with resistance of cells to infection (Ahmed *et al.*, 2001; Ahmed *et al.*, 2002; Schwartz *et al.*, 1997). It is possible that the antiviral activities of this and other cytokines are dampened by other anti-inflammatory processes that are not adequately regulated *ex vivo*.

4.4.3 CXCL10 is associated with increased susceptibility to SIV.

Subsequent analysis focused on the anti-inflammatory chemokine, gamma inducible protein 10 (IP-10), also called CXCL10. This α-chemokine is normally produced in response to IFNγ and is known to suppress production of other

cytokines. Like IL-1β, CXCL10 induces selective cell death in neuron cells *in vitro*, a process that requires the HIV-1 *nef* gene (van Marle *et al.*, 2004). In this study, CXCL10 in culture supernatants obtained at week 26 after first vaccine boosting was much lower in the Systemic group that also controlled SIV replication than either the Mucosal or Control group that did not control VVR. But on the day of challenge, CXCL10 in the Systemic group was significantly elevated, and these animals could no longer control their VVR, suggesting that this chemokine may have contributed to the reversal of virus kinetics in these PBMCs. By comparison, immunized animals secreted less CXCL10 in plasma before infection on DoC than control animals. After acute infection at 2 weeks, plasma CXCL10 was significantly increased in all animals compared to pre-infection plasma levels. Unlike in the pre-challenge plasma, these post-challenge plasma CXCL10 levels were slightly raised in immunised compared to control animals. This increased post-challenge plasma CXCL10 indicates that anamnestic responses after infection may drive antiviral T-cells into a state of immune exhaustion. The positive correlation between plasma CXCL10 and IL-10 indicates a possible antagonism between IL10-mediated virus suppression and CXCL10-mediated immune suppression.

A positive association has been reported between CXCL10 and SIV replication in both vaccine-naïve and immunised animals that were non-responsive to immunisation (Abel *et al.*, 2004). In this study, high amounts of CXCL10 in plasma just before SIVmac239 challenge were positively associated with *ex vivo* VVR of macaque PBMCs. It remains to be seen if blocking or depleting this chemokine reverses its immunosuppressive effect to allow immune recovery and efficient virus control.

4.5 *Ex vivo* model as a predictive surrogate for post-challenge outcome.

Neither IFNγ ELISPOT responses alone nor variations in the macaque MHC class 1 could offer independent explanations on why the studied animals differed in their *ex vivo* susceptibility to infection by SIV. Since immunisation was associated with virus suppression both *ex vivo* and *in vivo* after challenge, it was

hypothesised that susceptibility before challenge would determine the outcome of infection after challenge.

4.5.1 Intrinsic susceptibility predicts viremia and CD4+ T-cell memory after challenge.

Unimmunised and immunised macaques whose PBMCs replicated the virus less efficiently *ex vivo* also maintained significantly lower viremia and better preserved their memory CD4+ T-cell subsets *in vivo* after challenge than high replicators. The characteristically high T-cell memory in vaccinees was possibly the result of reduced viral burden or a reflection of vaccine-induced expansion of virus-specific cells (Staprans *et al.*, 2004). The preservation of memory T-cell subsets is associated with a better prognosis of HIV/SIV infection *in vivo* (Acierno *et al.*, 2006; Letvin *et al.*, 2006), but whether preservation of these T-cell subsets is already pre-defined before infection has not been examined. In this study, VVR on the day of challenge (DoC) was highly predictive of plasma viremia post-challenge in both immunised and non-immunised macaques. Similarly, VVR better predicted memory T-cell levels and offered a better indication of vaccine efficacy than IFNγ ELISPOT results. Overall, VVR still predicted plasma viremia and CD4+ T-cells during post-acute and chronic setpoint, an observation that shows the potential efficacy of this *ex vivo* model both in experimental vaccine testing and in pathogenesis studies.

4.5.2 Pre-challenge CNAR but not IFNγ ELISPOT predicts post-challenge plasma viremia and memory CD4+ T-cells.

Since epitope-specific CD8+ T-cells may alone not contribute to elite viral control (Chung *et al.*, 2006), virus suppression by CD8+ T-cells may additionally require non-cytolytic or other unidentified antiviral mechanisms. Suppression via the noncytotoxic mechanism is mediated by the CD8+ T-cell noncytotoxic antiviral response (CNAR) (Geiben-Lynn *et al.*, 2001; Walker *et al.*, 1991). Both CNAR and IFNγ-secreting cells were detected at significant amounts and were

associated with suppression of virus replication *ex vivo* (VVR). But only CNAR still significantly influenced VVR 44 weeks after immunization.

While there were no significant associations between pre-challenge IFNγ ELISPOT results and respective post-challenge outcomes, CNAR was highly predictive of acute through chronic viremia. CNAR was also associated with preserved acute and post-acute phase memory CD4+ T-cells. These associations could be attributed to sustained production of soluble factors as opposed to CTL responses. During viral latency, a critical microenvironment exists that sustains low-level infection (Kemball *et al.*, 2005; Kemball *et al.*, 2006). In the SIV model where there is no prolonged latency, this microenvironment may provide a survival advantage via an alternative innate mechanism before restoration of virus specific CTLs. The lack of association between pre-challenge IFNγ-ELISPOT and post-challenge plasma viremia or CD4+ T-cells can only be inferred. Multiple viral antigens are expressed simultaneously by multigenic vaccines (Hel *et al.*, 2006). These antigens compete for presentation, eventually dampening the quality antigen-specific T-cell responses. On the other hand, the ELISPOT technique only determines the number of CD8+ T-cells producing IFNγ upon stimulation with appropriate peptide mixture. However, these numbers may not accurately reflect the number of cells able to kill infected cells. In addition, this test does not measure the antiviral effect of soluble IFNγ. From these data, it is reasonable to postulate that post-acute and chronic viral infection is influenced by non-cytotoxic antiviral activities, which may play a major role in limiting viral replication as well as facilitating recovery of virus-specific immune responses. Vaccine designs that ensure sustained non-cytotoxic antiviral responses may improve robustness and efficacy of vaccines. Additional effort should focus on characterization of the mediators of CNAR in animal models and human elite controllers.

4.5.3 Beta chemokines correlate differentially with efficacy of vaccine-induced protection.

The effects of cytokines on *ex vivo* virus replication were addressed in section 4.4. This section examines whether the capacity to secret cytokines *ex vivo* can predict the control of viremia and preservation of memory CD4+ T-cells after challenge. High secreted levels of the pro-inflammatory proteins MIP-1β and IL-1β in the *ex-vivo* infected cultures were both associated with increased plasma viral load and with depressed memory CD4+ T-cells. Conversely, animals that produced high amounts of the immunomodulatory IL-10 in infected cultures also maintained low plasma viral loads during post-acute and chronic setpoint after challenge. This observation fits into a conflicting body of literature regarding the role of this cytokine in viral infection. During progressive HIV-1 infection, IL-10 may dampen the immune response by inhibiting both the function of natural killer cell activity and cell-to-cell contact-mediated cytolysis of infected cells (Elrefaei *et al.*, 2007). Moreover in chronic infection, IL-10 is expected to inhibit antiviral T-cell function (Brooks *et al.*, 2006; Ejrnaes *et al.*, 2006; Elrefaei *et al.*, 2006). This part of the paradigm supports IL-10 as a stimulator rather than inhibitor of viral replication (Chang *et al.*, 1996; Naif *et al.*, 1996). But IL10 also produces an entirely opposite effect. One study hypothesised that IL10 can induce viral latency *in vitro*, and that IL10-mediated virus regulation may be associated with the control of HIV-1 *in vivo* (Montaner *et al.*, 1994). Moreover, increased production of IL10 is associated with slow disease progression in HIV-1 infected adults (Andrade *et al.*, 2007). Put together, these data suggest that individual animals that harboured capacity to secrete sufficient amounts of IL-10 before infection also had the intrinsic capacity to control virus replication upon challenge with the pathogenic virus.

4.5.4 Pre-challenge levels of CXCL10 correlate with post-challenge plasma viremia and memory CD4+ T-cells.

Apart from high viral loads, not much is known about which factors drive the destruction of memory CD4+ T-cells during acute infection. Nevertheless, direct

killing of infected CD4 cells cannot solely explain their rapid decline. Here, elevated plasma CXCL10 on the day of challenge and during acute infection after challenge was associated with increased plasma SIV RNA load and low memory CD4+ T-cells. In people infected with HIV-1, high amounts of the stromal-derived factor-1 (SDF-1), a CXC chemokine, correlates with low serum viral burden and better survival time (Xiang *et al.*, 2004). In SIV infected animals, CXCL10 correlates positively with virus replication (Abel *et al.*, 2004). High CXCL10 has also been shown to correlate with reduced white blood cell counts in cerebrospinal fluid as well as with elevated plasma viral load (Cinque *et al.*, 2005). This chemokine is produced in response to increased IFNγ expression. In this study, immunised animals had high amounts of IFNγ-producing cells *ex vivo* and also secreted higher amounts of IFNγ in cultures compared to control animals. These pre-challenge IFNγ levels did not however, correlate with post-challenge plasma viremia or CD4+ memory T-cells. The lack of association may indicate a shift in immunological focus towards inflammation by inducing secretion of CXCL-10 that dampens virus-specific immunity. This IFNγ-driven CXCL10-mediated inflammation ultimately lowers the protective efficacy of candidate HIV-1/SIV vaccines (Abel *et al.*, 2004). This study hypothesises that CXCL10 may upregulate SIV infection leading to the destruction of virus-specific T-cell memory. The mechanism may involve chemokine-mediated engagement of virus regulatory machinery to drive the immune system into exhaustion and failure. It is important that vaccine designs ensure a balance between pro- and anti-inflammatory responses in order to ensure sustained vaccine effect.

5. CONCLUSIONS

In this study, an *ex vivo* infection model that has a reliable capacity to predict outcome of a pre-clinical HIV-1 vaccine has been developed. Multiple aspects of this model contribute to its efficacy as an infection surrogate. Using this *ex vivo* infection system, susceptibility to SIV infection was demonstrated to vary between individual animals before and during immunisation. The intrinsic variation before challenge was influenced differentially by β- and α-chemokines/cytokines and by other noncytotoxic antiviral response mechanisms. Moreover, the intrinsic susceptibility of individual animals accurately predicted the major outcome variables including plasma viral load and memory CD4+ T-cell counts after the macaques were exposed to the challenge virus.

It was also demonstrated that vaccinated animals produced less of most cytokines. It is worth considering vaccine designs that allow *de novo* regulation of cytokine synthesis. Avenues to consider include selective secretion of beneficial cytokines such as MIP-1α and IL-10 and down-regulation of CXCL10, IL-1β and MIP-1β. In order to mitigate the effects of CTL-mediated viral escape, candidate vaccines should also balance between cytotoxic and noncytotoxic responses. In addition, therapeutic vaccines should be designed to generate sustained responses against chronically replicating virus, should target escape viral mutants and activate the latent viruses.

Overall, this study shows that the *ex vivo* challenge model allows for evaluation of vaccine potency prior to challenge. In human AIDS vaccine trials, volunteer PBMCs could be used to rapidly determine the efficacy of candidate vaccines prior to infection exposure. This approach spares time and financial, human, and animal resources while circumventing ethical and design constraints. Independent investigations should confirm if the technique can be adapted to other unrelated viruses and vaccine studies.

6.0 SUMMARY

Efficacy assessment of AIDS vaccines relies both on pre-clinically challenging immunised monkeys with a pathogenic virus and subsequent monitoring of infection rates in large human trials. Conventional parameters of vaccine-induced immune responses do not completely predict outcome. Moreover, existing methods for testing cellular immunity are sophisticated and difficult to establish in resource-limited settings, thereby constraining large studies. There is a need for study models that bridge the gap between preclinical and clinical vaccine testing, and which are able to predict a virus-specific vaccine effect before actual challenge. Virus replication kinetics (VVR) on ConA-stimulated peripheral blood mononuclear cells (PBMC) was used as an *ex vivo* model to mimic the interaction between different components of the immune system and viral infection. PBMCs were obtained from the 17 experimental rhesus monkeys before immunisation and subsequently at 12, 26 and 44 weeks during immunisation (wdi). Before immunization, VVR of vaccine-naïve PBMCs varied between individual animals by between >430-fold and >60-fold after 7 and 10 days of infection cultures. VVR of sham-vaccinated control monkeys remained constant over 44 the weeks. However, VVR of immunised animals was significantly attenuated during this follow-up period. This effect was not influenced by the MHC- class 1 *Mamu-A*01* allele, which is normally associated with slow disease progression. VVR was instead dependent on the number of IFNγ-producing cells (p=0.001), CD8+ T-cell non-cytotoxic antiviral response (CNAR) (p=0.01) and MIP-1α (p=0.013). High VVR correlated with increased CXCL10, IL-1β and MIP-1β. Importantly, pre-challenge VVR, CXCL10, IL-1β and MIP-1β but not IFNγ correlated directly with acute plasma viremia and inversely with memory CD4+ T-cell counts after SIVmac239 challenge. VVR was thus able to predict disease progression and the protective capacity of the vaccine regime. Likewise, pre-challenge CNAR, MIP-1α and IL-10 were associated inversely with acute-phase plasma viremia and directly with memory CD4+ T-cell concentrations in blood. When applied to human studies, this *ex vivo* infection

technique could predict the efficacy of candidate AIDS vaccines prior to phase III clinical trials.

6.0 ZUSAMMENFASSUNG

Um die Wirksamkeit von Impfstoffen gegen AIDS zu untersuchen, werden in präklinischen Studien immunisierte Makaken mit pathogenem SIV (Simian Immunodefciency Virus) infiziert, oder die Infektionsraten in großen klinischen Studien am Menschen verglichen. Trotz aufwendiger Tests zur Überprüfung der Immunogenität solcher Impfstoffe kann die Wirksamkeit einer Vakzine nicht vorhergesagt werden. Es ist daher wichtig, ein *ex vivo* Modell zu entwickeln, um diese Lücke zu schließen. In der vorliegenden Arbeit wurden hierzu mononukleäre Blutzellen (PBMC) aus Affen isoliert, *in vitro* mit SIV infiziert und die Replikationskinetik des Virus (VVR) untersucht. Dieses *ex vivo* Modell simuliert die Interaktion des Virus mit verschiedenen Komponenten des Immunsystem. Die VVR wurde von 17 Rhesusaffen vor Immunisierung und in der 12., 26. und 44. Woche während der Immunisierungsphase untersucht. Vor der Immunisierung variierte die interindividuelle VVR bis zu 430-fach am Tag 7 und bis zu 60-fach am Tag 10 nach der Infektion. In den nicht immunisierten Kontrolltieren blieb die individuelle VVR während der Immunisierungsphase unverändert. Durch die Immunisierung wurde die VVR dagegen signifikant reduziert. Dieser Effekt wurde nicht durch ein MHC Klasse I-Allel, welches mit langsamem Krankheitsverlauf assoziiert ist, beeinflusst. In den immunisierten Tieren war die VVR abhängig von der Zahl IFNγ-produzierender Zellen ($p=0.001$), sowie einer durch lösliche Faktoren vermittelter antiviralen Aktivität (CNAR; $p=0.01$) und dem Chemokin MIP-1α ($p=0.013$). Hohe VVR korrelierte mit erhöhtem CXCL10, IL-1β und MIP-1β. Der Vergleich der Daten, die vor und nach der Belastungs-infektion der Versuchstiere gewonnen wurden, zeigte, dass hohe VVR sowie erhöhte Konzentrationen von CXCL10, IL-1β und MIP-1β, nicht aber virus-spezifische IFNγ-produzierende Zellen direkt mit der Virusbeladung im Plasma während der akuten Infektion und invers mit der Zahl der CD4+-Gedächtniszellen korrellierten. Die VVR, CNAR, MIP-1α und IL-10 waren invers mit der Virusbeladung während der akuten Infektion und direkt mit der Zahl der CD4+ Gedächtniszellen korreliert. Das hier vorgestellte *ex vivo* Modell ist daher geeignet, um den Krankheitsverlauf und die Wirksamkeit einer Vakzine gegen

AIDS vor einer Infektion zu prognostizieren. Wenn die Aussagekraft dieses Modell durch Untersuchungen am Menschen bestätigt wird, könnte die Wirksamkeit eines Impfstoffes vor der Durchführung eines klinischen Versuch der Phase III prognostiziert werden.

7.0 REFERENCES

Abel, K., La Franco-Scheuch, L., Rourke, T., Ma, Z. M., De Silva, V., Fallert, B., Beckett, L., Reinhart, T. A. & Miller, C. J. (2004). Gamma interferon-mediated inflammation is associated with lack of protection from intravaginal simian immunodeficiency virus SIVmac239 challenge in simian-human immunodeficiency virus 89.6-immunized rhesus macaques. *Journal of virology* **78**, 841-854.

Acierno, P. M., Schmitz, J. E., Gorgone, D. A. & other authors (2006). Preservation of functional virus-specific memory CD8+ T lymphocytes in vaccinated, simian human immunodeficiency virus-infected rhesus monkeys. *J Immunol* **176**, 5338-5345.

Ahmed, R. K., Nilsson, C., Biberfeld, G. & Thorstensson, R. (2001). Role of CD8+ cell-produced anti-viral factors in protective immunity in HIV-2-exposed but seronegative macaques resistant to intrarectal SIVsm challenge. *Scandinavian journal of immunology* **53**, 245-253.

Ahmed, R. K., Makitalo, B., Karlen, K., Nilsson, C., Biberfeld, G. & Thorstensson, R. (2002). Spontaneous production of RANTES and antigen-specific IFN-gamma production in macaques vaccinated with SHIV-4 correlates with protection against SIVsm challenge. *Clinical and experimental immunology* **129**, 11-18.

Allen, S. J., Crown, S. E. & Handel, T. M. (2007). Chemokine: receptor structure, interactions, and antagonism. *Annual review of immunology* **25**, 787-820.

Allen, T. M., Yu, X. G., Kalife, E. T. & other authors (2005). De novo generation of escape variant-specific CD8+ T-cell responses following cytotoxic T-lymphocyte escape in chronic human immunodeficiency virus type 1 infection. *Journal of virology* **79**, 12952-12960.

Anderson, D. E., Llenado, R. A. & Torres, J. V. (2004). Humoral immunity and the evolution of HIV-2. *Viral immunology* **17**, 436-439.

Andrade, R. M., Lima, P. G., Filho, R. G. & other authors (2007). Interleukin-10-secreting CD4 cells from aged patients with AIDS decrease in-vitro HIV replication and tumour necrosis factor alpha production. *AIDS (London, England)* **21**, 1763-1770.

Ashorn, P., McQuade, T. J., Thaisrivongs, S., Tomasselli, A. G., Tarpley, W. G. & Moss, B. (1990). An inhibitor of the protease blocks maturation of human and simian immunodeficiency viruses and spread of infection. *Proceedings of the National Academy of Sciences of the United States of America* **87**, 7472-7476.

Bagetta, G., Corasaniti, M. T., Berliocchi, L., Nistico, R., Giammarioli, A. M., Malorni, W., Aloe, L. & Finazzi-Agro, A. (1999). Involvement of interleukin-1beta in the mechanism of human immunodeficiency virus type 1 (HIV-1) recombinant protein gp120-induced apoptosis in the neocortex of rat. *Neuroscience* **89**, 1051-1066.

Barouch, D. H., Kunstman, J., Kuroda, M. J. & other authors (2002a). Eventual AIDS vaccine failure in a rhesus monkey by viral escape from cytotoxic T lymphocytes. *Nature* **415**, 335-339.

Barouch, D. H., Santra, S., Tenner-Racz, K. & other authors (2002b). Potent CD4+ T cell responses elicited by a bicistronic HIV-1 DNA vaccine expressing gp120 and GM-CSF. *J Immunol* **168**, 562-568.

Behbahani, H., Walther-Jallow, L., Klareskog, E. & other authors (2007). Proinflammatory and type 1 cytokine expression in cervical mucosa during HIV-1 and human papillomavirus infection. *Journal of acquired immune deficiency syndromes (1999)* **45**, 9-19.

Berrey, M. M., Schacker, T., Collier, A. C. & other authors (2001). Treatment of primary human immunodeficiency virus type 1 infection with potent antiretroviral therapy reduces frequency of rapid progression to AIDS. *The Journal of infectious diseases* **183**, 1466-1475.

Blackburn, S. D. & Wherry, E. J. (2007). IL-10, T cell exhaustion and viral persistence. *Trends in microbiology* **15**, 143-146.

Bontrop, R. E. & Watkins, D. I. (2005). MHC polymorphism: AIDS susceptibility in non-human primates. *Trends in immunology* **26**, 227-233.

Boven, L. A., Vergnolle, N., Henry, S. D., Silva, C., Imai, Y., Holden, J., Warren, K., Hollenberg, M. D. & Power, C. (2003). Up-regulation of proteinase-activated receptor 1 expression in astrocytes during HIV encephalitis. *J Immunol* **170**, 2638-2646.

Brave, A., Ljungberg, K., Boberg, A., Rollman, E., Engstrom, G., Hinkula, J. & Wahren, B. (2006). Reduced cellular immune responses following immunization with a multi-gene HIV-1 vaccine. *Vaccine* **24**, 4524-4526.

Brooks, D. G., Trifilo, M. J., Edelmann, K. H., Teyton, L., McGavern, D. B. & Oldstone, M. B. (2006). Interleukin-10 determines viral clearance or persistence in vivo. *Nature medicine* **12**, 1301-1309.

Brown, K., Gerstberger, S., Carlson, L., Franzoso, G. & Siebenlist, U. (1995). Control of I kappa B-alpha proteolysis by site-specific, signal-induced phosphorylation. *Science (New York, NY* **267**, 1485-1488.

Bryant, M. & Ratner, L. (1990). Myristoylation-dependent replication and assembly of human immunodeficiency virus 1. *Proceedings of the National Academy of Sciences of the United States of America* **87**, 523-527.

Brysha, M., Zhang, J. G., Bertolino, P., Corbin, J. E., Alexander, W. S., Nicola, N. A., Hilton, D. J. & Starr, R. (2001). Suppressor of cytokine signaling-1 attenuates the duration of interferon gamma signal transduction in vitro and in vivo. *The Journal of biological chemistry* **276**, 22086-22089.

Buchbinder, S. P., Katz, M. H., Hessol, N. A., O'Malley, P. M. & Holmberg, S. D. (1994). Long-term HIV-1 infection without immunologic progression. *AIDS (London, England)* **8**, 1123-1128.

Bushman, F. D., Fujiwara, T. & Craigie, R. (1990). Retroviral DNA integration directed by HIV integration protein in vitro. *Science* **249**, 1555-1558.

Capon, D. J. & Ward, R. H. (1991). The CD4-gp120 interaction and AIDS pathogenesis. *Annual review of immunology* **9**, 649-678.

Cardozo, T., Kimura, T., Philpott, S., Weiser, B., Burger, H. & Zolla-Pazner, S. (2007). Structural basis for coreceptor selectivity by the HIV type 1 V3 loop. *AIDS research and human retroviruses* **23**, 415-426.

Casimiro, D. R., Chen, L., Fu, T. M. & other authors (2003a). Comparative immunogenicity in rhesus monkeys of DNA plasmid, recombinant vaccinia virus, and replication-defective adenovirus vectors expressing a human immunodeficiency virus type 1 gag gene. *Journal of virology* **77**, 6305-6313.

Casimiro, D. R., Tang, A., Chen, L. & other authors (2003b). Vaccine-induced immunity in baboons by using DNA and replication-incompetent adenovirus type 5 vectors expressing a human immunodeficiency virus type 1 gag gene. *Journal of virology* **77**, 7663-7668.

Casimiro, D. R., Wang, F., Schleif, W. A. & other authors (2005). Attenuation of simian immunodeficiency virus SIVmac239 infection by prophylactic immunization with dna and recombinant adenoviral vaccine vectors expressing Gag. *Journal of virology* **79**, 15547-15555.

Castaldello, A., Brocca-Cofano, E., Voltan, R. & other authors (2006). DNA prime and protein boost immunization with innovative polymeric cationic core-shell nanoparticles elicits broad immune responses and strongly enhance cellular responses of HIV-1 tat DNA vaccination. *Vaccine* **24**, 5655-5669.

Castelli, J. C., Deeks, S. G., Shiboski, S. & Levy, J. A. (2002). Relationship of CD8(+) T cell noncytotoxic anti-HIV response to CD4(+) T cell number in untreated asymptomatic HIV-infected individuals. *Blood* **99**, 4225-4227.

Caulfield, M. J., Smith, J. G., Wang, S., Capen, R. C., Blondeau, C., Lentsch, S., Arminjon, F. & Sabouraud, A. (2000). Immunogenicity of a hexavalent combination vaccine in rhesus monkeys. *Vaccine* **19**, 902-907.

Cayabyab, M. J., Hovav, A. H., Hsu, T. & other authors (2006). Generation of CD8+ T-cell responses by a recombinant nonpathogenic Mycobacterium smegmatis vaccine vector expressing human immunodeficiency virus type 1 Env. *Journal of virology* **80**, 1645-1652.

Chang, J., Naif, H. M., Li, S., Jozwiak, R., Ho-Shon, M. & Cunningham, A. L. (1996). The inhibition of HIV replication in monocytes by interleukin 10 is linked to inhibition of cell differentiation. *AIDS research and human retroviruses* **12**, 1227-1235.

Chelucci, C., Casella, I., Federico, M. & other authors (1999). Lineage-specific expression of human immunodeficiency virus (HIV) receptor/coreceptors in differentiating hematopoietic precursors: correlation with susceptibility to T- and M-tropic HIV and chemokine-mediated HIV resistance. *Blood* **94**, 1590-1600.

Chen, B., Vogan, E. M., Gong, H., Skehel, J. J., Wiley, D. C. & Harrison, S. C. (2005). Structure of an unliganded simian immunodeficiency virus gp120 core. *Nature* **433**, 834-841.

Chen, L. F. & Greene, W. C. (2003). Regulation of distinct biological activities of the NF-kappaB transcription factor complex by acetylation. *Journal of molecular medicine (Berlin, Germany)* **81**, 549-557.

Chen, L. F. & Greene, W. C. (2004). Shaping the nuclear action of NF-kappaB. *Nature reviews* **5**, 392-401.

Chen, Z., Earl, P., Americo, J. & other authors (2007). Characterization of chimpanzee/human monoclonal antibodies to the vaccinia A33 glycoprotein and its variola virus homolog in vitro and in a vaccinia mouse protection model. *Journal of virology*.

Chun, T. W., Stuyver, L., Mizell, S. B., Ehler, L. A., Mican, J. A., Baseler, M., Lloyd, A. L., Nowak, M. A. & Fauci, A. S. (1997). Presence of an inducible HIV-1 latent reservoir during highly active antiretroviral therapy. *Proceedings of the National Academy of Sciences of the United States of America* **94**, 13193-13197.

Chun, T. W., Justement, J. S., Moir, S. & other authors (2001). Suppression of HIV replication in the resting CD4+ T cell reservoir by autologous CD8+ T cells: implications for the development of therapeutic strategies. *Proceedings of the National Academy of Sciences of the United States of America* **98**, 253-258.

Chung, C., Lee, W., Loffredo, J. T. & other authors (2006). Not all cytokine-producing CD8+ T-cells suppress simian immunodeficiency virus replication. *Journal of virology*.

Cinque, P., Bestetti, A., Marenzi, R., Sala, S., Gisslen, M., Hagberg, L. & Price, R. W. (2005). Cerebrospinal fluid interferon-gamma-inducible protein 10 (IP-10, CXCL10) in HIV-1 infection. *Journal of neuroimmunology* **168**, 154-163.

Cocchi, F., DeVico, A. L., Garzino-Demo, A., Arya, S. K., Gallo, R. C. & Lusso, P. (1995). Identification of RANTES, MIP-1 alpha, and MIP-1 beta as the major HIV-suppressive factors produced by CD8+ T cells. *Science* **270**, 1811-1815.

Cohen, E. A., Dehni, G., Sodroski, J. G. & Haseltine, W. A. (1990). Human immunodeficiency virus vpr product is a virion-associated regulatory protein. *Journal of virology* **64**, 3097-3099.

Corasaniti, M. T., Turano, P., Bilotta, A., Malorni, W., Stringaro, A. R., Nistico, R., Finazzi-Agro, A. & Bagetta, G. (2001). Evidence that increases of mitochondrial immunoreactive IL-1beta by HIV-1 gp120 implicate in situ cleavage of pro-IL-1beta in the neocortex of rat. *Journal of neurochemistry* **78**, 611-618.

Daniel, M. D., Letvin, N. L., King, N. W., Kannagi, M., Sehgal, P. K., Hunt, R. D., Kanki, P. J., Essex, M. & Desrosiers, R. C. (1985). Isolation of T-cell tropic HTLV-III-like retrovirus from macaques. *Science* **228**, 1201-1204.

Devadas, K., Hardegen, N. J., Wahl, L. M., Hewlett, I. K., Clouse, K. A., Yamada, K. M. & Dhawan, S. (2004). Mechanisms for macrophage-mediated HIV-1 induction. *J Immunol* **173**, 6735-6744.

Dittmar, M. T., McKnight, A., Simmons, G., Clapham, P. R., Weiss, R. A. & Simmonds, P. (1997). HIV-1 tropism and co-receptor use. *Nature* **385**, 495-496.

Donlon, T. A., Krensky, A. M., Wallace, M. R., Collins, F. S., Lovett, M. & Clayberger, C. (1990). Localization of a human T-cell-specific gene, RANTES (D17S136E), to chromosome 17q11.2-q12. *Genomics* **6**, 548-553.

Dykhuizen, M., Mitchen, J. L., Montefiori, D. C., Thomson, J., Acker, L., Lardy, H. & Pauza, C. D. (1998). Determinants of disease in the simian immunodeficiency virus-infected rhesus macaque: characterizing animals with low antibody responses and rapid progression. *J Gen Virol* **79 (Pt 10)**, 2461-2467.

Egan, M. A., Megati, S., Roopchand, V. & other authors (2006). Rational design of a plasmid DNA vaccine capable of eliciting cell-mediated immune responses to multiple HIV antigens in mice. *Vaccine* **24**, 4510-4523.

Ejrnaes, M., Filippi, C. M., Martinic, M. M., Ling, E. M., Togher, L. M., Crotty, S. & von Herrath, M. G. (2006). Resolution of a chronic viral infection after interleukin-10 receptor blockade. *The Journal of experimental medicine* **203**, 2461-2472.

Elrefaei, M., Barugahare, B., Ssali, F., Mugyenyi, P. & Cao, H. (2006). HIV-specific IL-10-positive CD8+ T cells are increased in advanced disease and are associated with decreased HIV-specific cytolysis. *J Immunol* **176**, 1274-1280.

Elrefaei, M., Ventura, F. L., Baker, C. A., Clark, R., Bangsberg, D. R. & Cao, H. (2007). HIV-specific IL-10-positive CD8+ T cells suppress cytolysis and IL-2 production by CD8+ T cells. *J Immunol* **178**, 3265-3271.

Fackler, O. T., Alcover, A. & Schwartz, O. (2007). Modulation of the immunological synapse: a key to HIV-1 pathogenesis? *Nature reviews* **7**, 310-317.

Faure, E., Lecine, P., Lipcey, C., Champion, S. & Imbert, J. (1997). Cell-to-cell contact activates the long terminal repeat of human immunodeficiency virus 1 through its kappaB motif. *European journal of biochemistry / FEBS* **244**, 568-574.

Feng, S. & Holland, E. C. (1988). HIV-1 tat trans-activation requires the loop sequence within tar. *Nature* **334**, 165-167.

Fernandez, E. J. & Lolis, E. (2002). Structure, function, and inhibition of chemokines. *Annual review of pharmacology and toxicology* **42**, 469-499.

Fitzgerald, J. C., Gao, G. P., Reyes-Sandoval, A., Pavlakis, G. N., Xiang, Z. Q., Wlazlo, A. P., Giles-Davis, W., Wilson, J. M. & Ertl, H. C. (2003). A simian replication-defective adenoviral recombinant vaccine to HIV-1 gag. *J Immunol* **170**, 1416-1422.

Flynn, N. M., Forthal, D. N., Harro, C. D., Judson, F. N., Mayer, K. H. & Para, M. F. (2005). Placebo-controlled phase 3 trial of a recombinant glycoprotein 120 vaccine to prevent HIV-1 infection. *J Infect Dis* **191**, 654-665.

Fouchier, R. A., Groenink, M., Kootstra, N. A., Tersmette, M., Huisman, H. G., Miedema, F. & Schuitemaker, H. (1992). Phenotype-associated sequence variation in the third variable domain of the human immunodeficiency virus type 1 gp120 molecule. *Journal of virology* **66**, 3183-3187.

Franke, E. K., Yuan, H. E. & Luban, J. (1994). Specific incorporation of cyclophilin A into HIV-1 virions. *Nature* **372**, 359-362.

Fridholm, H. & Everitt, E. (2005). Rapid and reproducible infectivity end-point titration of virulent phage in a microplate system. *J Virol Methods* **128**, 67-71.

Friedrich, T. C., Dodds, E. J., Yant, L. J. & other authors (2004). Reversion of CTL escape-variant immunodeficiency viruses in vivo. *Nature medicine* **10**, 275-281.

Fukasawa, M., Miura, T., Hasegawa, A., Morikawa, S., Tsujimoto, H., Miki, K., Kitamura, T. & Hayami, M. (1988). Sequence of simian immunodeficiency virus from African green monkey, a new member of the HIV/SIV group. *Nature* **333**, 457-461.

Fultz, P. N., McClure, H. M., Anderson, D. C., Swenson, R. B., Anand, R. & Srinivasan, A. (1986). Isolation of a T-lymphotropic retrovirus from naturally infected sooty mangabey monkeys (Cercocebus atys). *Proceedings of the National Academy of Sciences of the United States of America* **83**, 5286-5290.

Gallay, P., Swingler, S., Song, J., Bushman, F. & Trono, D. (1995). HIV nuclear import is governed by the phosphotyrosine-mediated binding of matrix to the core domain of integrase. *Cell* **83**, 569-576.

Gao, F., Bailes, E., Robertson, D. L. & other authors (1999). Origin of HIV-1 in the chimpanzee Pan troglodytes troglodytes. *Nature* **397**, 436-441.

Garzino-Demo, A., Moss, R. B., Margolick, J. B. & other authors (1999). Spontaneous and antigen-induced production of HIV-inhibitory beta-chemokines are associated with AIDS-free status. *Proceedings of the National Academy of Sciences of the United States of America* **96**, 11986-11991.

Gee, K., Angel, J. B., Mishra, S., Blahoianu, M. A. & Kumar, A. (2007). IL-10 regulation by HIV-Tat in primary human monocytic cells: involvement of calmodulin/calmodulin-dependent protein kinase-activated p38 MAPK and Sp-1 and CREB-1 transcription factors. *J Immunol* **178**, 798-807.

Geiben-Lynn, R., Kursar, M., Brown, N. V., Kerr, E. L., Luster, A. D. & Walker, B. D. (2001). Noncytolytic inhibition of X4 virus by bulk CD8(+) cells from human

immunodeficiency virus type 1 (HIV-1)-infected persons and HIV-1-specific cytotoxic T lymphocytes is not mediated by beta-chemokines. *Journal of virology* **75**, 8306-8316.

Goldstein, S., Brown, C. R., Dehghani, H., Lifson, J. D. & Hirsch, V. M. (2000). Intrinsic susceptibility of rhesus macaque peripheral CD4(+) T cells to simian immunodeficiency virus in vitro is predictive of in vivo viral replication. *Journal of virology* **74**, 9388-9395.

Goletti, D., Kinter, A. L., Hardy, E. C., Poli, G. & Fauci, A. S. (1996). Modulation of endogenous IL-1 beta and IL-1 receptor antagonist results in opposing effects on HIV expression in chronically infected monocytic cells. *J Immunol* **156**, 3501-3508.

Goletti, D., Macchia, I., Leone, P. & other authors (2006). Innate anti-viral immunity is associated with the protection elicited by the simian immunodeficiency virus (SIV) live attenuated virus vaccine in cynomolgus monkeys. *Med Sci Monit* **12**, BR330-340.

Gorse, G. J., Patel, G. B., Mandava, M. D., Arbuckle, J. A., Doyle, T. M. & Belshe, R. B. (2001). Cytokine responses to human immunodeficiency virus type 1 (HIV-1) induced by immunization with live recombinant canarypox virus vaccine expressing HIV-1 genes boosted by HIV-1(SF-2) recombinant GP120. *Vaccine* **19**, 1806-1819.

Gottlinger, H. G., Sodroski, J. G. & Haseltine, W. A. (1989). Role of capsid precursor processing and myristoylation in morphogenesis and infectivity of human immunodeficiency virus type 1. *Proceedings of the National Academy of Sciences of the United States of America* **86**, 5781-5785.

Graham, B. S. & Mascola, J. R. (2005). Lessons from failure--preparing for future HIV-1 vaccine efficacy trials. *J Infect Dis* **191**, 647-649.

Graziosi, C., Gantt, K. R., Vaccarezza, M. & other authors (1996). Kinetics of cytokine expression during primary human immunodeficiency virus type 1 infection. *Proceedings of the National Academy of Sciences of the United States of America* **93**, 4386-4391.

Greene, W. C. & Chen, L. F. (2004). Regulation of NF-kappaB action by reversible acetylation. *Novartis Foundation symposium* **259**, 208-217; discussion 218-225.

Greenland, J. R., Geiben, R., Ghosh, S., Pastor, W. A. & Letvin, N. L. (2007). Plasmid DNA vaccine-elicited cellular immune responses limit in vivo vaccine antigen expression through Fas-mediated apoptosis. *J Immunol* **178**, 5652-5658.

Harrich, D., Ulich, C. & Gaynor, R. B. (1996). A critical role for the TAR element in promoting efficient human immunodeficiency virus type 1 reverse transcription. *Journal of virology* **70**, 4017-4027.

Heinzinger, N. K., Bukinsky, M. I., Haggerty, S. A. & other authors (1994). The Vpr protein of human immunodeficiency virus type 1 influences nuclear localization of viral nucleic acids in nondividing host cells. *Proceedings of the National Academy of Sciences of the United States of America* **91**, 7311-7315.

Hel, Z., Tsai, W. P., Tryniszewska, E. & other authors (2006). Improved vaccine protection from simian AIDS by the addition of nonstructural simian immunodeficiency virus genes. *J Immunol* **176**, 85-96.

Hendel, H., Caillat-Zucman, S., Lebuanec, H. & other authors (1999). New class I and II HLA alleles strongly associated with opposite patterns of progression to AIDS. *J Immunol* **162**, 6942-6946.

Hirsch, V. M., Fuerst, T. R., Sutter, G. & other authors (1996). Patterns of viral replication correlate with outcome in simian immunodeficiency virus (SIV)-infected macaques: effect of prior immunization with a trivalent SIV vaccine in modified vaccinia virus Ankara. *Journal of virology* **70**, 3741-3752.

Hofmann-Lehmann, R., Swenerton, R. K., Liska, V., Leutenegger, C. M., Lutz, H., McClure, H. M. & Ruprecht, R. M. (2000). Sensitive and robust one-tube real-time reverse transcriptase-polymerase chain reaction to quantify SIV RNA load: comparison of one- versus two-enzyme systems. *AIDS research and human retroviruses* **16**, 1247-1257.

Horton, H., Frank, I., Baydo, R. & other authors (2006). Preservation of T cell proliferation restricted by protective HLA alleles is critical for immune control of HIV-1 infection. *J Immunol* **177**, 7406-7415.

Houglum, J. E. (1983). Interferon: mechanisms of action and clinical value. *Clin Pharm* **2**, 20-28.

Jacks, T., Power, M. D., Masiarz, F. R., Luciw, P. A., Barr, P. J. & Varmus, H. E. (1988). Characterization of ribosomal frameshifting in HIV-1 gag-pol expression. *Nature* **331**, 280-283.

Jinquan, T., Larsen, C. G., Gesser, B., Matsushima, K. & Thestrup-Pedersen, K. (1993). Human IL-10 is a chemoattractant for CD8+ T lymphocytes and an inhibitor of IL-8-induced CD4+ T lymphocyte migration. *J Immunol* **151**, 4545-4551.

Jones, K. A., Kadonaga, J. T., Luciw, P. A. & Tjian, R. (1986). Activation of the AIDS retrovirus promoter by the cellular transcription factor, Sp1. *Science (New York, NY* **232**, 755-759.

Jung, S., Knauer, O., Donhauser, N., Eichenmuller, M., Helm, M., Fleckenstein, B. & Reil, H. (2005). Inhibition of HIV strains by GB virus C in cell culture can be mediated by CD4 and CD8 T-lymphocyte derived soluble factors. *AIDS (London, England)* **19**, 1267-1272.

Kahn, J. O. & Walker, B. D. (1998). Acute human immunodeficiency virus type 1 infection. *The New England journal of medicine* **339**, 33-39.

Keele, B. F., Van Heuverswyn, F., Li, Y. & other authors (2006). Chimpanzee reservoirs of pandemic and nonpandemic HIV-1. *Science (New York, NY* **313**, 523-526.

Kemball, C. C., Lee, E. D., Vezys, V., Pearson, T. C., Larsen, C. P. & Lukacher, A. E. (2005). Late priming and variability of epitope-specific CD8+ T cell responses during a persistent virus infection. *J Immunol* **174**, 7950-7960.

Kemball, C. C., Lee, E. D., Szomolanyi-Tsuda, E., Pearson, T. C., Larsen, C. P. & Lukacher, A. E. (2006). Costimulation requirements for antiviral CD8+ T cells differ for acute and persistent phases of polyoma virus infection. *J Immunol* **176**, 1814-1824.

Kestler, H. W., 3rd, Ringler, D. J., Mori, K., Panicali, D. L., Sehgal, P. K., Daniel, M. D. & Desrosiers, R. C. (1991). Importance of the nef gene for maintenance of high virus loads and for development of AIDS. *Cell* **65**, 651-662.

Kiepiela, P., Ngumbela, K., Thobakgale, C. & other authors (2007). CD8+ T-cell responses to different HIV proteins have discordant associations with viral load. *Nat Med* **13**, 46-53.

Kiernan, R., Bres, V., Ng, R. W., Coudart, M. P., El Messaoudi, S., Sardet, C., Jin, D. Y., Emiliani, S. & Benkirane, M. (2003). Post-activation turn-off of NF-kappa B-dependent transcription is regulated by acetylation of p65. *The Journal of biological chemistry* **278**, 2758-2766.

Killian, M. S., Ng, S., Mackewicz, C. E. & Levy, J. A. (2005). A screening assay for detecting CD8+ cell non-cytotoxic anti-HIV responses. *J Immunol Methods* **304**, 137-150.

Kim, S. Y., Byrn, R., Groopman, J. & Baltimore, D. (1989). Temporal aspects of DNA and RNA synthesis during human immunodeficiency virus infection: evidence for differential gene expression. *Journal of virology* **63**, 3708-3713.

Kindberg, E., Hejdeman, B., Bratt, G., Wahren, B., Lindblom, B., Hinkula, J. & Svensson, L. (2006). A nonsense mutation (428G-->A) in the fucosyltransferase FUT2 gene affects the progression of HIV-1 infection. *Aids* **20**, 685-689.

Kinter, A. L., Ostrowski, M., Goletti, D. & other authors (1996). HIV replication in CD4+ T cells of HIV-infected individuals is regulated by a balance between the viral suppressive effects of endogenous beta-chemokines and the viral inductive effects of other endogenous cytokines. *Proceedings of the National Academy of Sciences of the United States of America* **93**, 14076-14081.

Kuroda, M. J., Schmitz, J. E., Charini, W. A., Nickerson, C. E., Lifton, M. A., Lord, C. I., Forman, M. A. & Letvin, N. L. (1999). Emergence of CTL coincides with clearance of virus during primary simian immunodeficiency virus infection in rhesus monkeys. *J Immunol* **162**, 5127-5133.

Laakso, M. M. & Sutton, R. E. (2006). Replicative fidelity of lentiviral vectors produced by transient transfection. *Virology* **348**, 406-417.

LaBarre, D. D. & Lowy, R. J. (2001). Improvements in methods for calculating virus titer estimates from TCID50 and plaque assays. *J Virol Methods* **96**, 107-126.

Laing, K. J. & Secombes, C. J. (2004). Chemokines. *Developmental and comparative immunology* **28**, 443-460.

Landau, N. R., Warton, M. & Littman, D. R. (1988). The envelope glycoprotein of the human immunodeficiency virus binds to the immunoglobulin-like domain of CD4. *Nature* **334**, 159-162.

Lapadat-Tapolsky, M., De Rocquigny, H., Van Gent, D., Roques, B., Plasterk, R. & Darlix, J. L. (1993). Interactions between HIV-1 nucleocapsid protein and viral DNA may have important functions in the viral life cycle. *Nucleic acids research* **21**, 831-839.

Lee, A. H., Suh, Y. S. & Sung, Y. C. (1999). DNA inoculations with HIV-1 recombinant genomes that express cytokine genes enhance HIV-1 specific immune responses. *Vaccine* **17**, 473-479.

Lee, C. G., Choi, S. Y., Park, S. H., Park, K. S., Ryu, S. H. & Sung, Y. C. (2005). The synthetic peptide Trp-Lys-Tyr-Met-Val-D-Met as a novel adjuvant for DNA vaccine. *Vaccine* **23**, 4703-4710.

Leslie, A. J., Pfafferott, K. J., Chetty, P. & other authors (2004). HIV evolution: CTL escape mutation and reversion after transmission. *Nature medicine* **10**, 282-289.

Letvin, N. L., Daniel, M. D., Sehgal, P. K. & other authors (1985). Induction of AIDS-like disease in macaque monkeys with T-cell tropic retrovirus STLV-III. *Science* **230**, 71-73.

Letvin, N. L. (2005). Progress toward an HIV vaccine. *Annual review of medicine* **56**, 213-223.

Letvin, N. L., Mascola, J. R., Sun, Y. & other authors (2006). Preserved CD4+ central memory T cells and survival in vaccinated SIV-challenged monkeys. *Science (New York, NY* **312**, 1530-1533.

Lewis, P., Hensel, M. & Emerman, M. (1992). Human immunodeficiency virus infection of cells arrested in the cell cycle. *The EMBO journal* **11**, 3053-3058.

Lifson, J. D., Nowak, M. A., Goldstein, S. & other authors (1997). The extent of early viral replication is a critical determinant of the natural history of simian immunodeficiency virus infection. *Journal of virology* **71**, 9508-9514.

Liu, J. & Roederer, M. (2007). Differential susceptibility of leukocyte subsets to cytotoxic T cell killing: Implications for HIV immunopathogenesis. *Cytometry A* **71**, 94-104.

Liu, L. J., Watabe, S., Yang, J., Hamajima, K., Ishii, N., Hagiwara, E., Onari, K., Xin, K. Q. & Okuda, K. (2001). Topical application of HIV DNA vaccine with cytokine-expression plasmids induces strong antigen-specific immune responses. *Vaccine* **20**, 42-48.

Loetscher, P., Seitz, M., Clark-Lewis, I., Baggiolini, M. & Moser, B. (1994). Monocyte chemotactic proteins MCP-1, MCP-2, and MCP-3 are major attractants for human CD4+ and CD8+ T lymphocytes. *Faseb J* **8**, 1055-1060.

Loffredo, J. T., Sidney, J., Piaskowski, S. & other authors (2005). The high frequency Indian rhesus macaque MHC class I molecule, Mamu-B*01, does not appear to be involved in CD8+ T lymphocyte responses to SIVmac239. *J Immunol* **175**, 5986-5997.

Loffredo, J. T., Maxwell, J., Qi, Y. & other authors (2007). Mamu-B*08-positive macaques control simian immunodeficiency virus replication. *Journal of virology* **81**, 8827-8832.

Luckay, A., Sidhu, M. K., Kjeken, R. & other authors (2007). Effect of plasmid DNA vaccine design and in vivo electroporation on the resulting vaccine-specific immune responses in rhesus macaques. *Journal of virology* **81**, 5257-5269.

Luke, W., Voss, G., Stahl-Hennig, C., Coulibaly, C., Putkonen, P., Petry, H. & Hunsmann, G. (1993). Protection of cynomolgus macaques (Macaca fascicularis) against infection with the human immunodeficiency virus type 2 strain ben (HIV-2ben) by immunization with the virion-derived envelope glycoprotein gp130. *AIDS research and human retroviruses* **9**, 387-394.

Lwembe, R., Ochieng, W., Panikulam, A. & other authors (2007). Anti-retroviral drug resistance-associated mutations among non-subtype B HIV-1-infected Kenyan children with treatment failure. *Journal of medical virology* **79**, 865-872.

MacArthur, R. D., Perez, G., Walmsley, S., Baxter, J. D., Mullin, C. M. & Neaton, J. D. (2005). Comparison of prognostic importance of latest CD4+ cell count and HIV RNA levels in patients with advanced HIV infection on highly active antiretroviral therapy. *HIV Clin Trials* **6**, 127-135.

Mackewicz, C. E., Craik, C. S. & Levy, J. A. (2003). The CD8+ cell noncytotoxic anti-HIV response can be blocked by protease inhibitors. *Proceedings of the National Academy of Sciences of the United States of America* **100**, 3433-3438.

Maghazachi, A. A., Al-Aoukaty, A. & Schall, T. J. (1996). CC chemokines induce the generation of killer cells from CD56+ cells. *European journal of immunology* **26**, 315-319.

Mahlknecht, U., Deng, C., Lu, M. C., Greenough, T. C., Sullivan, J. L., O'Brien, W. A. & Herbein, G. (2000). Resistance to apoptosis in HIV-infected CD4+ T lymphocytes is mediated by macrophages: role for Nef and immune activation in viral persistence. *J Immunol* **165**, 6437-6446.

Malkevitch, N., Rohne, D., Pinczewski, J., Aldrich, K., Kalyanaraman, V. S., Letvin, N. L. & Robert-Guroff, M. (2004). Evaluation of combination DNA/replication-competent Ad-SIV recombinant immunization regimens in rhesus macaques. *AIDS research and human retroviruses* **20**, 235-244.

Malkevitch, N. V., Patterson, L. J., Aldrich, M. K. & other authors (2006). Durable protection of rhesus macaques immunized with a replicating adenovirus-SIV multigene

prime/protein boost vaccine regimen against a second SIVmac251 rectal challenge: role of SIV-specific CD8+ T cell responses. *Virology* **353**, 83-98.

Mallardo, M., Dragonetti, E., Baldassarre, F., Ambrosino, C., Scala, G. & Quinto, I. (1996). An NF-kappaB site in the 5'-untranslated leader region of the human immunodeficiency virus type 1 enhances the viral expression in response to NF-kappaB-activating stimuli. *The Journal of biological chemistry* **271**, 20820-20827.

Malm, M., Rollman, E., Ustav, M., Hinkula, J., Krohn, K., Wahren, B. & Blazevic, V. (2005). Cross-clade protection induced by human immunodeficiency virus-1 DNA immunogens expressing consensus sequences of multiple genes and epitopes from subtypes A, B, C, and FGH. *Viral immunology* **18**, 678-688.

Mann, D. L., Garner, R. P., Dayhoff, D. E. & other authors (1998). Major histocompatibility complex genotype is associated with disease progression and virus load levels in a cohort of human immunodeficiency virus type 1-infected Caucasians and African Americans. *The Journal of infectious diseases* **178**, 1799-1802.

Mattapallil, J. J., Douek, D. C., Buckler-White, A., Montefiori, D., Letvin, N. L., Nabel, G. J. & Roederer, M. (2006). Vaccination preserves CD4 memory T cells during acute simian immunodeficiency virus challenge. *The Journal of experimental medicine* **203**, 1533-1541.

McGettigan, J. P., Koser, M. L., McKenna, P. M., Smith, M. E., Marvin, J. M., Eisenlohr, L. C., Dietzschold, B. & Schnell, M. J. (2006). Enhanced humoral HIV-1-specific immune responses generated from recombinant rhabdoviral-based vaccine vectors co-expressing HIV-1 proteins and IL-2. *Virology* **344**, 363-377.

McKay, P. F., Schmitz, J. E., Barouch, D. H., Kuroda, M. J., Lifton, M. A., Nickerson, C. E., Gorgone, D. A. & Letvin, N. L. (2002). Vaccine protection against functional CTL abnormalities in simian human immunodeficiency virus-infected rhesus monkeys. *J Immunol* **168**, 332-337.

Mellors, J. W., Rinaldo, C. R., Jr., Gupta, P., White, R. M., Todd, J. A. & Kingsley, L. A. (1996). Prognosis in HIV-1 infection predicted by the quantity of virus in plasma. *Science (New York, NY* **272**, 1167-1170.

Miller, M. D., Yamamoto, H., Hughes, A. L., Watkins, D. I. & Letvin, N. L. (1991). Definition of an epitope and MHC class I molecule recognized by gag-specific cytotoxic T lymphocytes in SIVmac-infected rhesus monkeys. *J Immunol* **147**, 320-329.

Miller, M. D., Warmerdam, M. T., Gaston, I., Greene, W. C. & Feinberg, M. B. (1994). The human immunodeficiency virus-1 nef gene product: a positive factor for viral infection and replication in primary lymphocytes and macrophages. *The Journal of experimental medicine* **179**, 101-113.

Milush, J. M., Stefano-Cole, K., Schmidt, K., Durudas, A., Pandrea, I. & Sodora, D. L. (2007). Mucosal Innate Immune Response Associated With A Timely Humoral Immune Response And Slower Disease Progression Following Oral Transmission Of SIV In Rhesus Macaques. *J Virol*.

Montaner, L. J., Griffin, P. & Gordon, S. (1994). Interleukin-10 inhibits initial reverse transcription of human immunodeficiency virus type 1 and mediates a virostatic latent state in primary blood-derived human macrophages in vitro. *The Journal of general virology* **75 (Pt 12)**, 3393-3400.

Moriuchi, H., Moriuchi, M., Combadiere, C., Murphy, P. M. & Fauci, A. S. (1996). CD8+ T-cell-derived soluble factor(s), but not beta-chemokines RANTES, MIP-1 alpha, and MIP-1 beta, suppress HIV-1 replication in monocyte/macrophages. *Proceedings of the National Academy of Sciences of the United States of America* **93**, 15341-15345.

Muhl, T., Krawczak, M., Ten Haaft, P., Hunsmann, G. & Sauermann, U. (2002). MHC class I alleles influence set-point viral load and survival time in simian immunodeficiency virus-infected rhesus monkeys. *J Immunol* **169**, 3438-3446.

Muller, M. C. & Barre-Sinoussi, F. (2003). SIVagm: genetic and biological features associated with replication. *Front Biosci* **8**, d1170-1185.

Munch, J., Schindler, M., Wildum, S., Rucker, E., Bailer, N., Knoop, V., Novembre, F. J. & Kirchhoff, F. (2005). Primary sooty mangabey simian immunodeficiency virus and human immunodeficiency virus type 2 nef alleles modulate cell surface expression of various human receptors and enhance viral infectivity and replication. *Journal of virology* **79**, 10547-10560.

Munoz, A., Kirby, A. J., He, Y. D., Margolick, J. B., Visscher, B. R., Rinaldo, C. R., Kaslow, R. A. & Phair, J. P. (1995). Long-term survivors with HIV-1 infection: incubation period and longitudinal patterns of CD4+ lymphocytes. *J Acquir Immune Defic Syndr Hum Retrovirol* **8**, 496-505.

Murphey-Corb, M., Martin, L. N., Rangan, S. R., Baskin, G. B., Gormus, B. J., Wolf, R. H., Andes, W. A., West, M. & Montelaro, R. C. (1986). Isolation of an HTLV-III-related retrovirus from macaques with simian AIDS and its possible origin in asymptomatic mangabeys. *Nature* **321**, 435-437.

Nabel, G. & Baltimore, D. (1987). An inducible transcription factor activates expression of human immunodeficiency virus in T cells. *Nature* **326**, 711-713.

Naif, H. M., Chang, J., Ho-Shon, M., Li, S. & Cunningham, A. L. (1996). Inhibition of human immunodeficiency virus replication in differentiating monocytes by interleukin 10 occurs in parallel with inhibition of cellular RNA expression. *AIDS research and human retroviruses* **12**, 1237-1245.

Negri, D. R., Borghi, M., Baroncelli, S., Macchia, I., Buffa, V., Sernicola, L., Leone, P., Titti, F. & Cara, A. (2006). Identification of a cytotoxic T-lymphocyte (CTL) epitope recognized by Gag-specific CTLs in cynomolgus monkeys infected with simian/human immunodeficiency virus. *The Journal of general virology* **87**, 3385-3392.

Nerrienet, E., Santiago, M. L., Foupouapouognigni, Y. & other authors (2005). Simian immunodeficiency virus infection in wild-caught chimpanzees from cameroon. *Journal of virology* **79**, 1312-1319.

Newberg, M. H., McEvers, K. J., Gorgone, D. A., Lifton, M. A., Baumeister, S. H., Veazey, R. S., Schmitz, J. E. & Letvin, N. L. (2006). Immunodomination in the evolution of dominant epitope-specific CD8+ T lymphocyte responses in simian immunodeficiency virus-infected rhesus monkeys. *J Immunol* **176**, 319-328.

Nielsen, M. H., Pedersen, F. S. & Kjems, J. (2005). Molecular strategies to inhibit HIV-1 replication. *Retrovirology* **2**, 10.

O'Connor, D. H., Mothe, B. R., Weinfurter, J. T. & other authors (2003). Major histocompatibility complex class I alleles associated with slow simian immunodeficiency virus disease progression bind epitopes recognized by dominant acute-phase cytotoxic-T-lymphocyte responses. *Journal of virology* **77**, 9029-9040.

O'Neil, P. K., Sun, G., Yu, H., Ron, Y., Dougherty, J. P. & Preston, B. D. (2002). Mutational analysis of HIV-1 long terminal repeats to explore the relative contribution of reverse transcriptase and RNA polymerase II to viral mutagenesis. *The Journal of biological chemistry* **277**, 38053-38061.

Ochieng, W., Ogoyi, D., Mulaa, F. J., Ogola, S., Musoke, R. & Otsyula, M. G. (2006). Viral load, CD4+ T-lymphocyte counts and antibody titres in HIV-1 infected untreated children in Kenya; implication for immunodeficiency and AIDS progression. *African health sciences* **6**, 3-13.

Ondoa, P., Vingerhoets, J., Vereecken, C., van der Groen, G., Heeney, J. L. & Kestens, L. (2002). In vitro replication of SIVcpz is suppressed by beta-chemokines and CD8+ T cells but not by natural killer cells of infected chimpanzees. *AIDS research and human retroviruses* **18**, 373-382.

Ondoa, P., Vereecken, C., Fransen, K., Colebunders, R., van der Groen, G., Heeney, J. L. & Kestens, L. (2003). Human and simian immunodeficiency virus-infected chimpanzees do not have increased intracellular levels of beta-chemokines in contrast to infected humans. *Journal of medical virology* **69**, 297-305.

Orandle, M. S., Williams, K. C., MacLean, A. G., Westmoreland, S. V. & Lackner, A. A. (2001). Macaques with rapid disease progression and simian immunodeficiency virus encephalitis have a unique cytokine profile in peripheral lymphoid tissues. *Journal of virology* **75**, 4448-4452.

Otting, N. & Bontrop, R. E. (1993). Characterization of the rhesus macaque (Macaca mulatta) equivalent of HLA-F. *Immunogenetics* **38**, 141-145.

Otting, N., Heijmans, C. M., Noort, R. C., de Groot, N. G., Doxiadis, G. G., van Rood, J. J., Watkins, D. I. & Bontrop, R. E. (2005). Unparalleled complexity of the MHC class I region in rhesus macaques. *Proceedings of the National Academy of Sciences of the United States of America* **102**, 1626-1631.

Pal, R., Venzon, D., Letvin, N. L. & other authors (2002). ALVAC-SIV-gag-pol-env-based vaccination and macaque major histocompatibility complex class I (A*01) delay simian immunodeficiency virus SIVmac-induced immunodeficiency. *Journal of virology* **76**, 292-302.

Pal, R., Kalyanaraman, V. S., Nair, B. C. & other authors (2006). Immunization of rhesus macaques with a polyvalent DNA prime/protein boost human immunodeficiency virus type 1 vaccine elicits protective antibody response against simian human immunodeficiency virus of R5 phenotype. *Virology* **348**, 341-353.

Palmieri, C., Trimboli, F., Puca, A., Fiume, G., Scala, G. & Quinto, I. (2004). Inhibition of HIV-1 replication in primary human monocytes by the IkappaB-alphaS32/36A repressor of NF-kappaB. *Retrovirology* **1**, 45.

Pandrea, I., Apetrei, C., Dufour, J. & other authors (2006). Simian immunodeficiency virus SIVagm.sab infection of Caribbean African green monkeys: a new model for the study of SIV pathogenesis in natural hosts. *Journal of virology* **80**, 4858-4867.

Parham, P. & Ohta, T. (1996). Population biology of antigen presentation by MHC class I molecules. *Science* **272**, 67-74.

Parkin, N. T., Chamorro, M. & Varmus, H. E. (1992). Human immunodeficiency virus type 1 gag-pol frameshifting is dependent on downstream mRNA secondary structure: demonstration by expression in vivo. *Journal of virology* **66**, 5147-5151.

Patterson, L. J., Malkevitch, N., Venzon, D. & other authors (2004). Protection against mucosal simian immunodeficiency virus SIV(mac251) challenge by using replicating adenovirus-SIV multigene vaccine priming and subunit boosting. *Journal of virology* **78**, 2212-2221.

Paxton, W., Connor, R. I. & Landau, N. R. (1993). Incorporation of Vpr into human immunodeficiency virus type 1 virions: requirement for the p6 region of gag and mutational analysis. *Journal of virology* **67**, 7229-7237.

Platanias, L. C. (2005). Mechanisms of type-I- and type-II-interferon-mediated signalling. *Nat Rev Immunol* **5**, 375-386.

Ploquin, M. J., Diop, O. M., Sol-Foulon, N. & other authors (2004). DC-SIGN from African green monkeys is expressed in lymph nodes and mediates infection in trans of simian immunodeficiency virus SIVagm. *Journal of virology* **78**, 798-810.

Pott, G. B., Sailer, C. A., Porat, R. & other authors (2007). Effect of a four-week course of interleukin-10 on cytokine production in a placebo-controlled study of HIV-1-infected subjects. *Eur Cytokine Netw* **18**, 1-10.

Pryciak, P. M. & Varmus, H. E. (1992). Nucleosomes, DNA-binding proteins, and DNA sequence modulate retroviral integration target site selection. *Cell* **69**, 769-780.

Quinto, I., Puca, A., Greenhouse, J. & other authors (2004). High attenuation and immunogenicity of a simian immunodeficiency virus expressing a proteolysis-resistant inhibitor of NF-kappaB. *The Journal of biological chemistry* **279**, 1720-1728.

Rabbi, M. F., Finnegan, A., Al-Harthi, L., Song, S. & Roebuck, K. A. (1998). Interleukin-10 enhances tumor necrosis factor-alpha activation of HIV-1 transcription in latently infected T cells. *J Acquir Immune Defic Syndr Hum Retrovirol* **19**, 321-331.

Ramakrishna, L., Anand, K. K., Mohankumar, K. M. & Ranga, U. (2004). Codon optimization of the tat antigen of human immunodeficiency virus type 1 generates strong immune responses in mice following genetic immunization. *Journal of virology* **78**, 9174-9189.

Resch, W., Hoffman, N. & Swanstrom, R. (2001). Improved success of phenotype prediction of the human immunodeficiency virus type 1 from envelope variable loop 3 sequence using neural networks. *Virology* **288**, 51-62.

Robinson, J., Waller, M. J., Parham, P., de Groot, N., Bontrop, R., Kennedy, L. J., Stoehr, P. & Marsh, S. G. (2003). IMGT/HLA and IMGT/MHC: sequence databases for the study of the major histocompatibility complex. *Nucleic acids research* **31**, 311-314.

Rosen, O., Sharon, M., Quadt-Akabayov, S. R. & Anglister, J. (2006). Molecular switch for alternative conformations of the HIV-1 V3 region: implications for phenotype conversion. *Proceedings of the National Academy of Sciences of the United States of America* **103**, 13950-13955.

Roth, S. J., Carr, M. W. & Springer, T. A. (1995). C-C chemokines, but not the C-X-C chemokines interleukin-8 and interferon-gamma inducible protein-10, stimulate transendothelial chemotaxis of T lymphocytes. *European journal of immunology* **25**, 3482-3488.

Roy, S., Delling, U., Chen, C. H., Rosen, C. A. & Sonenberg, N. (1990). A bulge structure in HIV-1 TAR RNA is required for Tat binding and Tat-mediated trans-activation. *Genes & development* **4**, 1365-1373.

Rubbert, A., Weissman, D., Combadiere, C., Pettrone, K. A., Daucher, J. A., Murphy, P. M. & Fauci, A. S. (1997). Multifactorial nature of noncytolytic CD8+ T cell-mediated suppression of HIV replication: beta-chemokine-dependent and -independent effects. *AIDS research and human retroviruses* **13**, 63-69.

Ruben, S., Perkins, A., Purcell, R., Joung, K., Sia, R., Burghoff, R., Haseltine, W. A. & Rosen, C. A. (1989). Structural and functional characterization of human immunodeficiency virus tat protein. *Journal of virology* **63**, 1-8.

Russo, R., Siviglia, E., Gliozzi, M., Amantea, D., Paoletti, A., Berliocchi, L., Bagetta, G. & Corasaniti, M. T. (2007). Evidence Implicating Matrix Metalloproteinases in the Mechanism Underlying Accumulation of IL-1beta and Neuronal Apoptosis in the Neocortex of HIV/gp120-Exposed Rats. *Int Rev Neurobiol* **82C**, 407-421.

Saha, K., Bentsman, G., Chess, L. & Volsky, D. J. (1998). Endogenous production of beta-chemokines by CD4+, but not CD8+, T-cell clones correlates with the clinical state of human immunodeficiency virus type 1 (HIV-1)-infected individuals and may be responsible for blocking infection with non-syncytium-inducing HIV-1 in vitro. *Journal of virology* **72**, 876-881.

Sato, A., Igarashi, H., Adachi, A. & Hayami, M. (1990). Identification and localization of vpr gene product of human immunodeficiency virus type 1. *Virus genes* **4**, 303-312.

Sauermann, U., Krawczak, M., Hunsmann, G. & Stahl-Hennig, C. (1997). Identification of Mhc-Mamu-DQB1 allele combinations associated with rapid disease progression in rhesus macaques infected with simian immunodeficiency virus. *AIDS (London, England)* **11**, 1196-1198.

Sauermann, U., Stahl-Hennig, C., Stolte, N. & other authors (2000). Homozygosity for a conserved Mhc class II DQ-DRB haplotype is associated with rapid disease progression in simian immunodeficiency virus-infected macaques: results from a prospective study. *The Journal of infectious diseases* **182**, 716-724.

Scarlatti, G., Tresoldi, E., Bjorndal, A. & other authors (1997). In vivo evolution of HIV-1 co-receptor usage and sensitivity to chemokine-mediated suppression. *Nature medicine* **3**, 1259-1265.

Schindler, M., Wildum, S., Casartelli, N., Doria, M. & Kirchhoff, F. (2007). Nef alleles from children with non-progressive HIV-1 infection modulate MHC-II expression more efficiently than those from rapid progressors. *AIDS (London, England)* **21**, 1103-1107.

Schubert, U., Bour, S., Ferrer-Montiel, A. V., Montal, M., Maldarell, F. & Strebel, K. (1996). The two biological activities of human immunodeficiency virus type 1 Vpu protein involve two separable structural domains. *Journal of virology* **70**, 809-819.

Schwartz, D. H., Castillo, R. C., Arango-Jaramillo, S., Sharma, U. K., Song, H. F. & Sridharan, G. (1997). Chemokine-independent in vitro resistance to human immunodeficiency virus (HIV-1) correlating with low viremia in long-term and recently infected HIV-1-positive persons. *The Journal of infectious diseases* **176**, 1168-1174.

Seman, A. L., Pewen, W. F., Fresh, L. F., Martin, L. N. & Murphey-Corb, M. (2000). The replicative capacity of rhesus macaque peripheral blood mononuclear cells for simian immunodeficiency virus in vitro is predictive of the rate of progression to AIDS in vivo. *The Journal of general virology* **81**, 2441-2449.

Seth, A., Ourmanov, I., Schmitz, J. E. & other authors (2000). Immunization with a modified vaccinia virus expressing simian immunodeficiency virus (SIV) Gag-Pol primes for an anamnestic Gag-specific cytotoxic T-lymphocyte response and is associated with reduction of viremia after SIV challenge. *Journal of virology* **74**, 2502-2509.

Shiver, J. W., Fu, T. M., Chen, L. & other authors (2002). Replication-incompetent adenoviral vaccine vector elicits effective anti-immunodeficiency-virus immunity. *Nature* **415**, 331-335.

Singhal, P. K., Rajendra Kumar, P., Subba Rao, M. R. & Mahalingam, S. (2006). Nuclear export of simian immunodeficiency virus Vpx protein. *Journal of virology* **80**, 12271-12282.

Stahl-Hennig, C., Voss, G., Nick, S., Petry, H., Fuchs, D., Wachter, H., Coulibaly, C., Luke, W. & Hunsmann, G. (1992). Immunization with tween-ether-treated SIV adsorbed onto aluminum hydroxide protects monkeys against experimental SIV infection. *Virology* **186**, 588-596.

Stahl-Hennig, C., Voss, G., Dittmer, U. & other authors (1993). Protection of monkeys by a split vaccine against SIVmac depends upon biological properties of the challenge virus. *AIDS (London, England)* **7**, 787-795.

Stahl-Hennig, C., Coulibaly, C., Petry, H. & other authors (1994). Immunization with virion-derived glycoprotein 130 from HIV-2 or SIV protects macaques against challenge virus grown in human or simian cells or prepared ex vivo. *AIDS research and human retroviruses* **10 Suppl 2**, S27-32.

Stahl-Hennig, C., Eisenblatter, M., Franz, M. & other authors (2007a). A single vaccination with attenuated SIVmac 239 via the tonsillar route confers partial protection against challenge with SIVmac 251 at a distant mucosal site, the rectum. *Front Biosci* **12**, 2107-2123.

Stahl-Hennig, C., Suh, Y. S., Park, K. S. & other authors (2007b). Immunogenicity of a DNA prime and recombinant adenovirus boost regime significantly varies between rhesus macaques of Chinese and Indian origins. *Journal of medical primatology* **36**, 195-205.

Staprans, S. I., Barry, A. P., Silvestri, G. & other authors (2004). Enhanced SIV replication and accelerated progression to AIDS in macaques primed to mount a CD4 T cell response to the SIV envelope protein. *Proceedings of the National Academy of Sciences of the United States of America* **101**, 13026-13031.

Steger, K. K., Dykhuizen, M., Mitchen, J. L. & other authors (1998). CD4+-T-cell and CD20+-B-cell changes predict rapid disease progression after simian-human immunodeficiency virus infection in macaques. *J Virol* **72**, 1600-1605.

Stranford, S. A., Ong, J. C., Martinez-Marino, B., Busch, M., Hecht, F. M., Kahn, J. & Levy, J. A. (2001). Reduction in CD8+ cell noncytotoxic anti-HIV activity in individuals receiving highly active antiretroviral therapy during primary infection. *Proceedings of the National Academy of Sciences of the United States of America* **98**, 597-602.

Strebel, K., Daugherty, D., Clouse, K., Cohen, D., Folks, T. & Martin, M. A. (1987). The HIV 'A' (sor) gene product is essential for virus infectivity. *Nature* **328**, 728-730.

Suh, Y. S., Park, K. S., Sauermann, U. & other authors (2006). Reduction of viral loads by multigenic DNA priming and adenovirus boosting in the SIVmac-macaque model. *Vaccine* **24**, 1811-1820.

Sun, Y., Schmitz, J. E., Buzby, A. P. & other authors (2006). Virus-specific cellular immune correlates of survival in vaccinated monkeys after simian immunodeficiency virus challenge. *Journal of virology* **80**, 10950-10956.

Sutherland, R., Yang, H., Scriba, T. J. & other authors (2006). Impaired IFN-gamma-secreting capacity in mycobacterial antigen-specific CD4 T cells during chronic HIV-1 infection despite long-term HAART. *AIDS (London, England)* **20**, 821-829.

Tan, J., Deleuran, B., Gesser, B., Maare, H., Deleuran, M., Larsen, C. G. & Thestrup-Pedersen, K. (1995). Regulation of human T lymphocyte chemotaxis in vitro by T cell-derived cytokines IL-2, IFN-gamma, IL-4, IL-10, and IL-13. *J Immunol* **154**, 3742-3752.

Ten Haaft, P., Verstrepen, B., Uberla, K., Rosenwirth, B. & Heeney, J. (1998). A pathogenic threshold of virus load defined in simian immunodeficiency virus- or simian-human immunodeficiency virus-infected macaques. *Journal of virology* **72**, 10281-10285.

Torres, K. J., Gutierrez, F., Espinosa, E., Mackewicz, C., Regalado, J. & Reyes-Teran, G. (2006). CD8+ cell noncytotoxic anti-HIV response: restoration by HAART in the late stage of infection. *AIDS research and human retroviruses* **22**, 144-152.

Trachtenberg, E., Korber, B., Sollars, C. & other authors (2003). Advantage of rare HLA supertype in HIV disease progression. *Nature medicine* **9**, 928-935.

Trkola, A., Paxton, W. A., Monard, S. P. & other authors (1998). Genetic subtype-independent inhibition of human immunodeficiency virus type 1 replication by CC and CXC chemokines. *Journal of virology* **72**, 396-404.

Tsujimoto, H., Cooper, R. W., Kodama, T. & other authors (1988). Isolation and characterization of simian immunodeficiency virus from mandrills in Africa and its relationship to other human and simian immunodeficiency viruses. *Journal of virology* **62**, 4044-4050.

Turnbull, E. L., Lopes, A. R., Jones, N. A. & other authors (2006). HIV-1 epitope-specific CD8+ T cell responses strongly associated with delayed disease progression cross-recognize epitope variants efficiently. *J Immunol* **176**, 6130-6146.

Uberla, K., Rosenwirth, B., Ten Haaft, P., Heeney, J., Sutter, G. & Erfle, V. (2007). Therapeutic immunization with Modified Vaccinia Virus Ankara (MVA) vaccines in SIV-infected rhesus monkeys undergoing antiretroviral therapy. *Journal of medical primatology* **36**, 2-9.

Van Heuverswyn, F., Li, Y., Neel, C. & other authors (2006). Human immunodeficiency viruses: SIV infection in wild gorillas. *Nature* **444**, 164.

van Marle, G., Henry, S., Todoruk, T. & other authors (2004). Human immunodeficiency virus type 1 Nef protein mediates neural cell death: a neurotoxic role for IP-10. *Virology* **329**, 302-318.

Van Rompay, K. K., Kearney, B. P., Sexton, J. J., Colon, R., Lawson, J. R., Blackwood, E. J., Lee, W. A., Bischofberger, N. & Marthas, M. L. (2006). Evaluation of oral tenofovir disoproxil fumarate and topical tenofovir GS-7340 to protect infant macaques against repeated oral challenges with virulent simian immunodeficiency virus. *J Acquir Immune Defic Syndr* **43**, 6-14.

Varin, A., Manna, S. K., Quivy, V., Decrion, A. Z., Van Lint, C., Herbein, G. & Aggarwal, B. B. (2003). Exogenous Nef protein activates NF-kappa B, AP-1, and c-Jun N-terminal kinase and stimulates HIV transcription in promonocytic cells. Role in AIDS pathogenesis. *The Journal of biological chemistry* **278**, 2219-2227.

Vezys, V., Masopust, D., Kemball, C. C., Barber, D. L., O'Mara, L. A., Larsen, C. P., Pearson, T. C., Ahmed, R. & Lukacher, A. E. (2006). Continuous recruitment of naive

T cells contributes to heterogeneity of antiviral CD8 T cells during persistent infection. *The Journal of experimental medicine* **203**, 2263-2269.

Vicenzi, E., Alfano, M., Ghezzi, S., Gatti, A., Veglia, F., Lazzarin, A., Sozzani, S., Mantovani, A. & Poli, G. (2000). Divergent regulation of HIV-1 replication in PBMC of infected individuals by CC chemokines: suppression by RANTES, MIP-1alpha, and MCP-3, and enhancement by MCP-1. *Journal of leukocyte biology* **68**, 405-412.

Vinner, L., Nielsen, H. V., Bryder, K., Corbet, S., Nielsen, C. & Fomsgaard, A. (1999). Gene gun DNA vaccination with Rev-independent synthetic HIV-1 gp160 envelope gene using mammalian codons. *Vaccine* **17**, 2166-2175.

Vodicka, M. A., Koepp, D. M., Silver, P. A. & Emerman, M. (1998). HIV-1 Vpr interacts with the nuclear transport pathway to promote macrophage infection. *Genes & development* **12**, 175-185.

Vogel, T. U., Evans, D. T., Urvater, J. A., O'Connor, D. H., Hughes, A. L. & Watkins, D. I. (1999). Major histocompatibility complex class I genes in primates: co-evolution with pathogens. *Immunological reviews* **167**, 327-337.

Walker, C. M., Erickson, A. L., Hsueh, F. C. & Levy, J. A. (1991). Inhibition of human immunodeficiency virus replication in acutely infected CD4+ cells by CD8+ cells involves a noncytotoxic mechanism. *Journal of virology* **65**, 5921-5927.

Wiskerchen, M. & Muesing, M. A. (1995). Human immunodeficiency virus type 1 integrase: effects of mutations on viral ability to integrate, direct viral gene expression from unintegrated viral DNA templates, and sustain viral propagation in primary cells. *Journal of virology* **69**, 376-386.

Wojcechowskyj, J. A., Yant, L. J., Wiseman, R. W., O'Connor, S. L. & O'Connor, D. H. (2007). Control of simian immunodeficiency virus SIVmac239 is not predicted by inheritance of Mamu-B*17-containing haplotypes. *Journal of virology* **81**, 406-410.

Xiang, J., George, S. L., Wunschmann, S., Chang, Q., Klinzman, D. & Stapleton, J. T. (2004). Inhibition of HIV-1 replication by GB virus C infection through increases in RANTES, MIP-1alpha, MIP-1beta, and SDF-1. *Lancet* **363**, 2040-2046.

Yant, L. J., Friedrich, T. C., Johnson, R. C. & other authors (2006). The high-frequency major histocompatibility complex class I allele Mamu-B*17 is associated with control of simian immunodeficiency virus SIVmac239 replication. *Journal of virology* **80**, 5074-5077.

Yu, X. G., Lichterfeld, M., Chetty, S. & other authors (2007). Mutually exclusive T-cell receptor induction and differential susceptibility to human immunodeficiency virus type 1 mutational escape associated with a two-amino-acid difference between HLA class I subtypes. *J Virol* **81**, 1619-1631.

Zack, J. A., Arrigo, S. J., Weitsman, S. R., Go, A. S., Haislip, A. & Chen, I. S. (1990). HIV-1 entry into quiescent primary lymphocytes: molecular analysis reveals a labile, latent viral structure. *Cell* **61**, 213-222.

Zapp, M. L. & Green, M. R. (1989). Sequence-specific RNA binding by the HIV-1 Rev protein. *Nature* **342**, 714-716.

Zhang, X., Divangahi, M., Ngai, P., Santosuosso, M., Millar, J., Zganiacz, A., Wang, J., Bramson, J. & Xing, Z. (2007a). Intramuscular immunization with a monogenic plasmid DNA tuberculosis vaccine: Enhanced immunogenicity by electroporation and co-expression of GM-CSF transgene. *Vaccine* **25**, 1342-1352.

Zhang, Z. Q., Schleif, W. A., Casimiro, D. R. & other authors (2004). The impact of early immune destruction on the kinetics of postacute viral replication in rhesus monkey infected with the simian-human immunodeficiency virus 89.6P. *Virology* **320**, 75-84.

Zhang, Z. Q., Casimiro, D. R., Schleif, W. A. & other authors (2007b). Early depletion of proliferating B cells of germinal center in rapidly progressive simian immunodeficiency virus infection. *Virology* **361**, 455-464.

Zhao, M. L., Kim, M. O., Morgello, S. & Lee, S. C. (2001). Expression of inducible nitric oxide synthase, interleukin-1 and caspase-1 in HIV-1 encephalitis. *Journal of neuroimmunology* **115**, 182-191.

APPENDIX

App. 1.1 REAGENTS AND MATERIALS USED FOR VARIOUS ASSAYS

App. Table 1.1a: Solutions for the Indicator cell-line suppression (CNAR) assay

Solution	Preparation
X-gal Stock (40mg/ml)	Dissolve 40 mg in 1 ml DMSO. Stored in 0.5 ml aliquots at -20°C in the dark. Discarded when it turns greenish-brown
DEAE-dextran stock (200μg/ml)	Prepared in DMEM (without FBS). Medium added first up to two-thirds of required volume, left to stand at 4°C for 2 hrs before topping up with DMEM. Stored at 4°C in the dark
0.2M Potassium ferricyanide	066 g dissolved in 1 ml PBS pH 7.2
0.2M Potassium ferrocyanide	0.0845 g dissolved in 1 ml PBS pH 7.2
2M Magnesium chloride	190.44 mg dissolved in 1 ml PBS pH 7.2
0.1 % Sodium azide	0.1 g dissolved in 100 ml PBS pH 7.2
Fixing Solution	1% formaldehyde and 0.2% glutaraldehyde prepared in PBS. Keep at 4°C in the dark

App. Table 1.1b: The staining and fixing solutions used for the CNAR assay

Components	***Per 1 millilitre***	**For 96 wells (10 millilitres)**
PBS	949 μl	9.49mL
0.2M potassium ferricyanide (in PBS)	20μl	0.2mL
0.2M potassium ferrocyanide (in PBS)	20μl	0.2mL
2M $MgCl_2$	1μl	0.01mL
40Mg/mL X-gal (in DMSO)	10μl	0.1mL

App. Table 1.2: Media and solutions used for various cell culture assays

Article	CAT #	Source
RPMI 1640	P04-18500	PAN™ Biotech
FBS; *heat inactivated at 56 °C, 30 minutes*	3302-P250316	PAN™ Biotech
Penicillin (10,000U/ml)/ Streptomycin (10 mg/ml)	P06-07100	PAN™ Biotech
IL-2, Lyophilised; (Specific activity $\geq 10^7$ U/mg). *Reconstituted in 50 ml RPMI =100,000 U/ml*	200-02	Peprotech Inc/ Tebu Bio
DMEM	P04-02500	PAN™ Biotech
Trypsin EDTA	P10-02300	PAN™ Biotech
37 % Formaldehyde	7398.1	ROTH
50 % Glutaraldehyde		
X-gal ($C_{14}H_{15}BrCINO_6$)	2315.4	ROTH
Sodium azide (NaN_3)	822335	MERCK
Potassium Ferrocyanide ($K_4Fe(CN)_6.3H_2O$	P-9387	SIGMA
Potassium Ferricyanide (III)	24.402-3	ALDRICH

App. Table 1.3: Primers and Probes for quantitative RT-PCR

Region	Oligonucleotide sequence	Source
SIVgag for. (1104-1130)	5'-ACC CAG TAC AAC AAA TAG GTG GTA ACT-3' (TM, 55 °C; GC, 40 %; Length, 27 mer)	Biomers GmbH, Ulm, Germany
SIV gag rev. (1077-1053)	5'-TCA ATT TTA CCC AGG CAT TTA ATG T-3' (TM, 55 °C; GC, 32%; Length, 25mer)	Biomers GmbH, Ulm, Germany
TaqMan Probe **(**1078-1102)	FAM-5'-TGT CCA CCT GCC ATT AAG CCC GAG-3'- TAMRA (TM, 65 °C; GC, 58%; Length, 24 mer)	Biomers GmbH, Ulm, Germany

Primers were designed using the gag sequence of the simian immunodeficiency virus of macaque isolate 239, clone lambda (SIVMM239). The virus sequence was retrieved from the NCBI sequence database (gene accession number; M33262).

App. Table 1.4: Reagents and buffers for MHC-1 allele typing

Buffer/Solution	Preparation/Components
5X Lysis buffer	67.55 g Tris pH 7.5 (5M) or 500 ml 1M Tris 548 g Saccharose 50 g Triton Brought to 1000 ml volume with ddH20 (Milli-Q purified) NB; Tris was prepared first, autoclaved then brought to pH with fuming HCL (ca.22 ml).
20X STE	67.55 g Tris 58.44 g NaCl 2.93 g EDTA Brought to 500 ml volume with ddH20 and autoclave
STE + H20	STE + H20
10% SDS	10 g SDS (weighed under the hood) 100 ml ddH20
20X TE	2.7 g Tris 0.6 g EDTA Brought to 100 ml volume with ddH20 and autoclave (Add ca. 2.5 ml fuming HCL to pH)
2X Proteinase K/ TE	30 mg Proteinase K 150 µl 20X TE 1350 µl ddH20 Prepared shortly before use (equivalent to 20 mg/ml) and frozen into single-use aliquots
6M NaCl solution	350 g NaCl Brought to 1000 ml volume with ddH20 and autoclave
80% Ethanol	833.33 ml of 96% Ethanol Brought to 1000 ml volume with ddH20
DNA solvent	88 ml H20 + 5 ml 20X STE

App. Table 1.5: *Macaca mulatta* (*Mamu*) MHC class 1 allele specific primers

Mamu	Oligonucleotide sequence	Source
A*01 for.	5′-AAA ACG ACG GCC AGT GAC AGC GAC GCC GCG AGC CAA-3′ (TM, 84.3°C; length, 36 mer; GC content, 63.9%)	VBC Biotech
A*01 rev.	5′-GAA ACA GCT ATG ACC GCT GCA GCG TCT CCT TCC CC-3′ (TM, 76.4°C; length, 35 mer; GC content, 60.9%)	
A*02 for.	5′-TGT AAA ACG ACG GCC AGT GGT GGA GCA GGA GGG TCC A-3′ (TM, >75°C; length, 37 mer; GC content, 59.5%)	MWG Biotech
A*02 rev.	5′-CAG GAA ACA GCT ATG ACC TCG TAG GCG GAC TGG TG-3′ (TM, 74.2°C; length, 35 mer; GC content, 57.1%)	
A*04 for.	5′-TGT AAA ACG ACG GCC AGT CCA TGA GCT ATT TCT ACA CCT A-3′ (TM, 71.5°C; length, 40 mer; GC content, 45%)	MWG Biotech
A*04 rev.	5′-CAG GAA ACA GCT ATG ACC GGT AGG TTC TGT GCT GCT C-3′ (TM, 73.9°C; length, 37 mer; GC content, 54.1%)	
MDRB5	5′-GCC TCG AGT GTC CCC CCA GCA CGT TTC-3′ (TM, 71.9°C; length, 27 mer; GC content, 66.7%)	VBC Biotech
3-MDR	5′-GCC GCA GCT TTC ACC TCG CCG CTG-3′ (TM, 72.4°C; length, 24 mer; GC content, 70.8%)	
B*17 for	5′-AAA ACG ACG GCC AGT GCG ACA CGG AGA GCC AAG GA-3′ (TM, 79.9°C; length, 35 mer; GC content, 60%)	VBC Biotech
B*17 rev	5′-GAA ACA GCT ATG ACC CCG CTC CGC ATA ACG GTT CC-3′ (TM, 75.6°C; length, 35 mer; GC content, 57.1%)	
B*22 for	5′-TGT AAA ACG ACG GCC AGT CCG AGG GAA CCT GAG GAC A-3′ (TM, 87°C; length, 37 mer; GC content, 56%)	Invitrogen
B*22 rev	5′-GAA ACA GCT ATG ACC CTG CTG CTC TGC CTC GCG-3′ (TM, 75.2°C; length, 33 mer; GC content, 60.6%)	VBC Biotech
B*30 for	5′-AAA ACG ACG GCC AGT GAG GCC CAC GCA CAG AAT C-3′ (TM, 78°C; length, 34 mer; GC content, 58.8%)	VBC Biotech
B*30 rev	5′-GAA ACA GCT ATG ACC CCT TGC CGT CGT AGG CAT A-3′ (TM, 72°C; length, 34 mer; GC content, 52.9%)	
B*57 for	5′-AAA ACG ACG GCC AGT TCC GAG AGA GGA GCC GCA-3′ (TM, 78°C; length, 33 mer; GC content, 60.6%)	VBC Biotech
B*57 rev	5′-GAA ACA GCT ATG ACC GGG GTG GTG GAT CAC ATG-3′ (TM, 72.7°C; length, 33 mer; GC content, 54.5%)	

App. Table 1.6: RNA and DNA preparation and PCR Kits

Description/ CAT#	***Purpose***	***Source***
RNeasy® Mini Kit/ 74104	Cell-associated RNA purification	Qiagen
QIAshredder™/ 79656	Cell-associated RNA purification	Qiagen
QIAamp® Viral RNA Mini Kit	Plasmid DNA purification	Qiagen
QIAamp® Viral RNA Mini Kit	Cell-free viral RNA purification	Qiagen
MagAttract Virus Mini M48 kit/ 955336	Cell-free viral RNA purification	Qiagen
QIAamp® DNA Mini Kit	Isolation of genomic DNA	Qiagen
QuantiTect® SYBR® Green RT-PCR	Optimisation of real-time PCR	Qiagen
QuantiTect™ Probe RT-PCR Kit	Optimisation of real-time PCR	Qiagen
TaqMan® One-Step RT-PCR Master Mix reagents Kit	Real-time RNA PCR	ABI
RNase-Free DNase Set/ 79254	Removal of genomic DNA from isolated RNA	Qiagen
RNase A/ 1018048	Removal of RNA from purified DNA plasmids.	Qiagen

App. Table 1.7: Cytokine assay kits

Description	*Components/Analytes*	*Catalogue*	*Source*
Fluorokine® MAP Human base Kit A (Cat # LUH000)	IFNγ	LUH285	R & D systems
	IL-1β	LUH201	R & D systems
	IL-10	LUH217	R & D systems
	MCP-1/CCL2	LUH279	R & D systems
	MIP-1α/CCL3	LUH270	R & D systems
	MIP-1β/CCL4	LUH271	R & D systems
	RANTES/CCL5	LUH278	R & D systems
	TNFα	LUH210	R & D systems
Fluorokine® MAP Human base Kit B (Cat # LUB000)	IP10/CXCL10	LUB266	R & D systems
Notes	Cross-reactive with Rhesus monkey cytokines. Each kit component comprised respective analyte-coated beads, analyte-specific biotinylated detection antibodies and Streptavidin phycoerythrin (PE) conjugate.		

Kit description and (CAT #)	**Source**
LiquiChip™ Control Bead Kit (922912)	Qiagen
LiquiChip™ Calibration Bead Kit (922911)	Qiagen

App. Table 1.8: Instruments and Softwares used

Instrument/Software	Purpose	Source
7500 Real-time PCR system/ 7500 Sequence Detection System	Real-time PCR	Applied Biosystems (ABI)
BioRobot M48 Workstation/ QIAsoft M Operating System	Viral RNA Isolation	Qiagen GmbH
Bioreader®-3000	ELISPOT and Indicator assay spot-detections	Bio-Sys GmbH, Karben
LiquiChip Workstation/ integrated system software for LiquiChip Workstation ver.2.3/ LiquiChip analyzer Ver. 1.0.5 + Luminex IS100	Cytokine bead array data collection, detection and analyses	Qiagen and Luminex
NanoDrop® ND-1000 Spectrophotometer/ ND-1000 v3.1.0	Spectrophotometric readings for nucleic acids (RNA and DNA)	PeQLab biotechnologies
Multifuge 3 $_{S-R}$	Centrifugation	Heraeus
Eppendorf centrifuge 5415 C	Centrifugation	Eppendorf
/SPSS version 15.0	Statistical data analyses	SPSS Inc

App. Table 1.9: Other Consumables

Item	Purpose	Source (CAT#)
PVDF MAIPS4510 plates	ELISPOT	Millipore
TC-Plate, 12-well	Cell culture	CELLSTAR®/Greiner bio-one (665180)
24-well cell culture cluster	Cell culture	Corning Inc. Costar®
TC-Plate 96-well, Flat-B	Cell culture/CNAR	SARSTEDT (83.1835.300)
MICROTEST™ Tissue culture plate, 96-well Flat-B	Cell culture/CNAR	Becton Dickinson
75 cm2 TC Flasks	Cell culture	CELLSTAR®/Greiner bio-one (658170/658175)
96-well Optical Reaction Plate with Barcode (128)	Real-time PCR	ABI (4306737)
Micro-Amp Optical adhesive Film	Real-time PCR, plate cover	ABI (4311971)

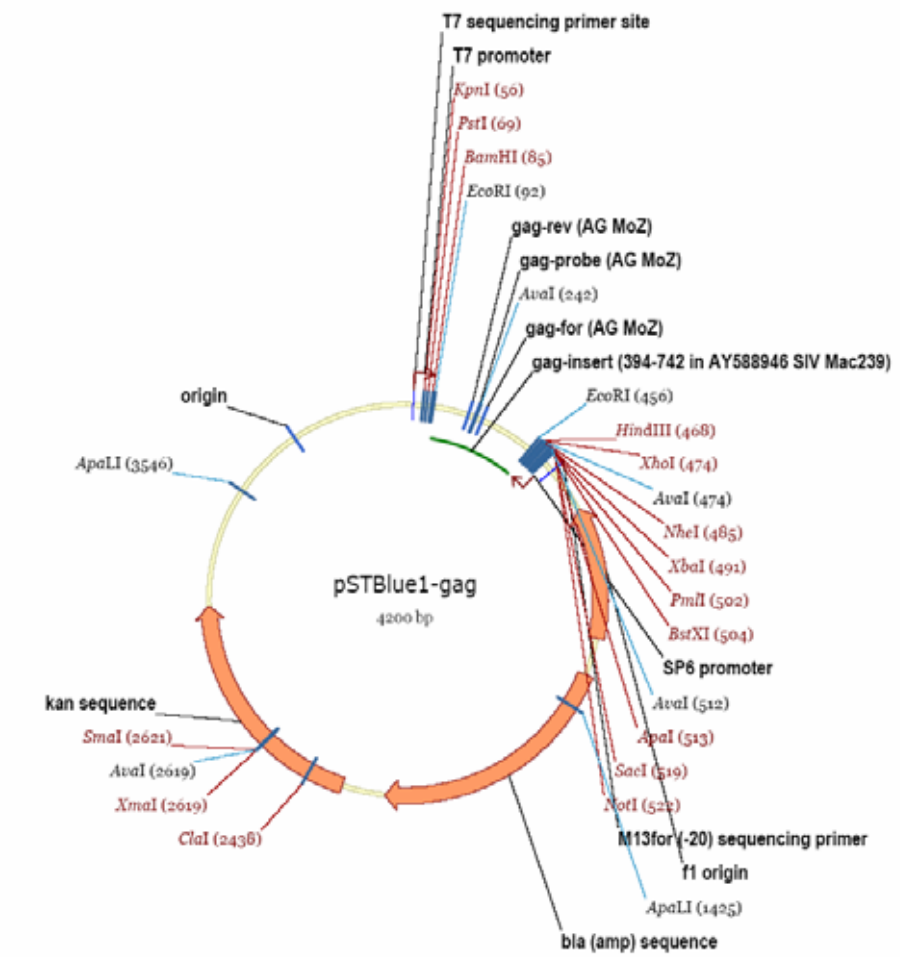

App. Fig. 1.1: The pSTBlue Vector used to prepare plasmid standards for RT-PCR

Vector sequence (Top) and map (below) of the pSTBlue1 plasmid used for *in vitro* transcription and preparation of RNA standards for real-time quantitative PCR. The vector contains a 349 base-pair SIVgag insert. This vector was re-sequenced by Dr. Dirk Motzkus, Deutsche Primatenzentrum, Goettingen and confirmed to contain the insert.

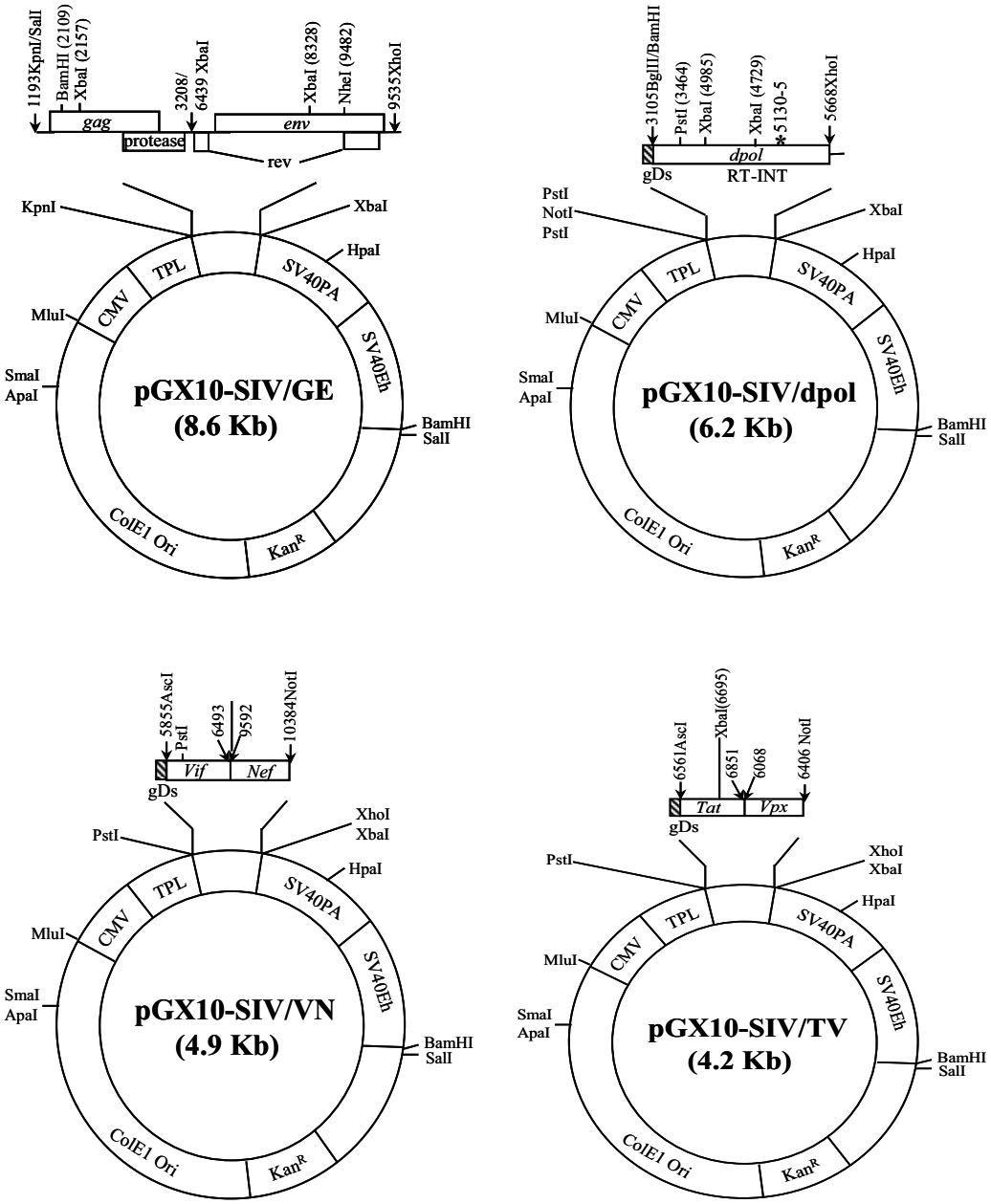

App. Fig. 1.2: The pGX10 plasmid vectors used as carriers of the DNA vaccine.

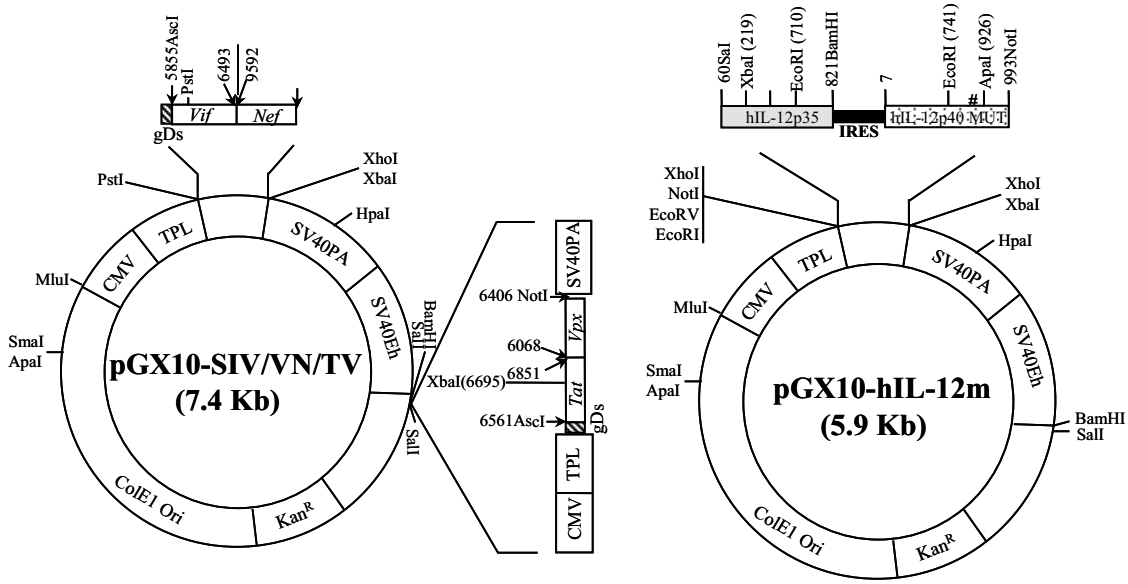

App. Fig. 1.2 continued: The pGX10 plasmid vectors used as carriers of the DNA vaccine.

ACKNOWLEDGEMENT

Many thanks to: The German Academic Exchange Services (DAAD) for supporting my study and stay in Germany and to the DPZ for hosting me. Special thanks to my Supervisor, Prof Dr. Hunsmann for replying that very first e: mail that enabled me secure the DAAD support. Thank you also for your able guidance. Words can not express how I am Indebted to Dr. Stahl-Hennig Christianne in whose lab I was based. Although most of the times I was running around in every lab, you were always generous with your advice and financial support for my experiments. Dr. Ulrike Sauermann was always there to listen to my every experimental need. I can say that the success of my work was tightly linked to your contribution from day 1. Your positive critique navigated this thesis to this end. Dr. PD Sieghart Sopper was never late from Wuersburg! Your arrival at DPZ gave my work another outlook for which I feel indebted. Thanks for the creative thinking that shaped my work too. How much more can I thank the four of you than to just say THANK YOU. Equal gratitude to Prof. Dr. Fritz who has followed up my progress since my first day as a PhD student. I will not forget the title 'Doktorvater' which made it easy to consult you. I also thank Prof. Dr Hardeland for accepting to be my 'Korreferent'. Vielen Dank. If and when any of you do make a SAFARI nach Kenia, do write me an email.

I have sincerely finished my work without knowing where the money came from! But one think I know is that some people were special in this arrangement. Many thanks to Prof. Sung who's Lab was central in the core vaccine study that gave birth to my Thesis. Thanks also for designing the vaccine used in this study. Many thanks too to Dr. Suh You-Suk for sharing his ELISPOT data for comparison with my own. Thanks too for inducting me to the ELISPOT assay. Many thanks to Prof Frank Kirchhoff of University of Ulm for the generous donation of the TZM-bl indicator cell lines and to the Institute of National Health, USA, that provided these cells in the first place. Many thanks to Prof. Dr K. Überla for donating the gag/pol genes used in the vaccine. I am grateful to the technicians who assisted me at various stages of my work. I do not want to forget the following names: Nicole Leuchte, Sandra Heine, Nicola, Lydia, Heidi and Judith Hampe. You Fox were special and played a special role! If I have to forget any of you, may I not. Nicole was unique and always multipurpose. Thank you all.

Mmmmh! That PhD room was special. Always quiet but with people. I thank my colleagues Reiner Schulte, Judith Montag, Jessica (who threw the towel at the last lap), Bianka Mussil, Tanja, Tina, Nadine, Andrea, Ahmed for making the environment complete.

Dirk, Andreas Stuecke and Monica for being liberal. I can't forget Andrea with the 'Monday English' adage. Karin Wolter's seat in Prof Dr. Hunsmann's office was a source of inspiration. If anyone made my life along the corridors of Viro and DPZ as a whole comfortable, it was Karin. Thanks a lot. If I have forgotten anyone, it is not deliberate. It is long since I first stepped in Deutschland and memory may fail, but my heart is grateful to you all.

The success of my work and stay in Germany could not have been realized without my loving wife, Dorothy. She is the greatest woman I have ever met and I am glad she was there for me every time; both at my highs and lows, sick and healthy. That she had to conduct her studies in German, write her thesis and still remain woman number one if an attribute from above! Thanks Hon.

How much more to my Dad Elgibor Rohi whose mighty Hand of support kept me going? Your Word kept me on top of health and in good spirits. The phone calls, the financial support in a tough economic system ensured that I was always watered and filled. Thanks to the First born of my Dad, Prince for always ensuring a continued link between me and Dad and that I always got what I wanted. My both parents are wonderful. Thanks mum for being strong. Thanks Mzee for being nice. You are such a gift.

And when all has been said and done, I ask myself if I really ever lived up to the call. When I don't know the answer to my own question, one thing is sure: the Light that shineth in darkness and the Voice that crieth in the wilderness gives me strength to say Thank You. Shalom.